

Remarks

Reconsideration of this Application is respectfully requested.

Upon entry of the foregoing amendment, claims 35-52 and 54-68 are pending in the application, with claim 35 being the sole independent. Claim 53 is sought to be cancelled without prejudice to or disclaimer of the subject matter therein. Applicants retain the right to pursue the subject matter of claim 53 in continuing applications. Claims 54-56, 58-61 and 65-68 have been amended in order to more clearly define the subject matter which Applicants regard as the invention. Applicants retain the right to pursue the subject matter of the claims prior to amendment in continuing applications. Support for the amendments to the claims can be found throughout the specification and the original claims. Support for the amendment to claims 54-56 can be found, *inter alia*, at page 4, lines 27-30. Support for the amendment to claims 58-61 can be found, *inter alia*, in Example 1. Support for the amendment to claims 65-68 can be found, *inter alia*, at page 13, lines 5-8. These changes are believed to introduce no new matter, and their entry is respectfully requested.

Based on the above amendment and the following remarks, Applicants respectfully request that the Examiner reconsider all outstanding objections and rejections and that they be withdrawn.

A. Claim Rejections Under 35 U.S.C. § 112, First Paragraph

The Examiner has rejected claims 53-57 and 65-68 under 35 U.S.C. § 112, first paragraph, as allegedly not enabled by the specification. (Paper No. 13, page 2.) Specifically, the Examiner has asserted that:

For the purpose of examination under 35 U.S.C. 112, first paragraph,
"pharmaceutical compositions", and compositions comprising

therapeutically active substances must be enabled for their therapeutic use.

(*Id.* at page 3.) For the reasons set forth in Applicants Preliminary Amendment and Remarks of January 17, 2001, Applicants respectfully disagree.

However, solely to advance prosecution and not in acquiescence to the Examiner's rejection, claims 54-57 have been amended to no longer recite "therapeutically active" nucleic acids. Claim 53 has been cancelled. Further, claims 65-68 have been amended to no longer recite "pharmaceutical" compositions. Accordingly, the Examiner's rejections are rendered moot. Applicants respectfully request that the Examiner reconsider and withdraw the rejections.

B. Claims rejections Under 35 U.S.C. § 112, Second Paragraph

The Examiner has rejected claims 58-63 under 35 U.S.C. § 112, second paragraph as allegedly being indefinite. (Paper No. 13, page 6.) Applicants respectfully traverse the Examiner's rejections.

The Examiner has alleged that the term "dilute" is a relative term which renders claim 58 and the associated dependent claims indefinite. (*Id.*) Solely to advance prosecution and not in acquiescence to the Examiners' rejection, Applicants have deleted the term "dilute" from the claims. Accordingly the Examiner's rejection is rendered moot and Applicants respectfully request that the rejection be reconsidered and withdrawn.

The Examiner has asserted that claims 59 and 60 are indefinite because it is unclear whether the recited DNA concentrations are starting concentrations or final concentrations. (Paper No. 13, page 7.) Applicants have amended claims 59 and 60 in order to make clear that the recited DNA concentrations are final concentrations. Accordingly, Applicants respectfully request that the Examiner reconsider and withdraw the rejection.

The Examiner has asserted that claims 61 and 62 are indefinite because it is unclear what salt concentration is intended by "physiological value." (*Id.*) Applicants have amended the claims in order to make clear what salt concentration is being referred to in the claims. Accordingly, Applicants respectfully request that the Examiner reconsider and withdraw the rejection.

C. Claim Rejections Under 35 U.S.C. § 102

The Examiner has rejected claims 35-43 and 49 under 35 U.S.C. § 102(e) as being anticipated by Yin *et al.*, U.S. Patent No. 5,919,442 or Tomalia *et al.*, U.S. Patent No. 5,714,166. (Paper No. 13, page 7.) Applicants respectfully traverse the Examiner's rejection.

I. One Skilled in the Art Would Recognize the Term "PEI" to be Random, Branched PEI

In Applicants' Preliminary Amendment and Remarks, filed January 17, 2001, Applicants indicated that the PEI of the invention is limited to the PEI disclosed in the specification. With regards to these statements, the Examiner has stated that "the specification provides no limiting definition with regard to the nature of the PEI which may be used in the instant invention." (Paper No. 13, page 9.) Applicants respectfully disagree.

As discussed in Applicants' Preliminary Amendment and Remarks, the term "polyethyleneimine" or "PEI", when used alone and without any modifying adjective or other descriptive term, is recognized in the art to mean random branched PEI, which is the "regular" PEI that has been commercially available for a long time. If using other, more unusual forms of PEI (e.g., dendrimer PEI or hyper-comb branched PEI), one skilled in the art would certainly use the specific modifying adjective. In this connection, Applicants submit herewith a Declaration Under 37 C.F.R. 1.132 signed by inventor Manfred Ogris. In the Declaration, Dr. Ogris explains how one

skilled in the art would understand the term PEI (without further descriptive modification). Applicants also note that the example PEIs provided in the specification at page 6, lines 1-10 and Example 1, lines 19-20 are all examples of "random branched" PEI.

Given the examples provided in the specification and the art-recognized meaning of the term "PEI", one skilled in the art would understand the claimed invention to be directed to PEI that is random branched. Thus, contrary to the Examiner's statements, the specification does indeed provide a limiting definition with regard to the nature of the PEI used in the invention. Applicants remind the Examiner that the specification need not literally describe the claims. (M.P.E.P. § 2163.03.)

II. Neither Yin et al., Tomalia et al. nor Bogdanov et al. Anticipate the Claims

In order for a reference to anticipate under 35 U.S. C. § 102(e), the reference must teach every element of the claim. *See* M.P.E.P. § 2131; *Verdegaal Bros. v Union Oil Co. of California*, 814 F.2d 628,631 (Fed. Cir. 1987). As further discussed below, neither *Yin et al.*, *Tomalia et al.*, nor *Bogdanov et al.* teach the use of *complexes* of nucleic acid and *randomly branched* PEI, which is covalently modified with a hydrophillic polymer. Thus, neither *Yin et al.*, *Tomalia et al.*, nor *Bogdanov et al.* anticipate the claims.

A. Yin et al.

Yin et al. teach hyper comb-branched polymers. Hyper comb-branched polymers comprise successive generations of branches branching off of prior generations of branches resulting in a structure with an exceedingly high degree of branching. (Column 3, lines 33-49.) More specifically, *Yin et al.* teach that:

Hyper comb-branched polymers are defined based upon the number of generations or grafting steps. As illustrated in FIG.2, a hyper

comb-branched polymer is constructed by grafting or attaching a series of branching arrays to a core, or predecessor branches. The first grafting array is defined as generation 0 (G0), the second generation is generation 1 (G1), the third grafting array is generation 2 (G2), the fourth array is generation 3 (G3), and so on. This novel design not only significantly reduces the synthetic effort for obtaining higher molecular weight (i.e. greater than 10 million, with a molecular weight distribution of about 1.2) or larger size (i.e. a diameter greater than about 100 nm) dendritic polymers, but also enables the designer to tailor particular structural attributes of the hyper comb-branched polymers.

(Column 3, lines 50-65.) Based upon this description, it is clear that the polymer branches of Yin *et al.* are highly *organized* into successive generations which "enables the designer to tailor particular structural attributes of the hyper-comb branched polymers." (*Id.*) In contradistinction to the compositions of Yin *et al.*, Applicants' claimed invention does not employ hyper comb-branched polymers. Applicants' claimed invention comprises *random* branched PEI. Accordingly, Yin *et al.* do not teach each element of the claims.

B. Tomalia *et al.*

Tomalia *et al.* teach "dense star" polycation polymers. A dense star or "starburst" polymer of PEI is a dendritic polymer exhibiting regular dendritic branching formed by the sequential or generational addition of branched layers to or from a core. (Column 2, lines 32-45.) Dendritic polymers encompass dendrimers, which are characterized by a core, at least one interior branched layer, and surface branched layers. (*Id.*) They are distinguished from randomly branched polymers by the inclusion of precisely one branch point per repeat unit. (See PANAMA Starburst Dendrimers, <www.columbia.edu/~jlt32/Dendrimer.pdf, page 1> (visited August 1, 2001) (Exhibit A); see also Tomalia *et al.*, *Polymer. Mat.* 3: 1814-30 (1996) (Exhibit B).) Accordingly, Tomalia *et al.* do not

teach the use of randomly branched PEI. Thus, Tomalia *et al.* do not teach every element of the claims.

In addition, Tomalia *et al.* do not teach covalent attachment of hydrophilic polymers to the PEI polymer. Tomalia *et al.* teach that polycation polymers may be "coated" or "shielded" with PEG. (Column 22, lines 36-37.) However, there is no teaching that PEG should be covalently attached to the PEI. In response to Applicants' previous assertions on this issue, the Examiner has alleged that Tomalia *et al.* teach that PEG is "attached" to PEI and that "the specification clearly indicates that 'attachment' encompasses covalent linkage. See column 17, lines 45-48." (Paper No. 13, page 10.) Applicants respectfully disagree. Applicants have failed to find where Tomalia *et al.* teach that PEG can be "attached" to PEI. Further, while the specification indicates that "attachment" may encompass covalent linkage, said attachment is discussed in terms of the "carried materials" that are physically entrapped or encapsulated within the core of the dendrimers. (Column 17, lines 41-43.) PEG is not a "carried material" within the context of the paragraph that the Examiner cites. Thus, Tomalia *et al.* do not teach covalent attachment of PEG to PEI.

In view of the above, Applicants assert that neither Yin *et al.* nor Tomalia *et al.* teach every element of the claims. Accordingly, Applicants assert that the rejection under 35 U.S.C. § 102(e) is improper and Applicants respectfully request that the Examiner reconsider and withdraw the rejection.

C. Bogdanov *et al.*

The Examiner has rejected claims 35, 41-45, 49 and 52 under 35 U.S.C. § 102(e) as allegedly being anticipated by Bogdanov *et al.*, U.S. Patent No. 5,871,710. (Paper No. 13, page 9.) Applicants respectfully traverse the Examiner's rejection.

The Examiner has asserted that "Bogdanov teaches a block copolymer of PEG and nucleic acids which is covalently attached to PEI." (Paper No. 13, page 10.) As discussed in Applicants' Preliminary Amendment and Remarks of January 17, 2001, Bogdanov *et al.* do not teach PEI/nucleic acid *complexes* as required by the claims and taught in the specification. According to the online version of the Merriam-Webster Collegiate Dictionary, a complex is "a chemical association of two or more species (as ions or molecules) joined usually by weak electrostatic bonds rather than covalent bonds." (See Exhibit C.) The art recognizes this definition of "complex." See THEODORE L. BROWN & H. EUGENE LEMAY, CHEMISTRY, THE CENTRAL SCIENCE 863-64 (Prentice Hall, 4th ed. 1988) (Exhibit D) (discussing the charge interaction between molecules within complexes); See also Abdallah *et al.*, *Hum. Gen. Ther.* 7:1947, 1953 (1996) (Exhibit E) (discussing the charge ratios of DNA/PEI complexes). The specification also discusses the importance of charge in relation to the DNA/PEI complex. Thus, it is clear from the claims, the teachings in the art, and the specification that the association between the PEI and DNA is an electrostatic association. According to the Examiner, Bogdanov *et al.* teach *covalent attachment* of nucleic acids to PEI. Thus, Bogdanov *et al.* do not teach *complexes* of nucleic acid and polyethyleneimine, as required by the claims. Because Bogdanov *et al.* do not teach every element of the claims, Bogdanov *et al.* do not anticipate the claims. Applicants respectfully request that the Examiner reconsider and withdraw the rejection.

III. Claim Rejections Under 35 U.S.C. § 103

The Examiner has rejected claims 44-51 and 64 under 35 U.S.C. § 103(a) as allegedly being unpatentable over Yin *et al.* or Tomalia *et al.*, either one in view of Szoka *et al.*, U.S. Patent No. 5,661,025. (Paper No. 13, page 11.) Applicants respectfully traverse the Examiner's rejection.

The defects of Yin *et al.* and Tomalia *et al.* have been described above in relation to the Examiner's rejection under 35 U.S.C. § 102(e). Szoka *et al.* do not cure the defects of Yin *et al.* or Tomalia *et al.* in order to render the subject matter of claims 44-51 and 64 obvious. Accordingly, Applicants respectfully request that the Examiner reconsider and withdraw the rejection.

The Examiner has rejected claim 52 under 35 U.S.C. § 103(a) as allegedly being unpatentable over Yin *et al.* or Tomalia *et al.*, either one in view of Szoka *et al.* in further view of Bogdanov *et al.* (Paper No. 13, page 16.) Applicants respectfully traverse the Examiner's rejection.

The defects of Yin *et al.* and Tomalia *et al.* have been described above in relation to the Examiner's rejection under 35 U.S.C. § 102(e). Szoka *et al.* in further view of Bogdanov *et al.* do not cure the defects of Yin *et al.* or Tomalia *et al.* in order to render the subject matter of claim 52 obvious. Accordingly, Applicants respectfully request that the Examiner reconsider and withdraw the rejection.

Conclusion

All of the stated grounds of objection and rejection have been properly traversed, accommodated, or rendered moot. Applicants therefore respectfully request that the Examiner reconsider all presently outstanding objections and rejections and that they be withdrawn. Applicants believe that a full and complete reply has been made to the outstanding Office Action and, as such, the present application is in condition for allowance. If the Examiner believes, for any reason, that personal communication will expedite prosecution of this application, the Examiner is invited to telephone the undersigned at the number provided.

Prompt and favorable consideration of this Amendment and Reply is respectfully requested.

Respectfully submitted,

STERNE, KESSLER, GOLDSTEIN & FOX P.L.L.C.



Eric K. Steffe
Attorney for Applicants
Registration No. 36,688

Date: 8/25/01

1100 New York Avenue, N.W.
Suite 600
Washington, D.C. 20005-3934
(202) 371-2600

Version with markings to show changes made

53. (Cancelled)

54. (Once amended) Complexes according to claim [53]35, characterised in that the [therapeutically active] nucleic acid codes for one or more cytokines.

55. (Once amended) Complexes according to claim [53]35, characterised in that the [therapeutically active] nucleic acid codes for one or more tumor antigens or fragments thereof.

56. (Once amended) Complexes according to claim [53]35, characterised in that the [therapeutically active] nucleic acid is a suicide gene.

58. (Twice amended) Process for preparing complexes according to claim 35, characterised in that first DNA and PEI, optionally modified with a cellular ligand, are complexed by mixing [dilute] solutions of the DNA and the PEI and then the hydrophilic polymer is bound to PEI.

59. (Once amended) Process according to claim 58, characterised in that the final DNA concentration is about 5 to 50 µg of DNA/ml.

60. (Once amended) Process according to claim 59, characterised in that the final DNA concentration is about 10 to 40 µg of DNA/ml.

61. (Twice amended) Process according to claim 59, characterised in that the complexing is carried out at a salt concentration below [physiological value] the concentration of salt in HBS (150 mM NaCl, 20 mM HEPES, pH 7.3).

65. (Once amended) [Pharmaceutical]A composition containing one or more complexes according to claim [53]35.

66. (Once amended) [Pharmaceutical]The composition according to claim 65, characterised in that it contains the complexes in a concentration of about 200 µg/ml to about 1 mg/ml, based on DNA.

67. (Once amended) [Pharmaceutical]The composition according to claim 65, characterised in that the complexes contain DNA which codes for one or more cytokines.

68. (Once amended) [Pharmaceutical]The composition according to claim 65 [in the form of a tumor vaccine], characterised in that the complexes contain DNA which codes for one or more tumor antigens or fragments thereof, optionally combined with DNA which codes for one more cytokines.

PAMAM Starburst Dendrimers

Dendritic polymers are a novel class of macromolecules, distinguished from linear and randomly branched polymers by the inclusion of precisely one branch point per repeat unit.¹ Polyamidoamine ("Starburst") dendrimers, Figure 1, are synthesized by the repetitive addition of a branching unit to an amine core (typically ammonia or ethylene diamine.) The repeat unit is added to the growing polymer in two steps: Michael addition of methacrylate to the amine, followed by regeneration of amine termini with ethylene diamine.² Each complete grafting cycle is termed a generation. Branching occurs at the terminal amine, since two methacrylate monomers will be added to each amine. Consequently, each generation of growth doubles the number of termini and approximately doubles the molecular weight. The Starburst dendrimers to be used in the work proposed herein will be provided through a collaborative arrangement with Professor D. Tomalia. Dendrimers from generation 0 to generation 10 will be available, which span a range of molecular weight from 517 to 935000 Daltons, and contain from 4 to 4096 terminal amines.



Figure 1. Ball-and-stick molecular models of G0, G1, G2, G3, G4, and G6 dendrimers, with the dendrimer diameter (as measured by size exclusion chromatography) listed below.

In many ways, starburst dendrimers resemble globular proteins more than they do linear high polymers. First, like proteins found in nature, and in contrast to synthetic high polymers, stepwise synthesis of the dendrimer leads to well-defined composition, topology, and uniform molecular weight. Second, dendrimers are much more compact than a linear chain. In fact, at very high generations (ca. generation 10 and above for PAMAM dendrimers), uniform dendrimer growth becomes impossible due to the close packing of the branches. Since dendrimer volume grows roughly exponentially with generation, while the radius can grow only linearly, a limiting generation exists for each dendrimer chemistry - the so-called deGennes dense packing limit.³

DNA

Because of their well-controlled molecular properties and low toxicity, PAMAM starburst dendrimers have been attractive polymers for potential biomedical applications. In particular, higher generation PAMAM starburst dendrimers have shown extraordinary efficacy as vectors for the transfection of DNA into mammalian cells.⁴⁻⁸ Some of this efficacy is probably due to the ability of the polycationic dendrimer to form a tight, charge-neutralized complex with polyanionic DNA, since neutral molecules are better able to permeate the lipid membranes that surround cells. However, additional factors must be important, since starburst dendrimers are much more effective at DNA transfection than linear polymers, such as polylysine, and are more effective than hyperbranched polyethyleneimine.⁸ Moreover, simply neutralizing the charge on a macromolecule is not sufficient for membrane permeation, since neutral, hydrophilic polymers such as dextran or polyethyleneoxide are not membrane permeant.

Several unique properties of starburst dendrimers and their complexes with DNA may be important for transfection, and these properties need to be elucidated. These include:

(1) Packing of DNA. Dendrimers of generation 6 and higher possess sizes as large as the eukaryotic DNA packing proteins, the histones.² It is possible that dendrimers serve as templates which condense DNA into a structure that is more readily transported across biological membranes.

(2) Membrane binding. As discussed below, the putative pathway for cellular entry of dendrimer-DNA complexes is by entrapment into vesicles that originate as invaginations from the cell surface. However, it has not been definitively established whether the entrapped complexes are first bound to the cell surface, or are simply captured in the fluid that is taken into the forming vesicle. The binding of dendrimers and dendrimer-DNA complexes to lipid membranes may depend on the membrane composition and the stoichiometry of the complexes.

(3) Titration properties. DNA transfection by dendrimers is thought to proceed via the so-called endocytic pathway.⁸ In this process, the cell membrane surface forms an invagination which pinches off from the extracellular medium, forming a lipid vesicle within the cellular cytoplasm (Figure 2.) This "endosomal vesicle" entraps some of the extracellular fluid, as well as any membrane-bound molecules; dendrimer-DNA complexes may be in solution or membrane adherent. Once inside the cytoplasm, the endosomal vesicle is actively acidified by proton-pumping enzymes and anion channels in the endosome membrane. If the pH in the endosome is unusually well-buffered, then acidification can result in a large osmotic imbalance ($\Delta\pi$) caused by the large influx of H^+ and anions. Weak bases, which concentrate in endosomes and act as pH-buffers, can cause endosomal rupture by this mechanism.⁹ Haensler and Szoka⁸ have proposed that dendrimers act similarly, with the physiologically relevant buffering capacity provided by the internal, tertiary

amines. In support of this hypothesis, hyperbranched poly(ethyleneimine) is also very effective for transfection.

(4) Membrane Disruption. Cell membranes are composed of a mixture of lipids and proteins, and carry a substantial negative surface charge on glycosylated proteins and acidic lipids. The maintenance of the bilayer structure and integrity may require that these molecules are well-mixed.¹⁰ The adsorption of a polycationic dendrimer on a membrane may result in lateral phase separation¹¹ and destabilization.

(5) DNA Release. The efficacy of a transfection vector may depend not only on its ability to transport DNA across cell membranes, but also on the accessibility of the DNA once inside the cell. Since cell membranes are anionic, they may compete with DNA for dendrimer binding. In principle, such competition could result in partial or total liberation of DNA from DNA-dendrimer complexes, freeing the DNA to integrate into the host genome.

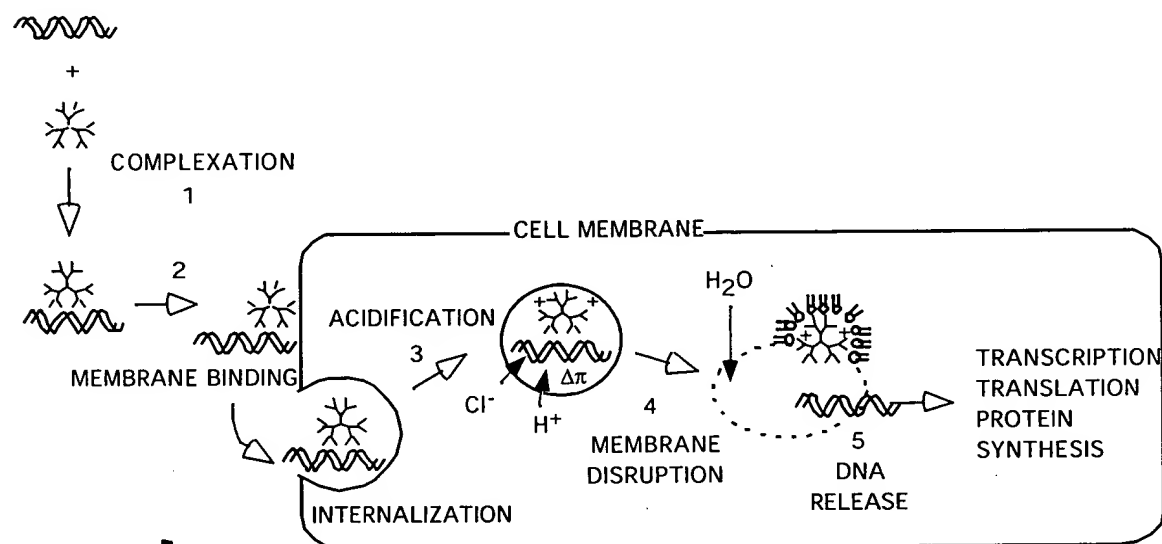


Figure 2. Putative pathway for dendrimer-mediated transfection.

Research is proposed herein which will examine in detail the interactions between polyamidoamine dendrimers, DNA, and phospholipid bilayer membranes. These interactions are an integral part of a current working hypothesis of the mechanism of dendrimer-mediated transfection, Figure 2. The research is aimed at understanding the physicochemical factors that are relevant to the exceptional efficacy of dendrimer-mediated transfection. These factors will be studied by systematic variation of the molecular components: DNA length and sequence, dendrimer generation, and membrane composition.

Research Objectives and Methods

Motivated by the success of starburst dendrimers in promoting DNA transfection,^{4, 7, 8} we propose research that will lead to an improved understanding of how these dendrimers interact with both polynucleic acids and biomimetic membranes. The research is organized around the working hypothesis presented in Figure 2; the physical chemistry of each step will be studied in appropriate model systems. DNA complexation (Step 1) will be studied to determine systematically the roles of DNA sequence and length, and dendrimer generation, in the formation of complexes. Membrane binding (Step 2) by dendrimers and dendrimer/DNA complexes will be characterized, using phospholipid vesicles with simple compositions, designed to mimic important properties of biological membranes. Titration of dendrimer, dendrimer/DNA, and dendrimer/DNA/vesicle systems will be used to verify the buffering capabilities of these complexes in the relevant pH range (Step 3). The ability of dendrimers and DNA/dendrimer complexes to disrupt lipid vesicles, and to sensitize vesicles to osmotic stress, will be determined (Step 4). Finally, the competition between the binding to anionic membranes and anionic DNA will be explored, to determine if this is a plausible mechanism for release of DNA to the cellular cytosol (Step 5), and to explore whether stoichiometric dendrimer-lipid complexes can be formed. Such complexes could prove useful for drug delivery and controlled release applications.

The research proposed herein will quantitatively characterize these molecular interactions, focusing on changes in structure, supramolecular organization, solution properties, and to the extent possible, dynamics. The work proposed is important in order to better understand the mechanisms of dendrimer facilitated DNA delivery, and will be important in the further design of transfection agents and drug delivery formulations with PAMAM dendrimers.

Specific objectives of the research are

- (1) To systematically determine the association parameters (binding constants, off-rates, enthalpy) of the binding of a series of starburst dendrimers (generation 1 to generation 10) to polynucleic acids. Double stranded DNA, single stranded DNA, and short DNA fragments will all be examined. pH and temperature effects will also be examined.
- (2) To determine the accessibility of DNA in DNA/dendrimer complexes to a variety of fluorescent probes that are known to bind free DNA. The accessibility of the DNA may correlate with its ability to integrate into a host genome; moreover, accessibility can provide an estimate of ease or difficulty with which dendrimers can be displaced from the polynucleotide.
- (3) To determine the ability of anionic lipids to release DNA from bound dendrimers.
- (4) To determine the extent of adsorption of dendrimers onto lipid membranes of varying composition.
- (5) To identify membrane compositions that are responsive to the adsorption of dendrimers, either through permeabilization, or weakening to osmotic stress.

(6) To construct polyelectrolyte-surfactant complexes of dendrimers and anionic lipids.

The principal methods to examine the structures and dynamic characteristics of these complexes will be fluorescence spectroscopy and electron spin resonance (ESR). Circular dichroism spectroscopy, X-ray diffraction, and quasielastic light scattering will be used for further structural characterization in some instances. Fluorescence spectroscopy is a highly sensitive probe for molecular environment. By using quenching and energy transfer techniques, fluorescence has been used to examine molecular conformations, biomolecule binding, lipid vesicle permeabilization and fusion, and mobility of molecules adsorbed or incorporated into lipid vesicles.¹² ESR techniques provide complementary and corroborating data, by yielding information on short-range diffusion (through τ_c , the correlation time), environmental polarity (through the hyperfine coupling constant, A), and probe density (through the spin exchange frequency, ω).¹³ The PI will have direct access to a Bruker ESP-300/380 and a Bruker ER 100D X-band spectrometer on the Columbia campus, in the laboratory of Professor Nicholas Turro.

The ready availability of all polyamidoamine dendrimers from G0 through G10 (kindly provided by Professor D. Tomalia) provides a unique opportunity to *systematically* vary the three molecular constituents of these supramolecular complexes, and to thereby ascertain the role of each constituent in the properties of the complexes. DNA length and sequence will be varied. Some sequences, most notably poly(A)-poly(T) and poly(G)-poly(C), are unable to wrap around histone proteins to form nucleosomal core particles,^{14, 15} presumably owing to their increased rigidity compared with alternating or varied sequences. These homopolymers may also exhibit reduced affinity for dendrimers. Dendrimer generation will be varied, and pH will be used to control the degree of dendrimer ionization and the nature of the charged groups. (At lower pH, the "internal" tertiary amines can become protonated.⁸) Membrane properties will be varied by incorporating differing amounts of anionic lipids, and by including lipids with different phase preferences.

Preliminary Results

Fluorescence Probes of DNA/Dendrimer Interactions

Preliminary results addressing several of the specific objectives have been obtained, and are presented here. To explore the binding of dendrimers to DNA, and the DNA accessibility, the fluorescent dye ethidium bromide (EtBr, Figure 9) was allowed to bind to DNA in the presence and absence of starburst dendrimers of generation 2 (G2) and generation 7 (G7). Ethidium binds to DNA by intercalating between bases.¹⁶ Intercalated ethidium has a 20-30 fold fluorescence increase over ethidium in solution, a red-shifted excitation maximum, and a blue-shifted emission maximum.¹⁷ The ethidium fluorescence enhancement on binding to DNA can be used to measure the amount of bound and free ethidium. A Scatchard plot is then used to estimate the binding constant for ethidium binding to DNA, Figure 3. In the presence of G2 or G7 dendrimers, the

binding of ethidium was weakened, as evidenced by the diminished slopes of the the Scatchard plots. Remarkably, even at very high ethidium concentrations some of the DNA remained inaccessible when dendrimers were present - i.e., the ethidium fluorescence enhancement in the presence of dendrimers was significantly reduced, even at very high ethidium concentrations, where one might expect that ethidium could displace bound dendrimers.

To summarize, we have observed two effects of dendrimers on ethidium binding: first, an overall weakening of ethidium binding, and second, complete inhibition of ethidium binding to a fraction of the available sites. The presence of both effects suggests that dendrimers may have two (or more) "modes" of DNA binding, one of which is much tighter than ethidium-DNA binding.

It is also possible that the same dendrimer molecule may shield some sites strongly, and others weakly. This could occur if the dendrimer has different affinities for different sequences on calf thymus DNA; for example, the affinity could be higher for the some sequences, which might be better able to "wrap" around a dendrimer, in a manner similar to the way in which DNA wraps

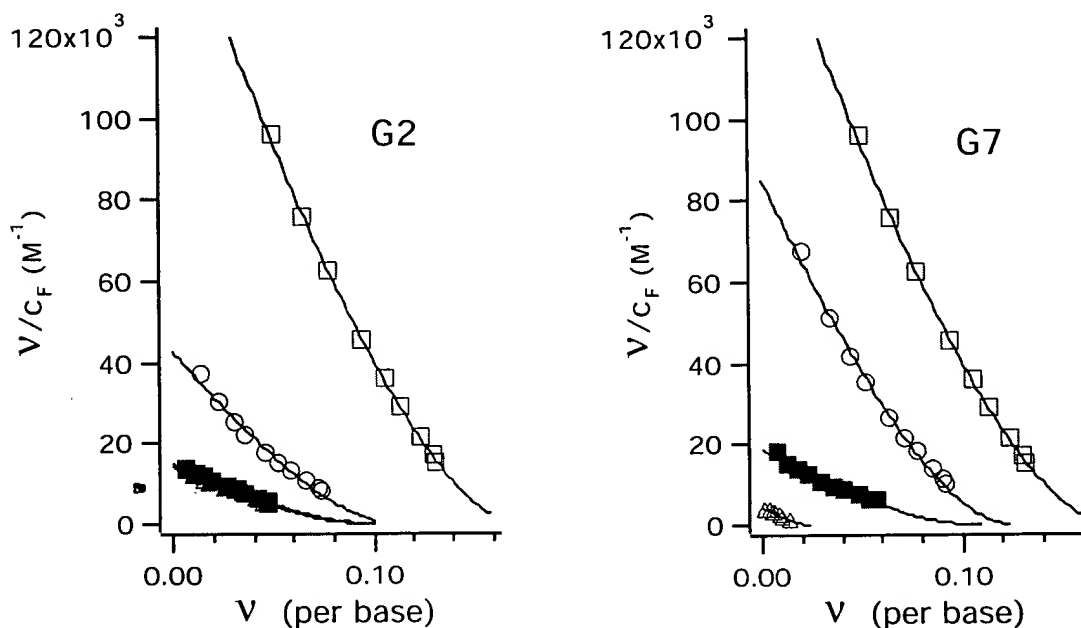


Figure 3. Scatchard plot of the binding of EtBr to calf thymus DNA in the presence and absence of polyamidoamine dendrimers of generation 2 (left) and 7 (right). v is the ratio of bound dye to the number of bases, C_F is the free dye concentration. Symbols represent different amounts of added dendrimer, given as equivalents (1° amine:DNA phosphate): □, no dendrimer; ○, 0.5 equivalents; ■, 1 equivalent; Δ, 2 equivalents. The curves were fit using the excluded site model of McGhee and von Hippel¹⁸. Dendrimers reduce the affinity of some sites for ethidium binding, as evidenced by the reduced slope, but also completely block other sites, as shown by a reduced x-intercept.¹⁹ (The x-intercept represents the maximal ethidium binding; i.e., that achieved at infinite C_F .)

around histone complexes. Different behavior of different intercalation sites on the DNA could also arise from interactions of different parts *of the same dendrimer* with the DNA. Some part of the DNA may be buried within the "core" of the dendrimer, and therefore entirely inaccessible. Further experiments (using higher affinity intercalating dyes, *vide infra*) will be needed to evaluate and discriminate between these possibilities.

It is interesting to compare our results on the accessibility of DNA to ethidium with the effects of dendrimers on transcription and transcriptional initiation, as observed by Bielinska, et al.²⁰ They found that these dendrimers strongly inhibited initiation, which requires the binding of RNA polymerase, but *not* transcriptional elongation, in which the polymerase undergoes translational motion along the DNA strand. This supports our observation that dendrimers can be very difficult to displace from DNA, but also raises the intriguing possibility that dendrimers may be rather easily displaced *along* the DNA polymer, as would be required for effective transcription.

DNA/nucleosome (histone) complexes bind ethidium weakly, but highly cooperatively. In other words, the binding of ethidium becomes progressively stronger after the first few ethidium molecules have bound.²¹ This apparent cooperativity is thought to arise from the progressive dissociation of the DNA from the nucleosome. The first few ethidium molecules disrupt the conformation of the DNA so that binding to the histone complex is weakened; subsequent molecules of ethidium can then bind more easily to the liberated sites on the DNA. The lack of apparent cooperativity in ethidium binding to DNA/dendrimer complexes that we have observed may indicate that ethidium-induced conformational changes in DNA do not liberate high-affinity binding sites on the DNA.

ESR

ESR measurements of the interactions of dendrimers and dimyristoyl phosphatidylcholine (DMPC, Figure 4) liposomes have been carried out in collaboration with Professor M.F. Ottaviani of the University of Florence, one of the world's experts on the use of ESR techniques to study supramolecular structures involving dendrimers. ESR work proposed herein will also be performed in collaboration with Professor Ottaviani.

Polyamidoamine dendrimers are easily labelled with spin probes (e.g. iodoacetamido-TEMPO, Figure 5) by coupling to a small fraction of the terminal amines. G6 dendrimers were labelled at ca. 3% of their terminal amines with TEMPO, and the ESR spectra for the dendrimers in the presence and absence of DMPC vesicles, Figure 6. The ESR spectra were then fit by the procedure of Schneider and Freed;¹³ the fit curves are shown as dashed lines. The spectrum in the presence of the vesicles was fit with two components; the data indicate that the vesicles provide a probe

environment that is less polar and slightly more viscous than when the dendrimer is in a pure aqueous phase. These results are especially exciting, since strong interactions between the cationic dendrimer and these zwitterionic membranes were not expected. Nonetheless, there is clear evidence for some interaction, perhaps mediated through the interaction of the phosphate group with the terminal amines of the dendrimer.

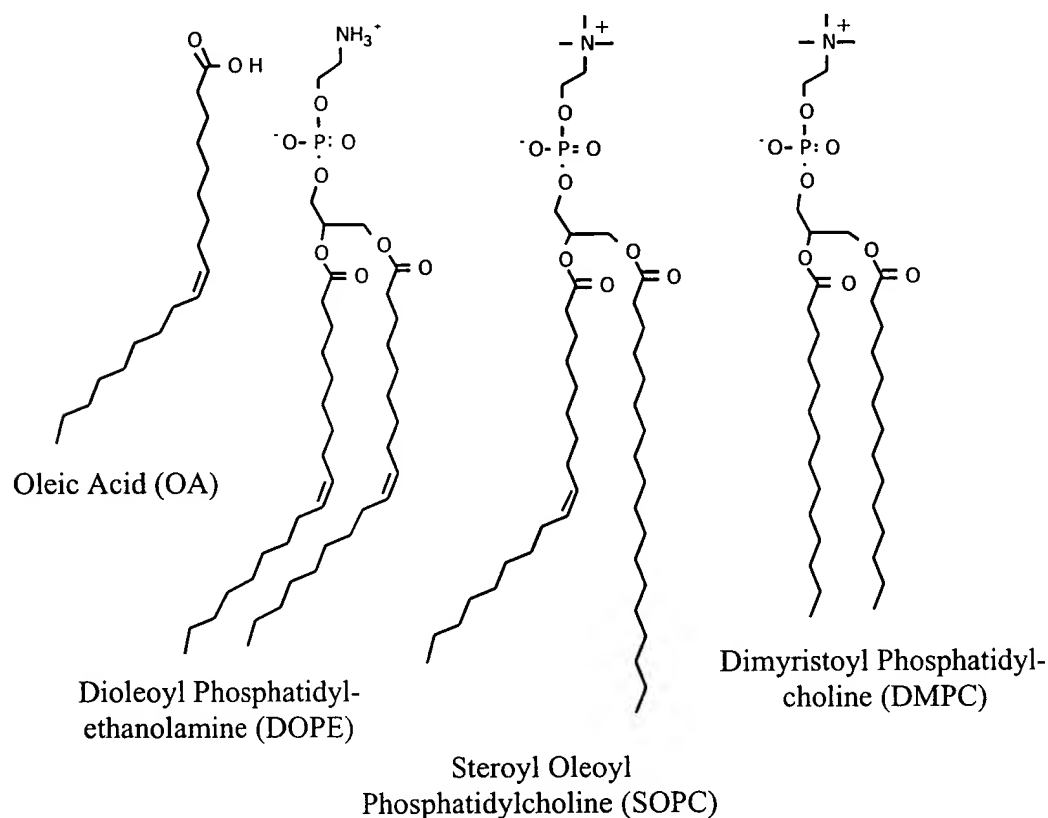


Figure 4. Structures of lipids used for model membranes in this proposal.

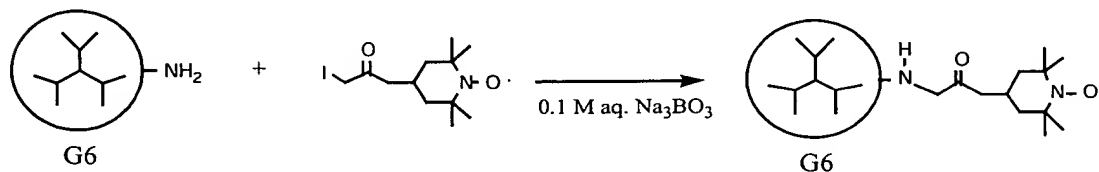


Figure 5 Spin labelling of starburst dendrimers.

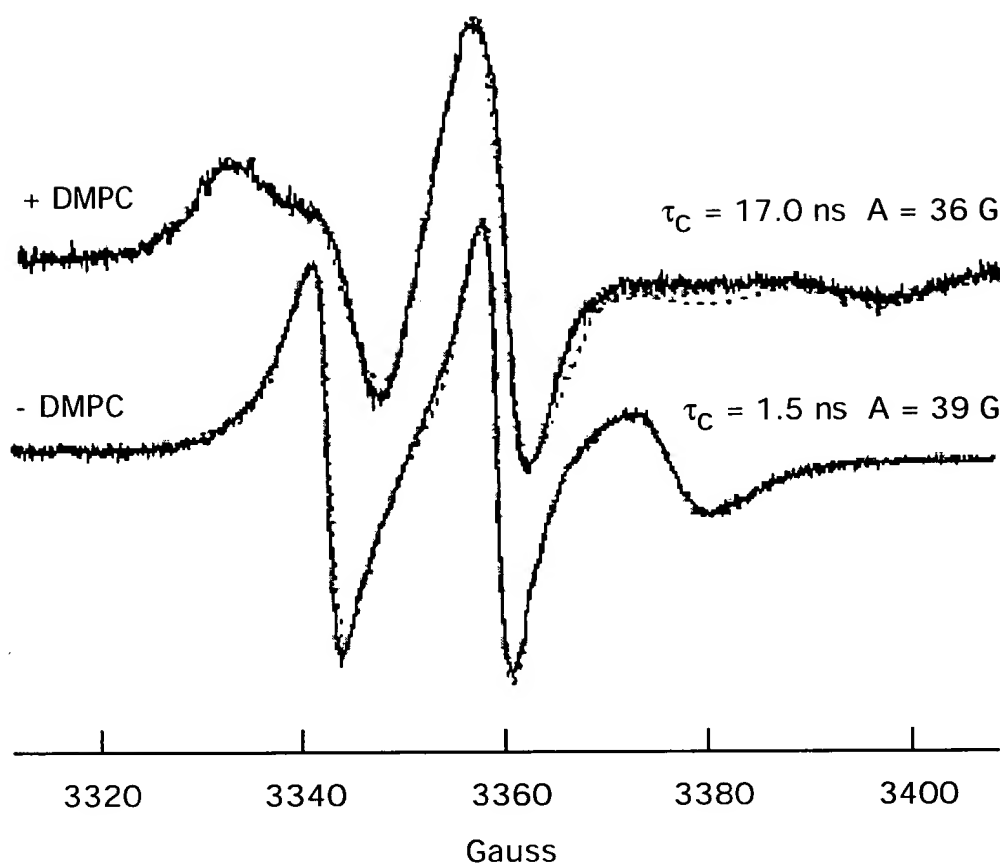


Figure 6. ESR spectra of spin labelled G6 dendrimers in the presence (top) and absence (bottom) of DMPC vesicles. The best fits to the spectra are shown as dashed lines, using the procedure of Schneider and Freed.¹³ The $m=\pm 1$ peaks have a dramatically altered lineshape, which is interpreted as a less polar probe environment and a slower probe correlation time.

Membrane Disruption

We have found that PAMAM dendrimers are able to affect the permeability properties of small vesicles containing an entrapped fluorescent dye, as indicated by the following results. Liposomes containing 60 mM calcein (Figure 11) were formed from different lipid compositions, and external dye was removed using a Sepharose 4B-200 gel column (4x1 cm dia). At moderate concentrations, calcein excitation energy is dissipated non-radiatively, due to interactions between a fluorophore in its excited state and nearby ground-state dye molecules. This "self-quenching" is quite efficient at 60 mM, so that the calcein dye entrapped in the interior of the vesicles shows very little fluorescence. If the local calcein concentration is reduced, for example by leakage from a dilute

sample of calcein-containing liposomes, the dye is diluted and the fluorescence increases dramatically. Thus, the intensity of fluorescence is a simple probe of the breakdown of the vesicle membrane. Liposomes composed of egg phosphatidylcholine (predominantly steroyl-oleoyl and palmitoyl-oleoyl fatty acid composition) and liposomes of dioleoyl phosphatidylethanolamine and oleic acid have been used in preliminary studies, Figure 4. Again, in these studies with a fluorescent probe, some evidence for an interaction between dendrimers and the zwitterionic phosphatidylcholine was found, since phosphatidylcholine liposomes were actually slightly stabilized in the presence of dendrimer. Untreated PC liposomes lost about 15% of the entrapped dye over a 30 hour period whereas dendrimer-treated PC liposomes lost less than 5% of the entrapped calcein. This effect may be due to a slight strengthening of the liposome by a peripheral adsorption of dendrimer, or to decreased liposome-liposome contact from charge repulsion or steric interactions of adsorbed dendrimer. (Covalently attached polyethylene glycol also stabilizes liposomes, perhaps due to reduced liposome-liposome contact.^{22, 23})

More dramatic are the results obtained with the DOPE/OA liposomes. This combination was chosen because (1) strong Coulomb interactions between anionic oleate (at neutral and alkaline pH) and the polycationic dendrimer were expected, and (2) DOPE, by itself, does not form stable bilayers.^{24, 25} Lipids which prefer non-lamellar phases are a significant constituent of biological membranes, and the stability of membranes may depend on the proper mixing of these non-lamellar lipids with other, stabilizing species.¹⁰ As expected, addition of dendrimers causes a sudden and dramatic leakage of calcein from these liposomes, Figure 7.

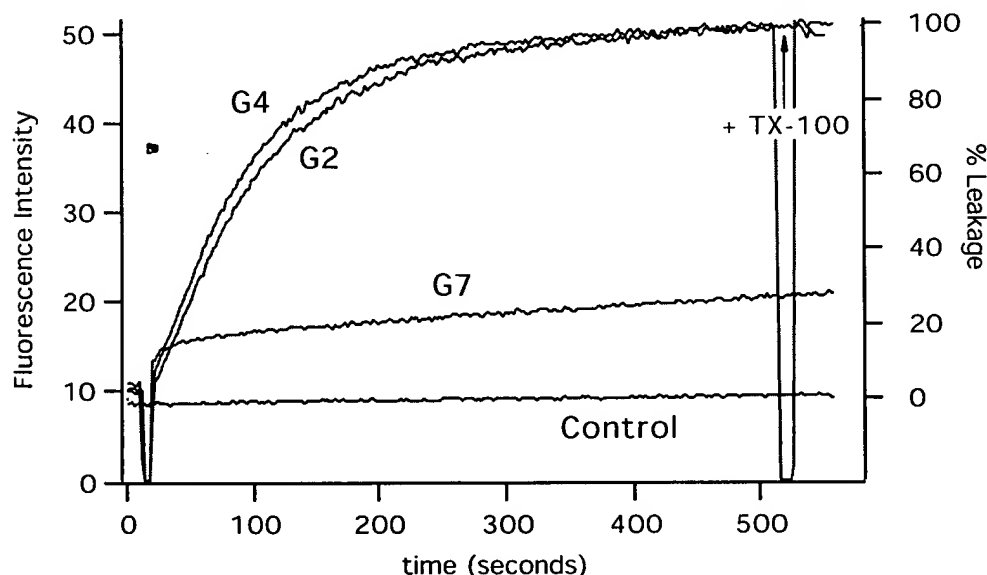


Figure 7. G2 and G4 dendrimers at 0.1 g/L cause rapid and complete leakage of calcein from DOPE/PE liposomes; G7, at the same weight concentration, causes a slower leakage.

Proposed Research

An investigation of the important physicochemical processes underlying dendrimer-based DNA transfection (Figure 2) is proposed herein. The processes of dendrimer-DNA complexation, membrane binding, and membrane disruption will be studied by systematically varying dendrimer generation and ionization, DNA length and composition, and membrane composition.

Characterization of binding constants and off-rates of dendrimers with DNA vs. temperature, pH, ionic strength.



As discussed in the introduction, the first step in dendrimer-mediated transfection is the formation of a dendrimer-DNA complex. Although these complexes have been examined by electron microscopy,^{6, 7} little work has been done characterizing the physical chemistry of their formation and their nanoscopic structure. Measurements of binding constants and off-rates, when studied by systematically varying the DNA composition and dendrimer generation, will provide insight into the mechanism of complex formation.

In addition to the ethidium competition assays that have already been performed, a direct measurement of the binding of dendrimers to calf thymus DNA will be done. Ideally, binding measurements can be made by observing the change in a spectroscopic property as the concentration of dendrimers is changed.²⁶ We propose to study the ESR spectra of labeled dendrimers interacting with DNA; the spectral changes on binding may permit an estimate of binding constants.

To corroborate results from ESR spectroscopy, we will prepare fluorescently-labeled DNA that can be used in a direct binding assay, i.e. an assay in which DNA-dendrimer complexes are separated from unbound dendrimers or unbound DNA, either by dialysis or filtration. DNA fragments can be fluorescently labelled on phosphate termini with "kits" available commercially from Molecular Probes, Inc. (Eugene, OR) to produce phosphoramidate adducts. The fluorescent moiety will be Bodipy-TR, which has an absorption maximum at 588 nm. Using a dye in the far

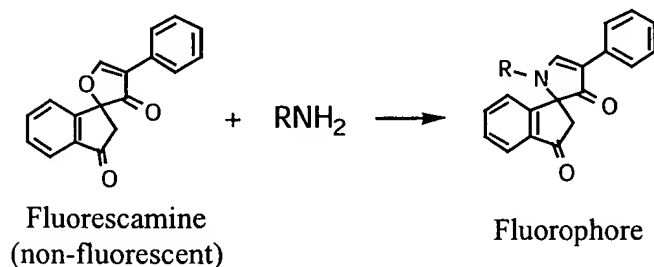


Figure 8. Reaction of fluorescamine with primary amines produces a fluorescent product. From Udenfriend et al.²⁷

red allows the use of a fluorescence assay for amines without interference or energy transfer.

Equilibrium dialysis and ultrafiltration measurements of the binding of G1- G10 dendrimers to calf thymus DNA will be performed. The dialyzate and dialyzing solution

will be analyzed for dendrimer content by a fluorescamine assay²⁷ (Figure 8) and for labelled DNA by fluorescence. (By correcting for scattering background, DNA concentration may also be estimated by UV absorption.) By studying binding at several temperatures, a van't Hoff analysis will determine the entropic and enthalpic contributions to the binding free energy.²⁸ Finally, the ionic strength and pH will be varied to measure the binding under conditions that mimic extracellular, endosomal, and intracellular compartments.

Binding constants will provide insight into the strength and nature of the bound complex. In particular, the entropy change on binding may be unusually large (and negative) if numerous *mobile* branches of the dendrimer each bind to the DNA. If the dendrimer branches are rather immobile in the free dendrimer, then a smaller reduction in entropy would be expected on binding. In studies of thermodynamics of dendrimer binding, special emphasis will be placed on the effect of dendrimer generation, since the packing and mobility of the dendrimer branches is known to depend sharply on generation number. A sharp increase in transfection efficiency has been noted as generation number increases, and the dendrimer binding of several photoluminescent probes shows an abrupt onset at generation 4.²⁹

The binding strength and structures of complexes of dendrimers and polynucleic acids may vary with the length and the sequence of the nucleotide chain. To understand the roles played by these factors, we will study the binding of dendrimers to short DNA fragments, and to specific DNA sequences. The binding to DNA fragments cannot be measured by dialysis, since the fragments and the dendrimers will be of similar size. A nitrocellulose filter assay³⁰ will be used to measure the affinities of dendrimers for DNA fragments. In this assay, uncomplexed DNA is free to pass through the filter, while complexed DNA is retained. DNA fragment ladders, consisting of either 2, 50, or 123 bp increments, are commercially available (Sigma Chemical Company, St. Louis, MO).

Preliminary observations with ethidium bromide labeled DNA have suggested very tight binding in the dendrimer-DNA complex, as indicated by the inability of ethidium bromide to bind to all sites. Such binding could result from a "wrapping" of the DNA around the dendrimer, much as DNA is wrapped around a nucleosome. A study of the affinities of DNA fragments can help confirm such a binding model, since the model predicts increasing affinity up to DNA lengths at least as large as the dendrimer circumference, ca. 120 base pairs for G7. If the DNA is not bent by its interaction with the dendrimer, then fragments longer than the dendrimer diameter (equivalent to about 40 base pairs) should show saturation in their binding affinity. Other differences distinguish "wrapping" models from more linear binding conformations: the former mechanism should produce a composition-dependent binding. For example, neither poly(dA)poly(dT) nor poly(dG)poly(dC) DNA can be reconstituted into nucleosome core particles.¹⁵ These sequences form helices that cannot flex enough to wrap around histones. In contrast, mixed sequence DNA

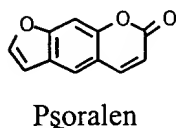
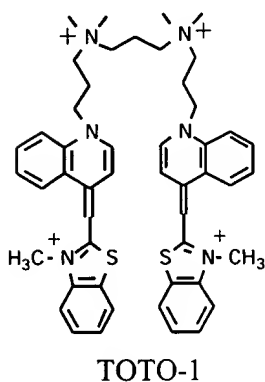
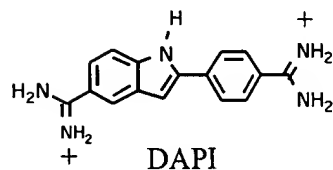
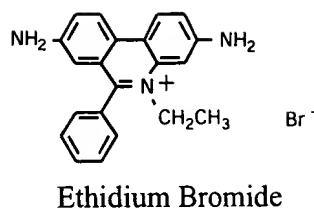


Figure 9. Fluorescent probes of DNA.

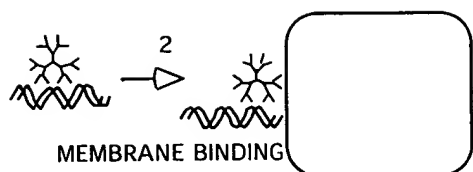
has greater flexural freedom. (This is not to say that it has a shorter persistence length. Curvature of DNA in nucleosomes is high compared with DNA persistence lengths, typically 150 nm, so that sequence-dependent DNA curvature is thought to facilitate nucleosome formation.³¹) We propose to study the sequence-dependent binding properties of dendrimers, using commercially available DNA polymers of pure or alternating sequence. A summary of the proposed systematic variation of the DNA composition and length is presented in Figure 10, as one of the three components (dendrimer, DNA, membrane) that will be controlled.

Additional and corroborative studies on dendrimer/DNA binding will be undertaken using the spin-labeled dendrimers. Complexation of the dendrimers with DNA is expected to change the correlation time and polarity of the spin label, and a two-component analysis of the ESR spectra may be used to estimate bound and unbound fractions.

Accessibility of DNA complexed to Dendrimers.

A variety of probes of nucleic acid structure are commercially available from Molecular Probes, Inc., (Eugene, OR), Figure 9. These include both cationic and neutral probes that exhibit a variety of different binding modes. Dicationic DAPI (4'-6-diamidino-2-phenylindole) binds in the minor groove with a 20-fold fluorescence enhancement, compared to its emission in an aqueous environment. The dimeric cyanine dye TOTO-1 has a much higher affinity for DNA than ethidium ($>> 1.5 \times 10^5 \text{ M}^{-1}$) and shows a 100-1000 fold fluorescence enhancement on binding;

it will be interesting to explore whether dendrimers can prevent TOTO-1 binding, as they do with ethidium. Psoralen (furocoumarin) is quenched when intercalated into DNA, but is neutral, rather than cationic. Studies of competition between dendrimers and psoralen will determine the role of charge in the screening of DNA by dendrimers.



Adsorption of Dendrimers to Lipid Membranes, and Membrane Destabilization.

Although osmotic effects may be important in dendrimer-DNA release from endosomes, it is likely that direct dendrimer-lipid interactions are important. The binding of dendrimers (and their complexes with DNA) to membranes would result in a greater cellular uptake of the complexes via the endocytic pathway, while perturbation of the membrane by PAMAM dendrimers could destabilize or even permeabilize the endosomal membrane and allow DNA permeation to the cytoplasm.

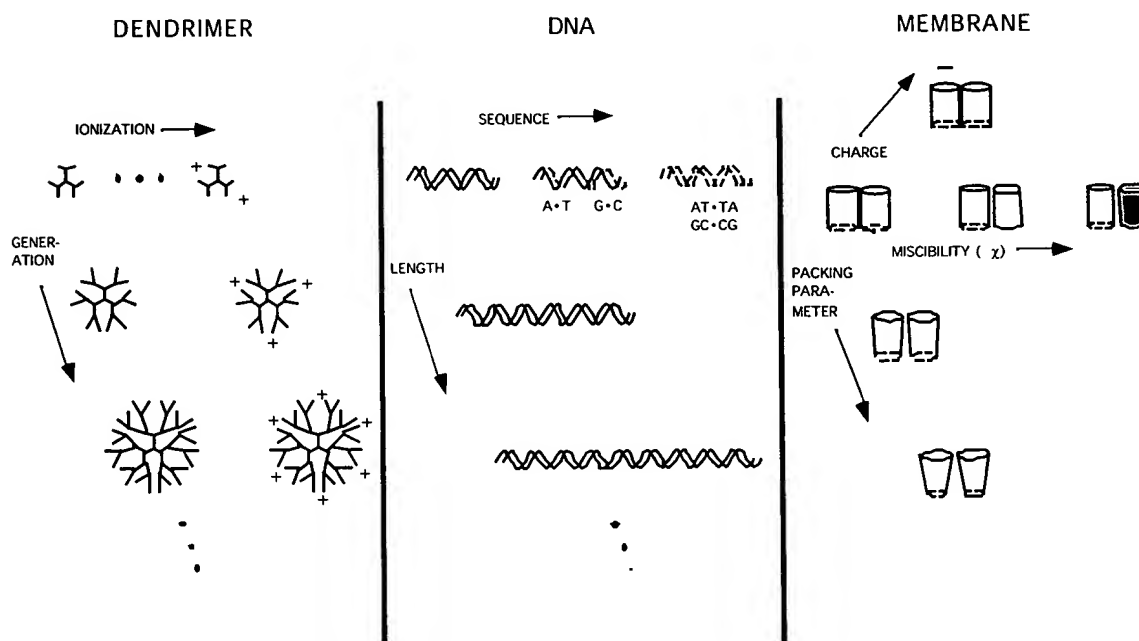


Figure 10. Systematic variation of the three components in dendrimer/DNA/membrane complexes. The effects of dendrimer size (generation) and ionization will be studied, as will DNA length and sequence, and membrane lipid shape, charge, and lateral miscibility (in two component membranes).

To explore these roles for PAMAM dendrimers in transfection, we will measure the adsorption of dendrimers to large unilamellar lipid vesicles of varying composition, using the centrifugation assay developed by Ben-Tal and McLaughlin.³² Liposomes are prepared by extrusion of an aqueous lipid suspension through polycarbonate membranes of defined pore size, which breaks the very large multilamellar aggregates into 100 nm diameter, single wall liposomes.³³⁻³⁵ If this is done in a sucrose-containing buffer, the density of the resulting liposomes can be made high enough to render them susceptible to centrifugation (100,000 g, 1 hr) from an isoosmotic salt

The results from this direct binding assay will be compared with ESR results using spin-labelled dendrimers and membranes of the same compositions.

dendrimers? Can lipids which are more prevalent than DOPE in biological membranes, such as asymmetric chain steroyl-oleoyl and palmitoyl-oleoyl phosphatidyl-ethanolamines, also yield dendrimer-responsive membranes? Is it important that the membrane component with the packing parameter < 1 (oleic acid in our preliminary work) be the component that is (putatively) aggregated by the dendrimer, or does the aggregation of either component result in membrane destabilization? Moreover, if a charge-induced lateral phase separation is critical for the destabilization of these membranes, any stabilizing anionic lipid should be able to substitute for the oleate anion, while a neutral stabilizing lipid should result in a loss of responsiveness. Additionally, lipid mixtures that are closer to spontaneous phase separation (due to differing acyl chain compositions, for example) should be more easily disrupted. The principal goal of this work is to systematically map out membrane compositions that are responsive to dendrimer adsorption, and to correlate

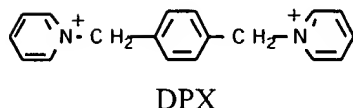


Figure 11. Fluorescent probes of membrane permeabilization.

those compositions with the simple physical parameters characterizing the membrane. The compositions and the parameters will then be compared with those found in cell membranes and endosomes.

In addition to studying dendrimer-lipid binding, we will also investigate the dendrimer induced leakage of entrapped aqueous fluorophores, including calcein, and ANTS / DPX, Figure 11. ANTS / DPX can be used to examine the mechanism of leakage (i.e. all-or-none leakage from a few vesicles vs. slow permeation of the vesicle population) by the method of "fluorescence requenching"³⁸ Briefly, the ANTS fluorophore is quenched by DPX, when both are entrapped in vesicles. When a fluorescence increase is observed, it may be due to leakage of ANTS, DPX, or both. Back addition of the quencher can be used to determine, indirectly, the extent to which dye molecules *remaining inside vesicles* are still quenched. If the quenching of dye remaining inside vesicles is unchanged, then release can only be all-or-none; if the dye remaining in the vesicles is progressively less quenched, the release is graded, Figure 12.

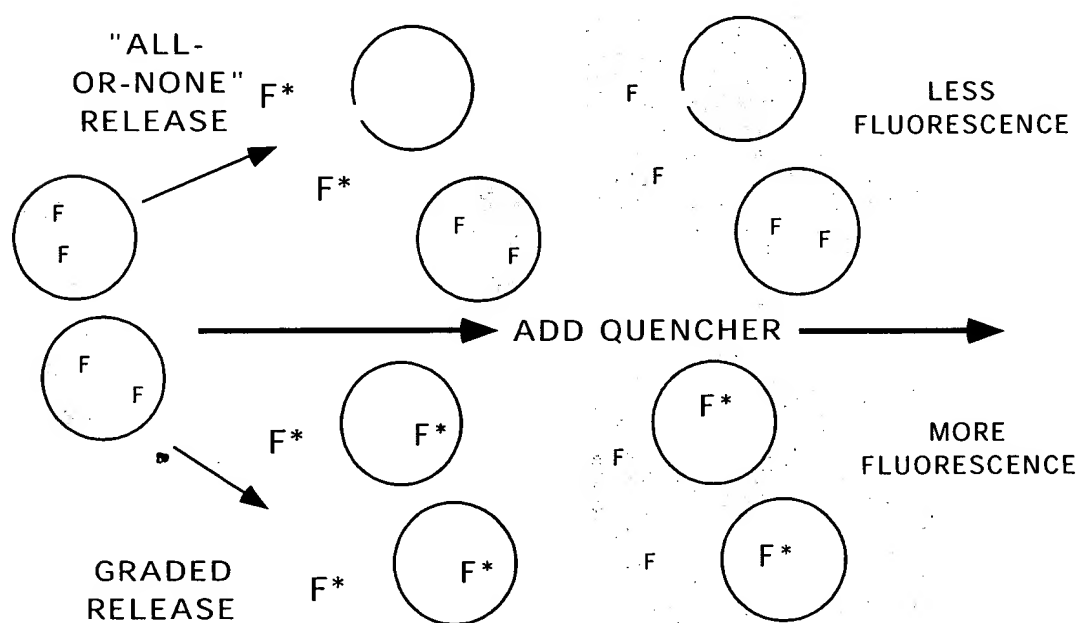
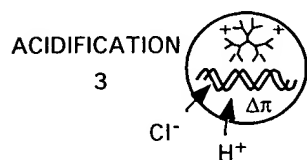


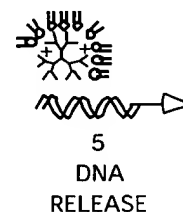
Figure 12. Fluorescence requenching. By adding additional quencher (dots) after leakage has occurred, the fluorescence of the dye (F) that remains entrapped can be determined. When release of quencher is graded, the fluorescence of the entrapped dye increases. (Note that the requenching measurement must be made quickly, since the added quencher will eventually permeate into the liposomes and quench the entrapped as well as the free dye.)

Since there is reason to expect that osmotic forces play a role in endosomal destabilization in DNA/dendrimer complexes, these leakage experiments will also be conducted in hypo-osmotic media.³⁹ Hypoosmotic conditions cause liposome swelling and increase membrane tension.



Titration of PAMAM dendrimers and dendrimer / DNA complexes

Titration measurements will be performed on free dendrimers and on dendrimers bound to DNA. Titration of polyelectrolytes is a classic method for observing conformational transitions. The principle is straightforward: since pK_a depends on the presence of nearby charged groups, conformational transitions affect pK_a . In polymeric systems, pK_a varies with α , the fractional ionization of the polymer. Titration measurements will determine the buffering capacity of dendrimer / DNA complexes throughout the full range of pH, including the physiologically relevant range of pH 7.4 (extracellular) to pH 5.0 (endosomal).



Liberation of DNA from dendrimers by anionic lipids

An important issue in DNA transfection is the availability of the DNA, once inside the cell, for integration into the genome or binding to antisense message. DNA could become more available if dendrimer carrier molecules were stripped from the DNA by interactions with anionic lipids that are commonplace in cell membranes. The preliminary experiments on the accessibility of calf thymus DNA to ethidium will be extended to include anionic lipid vesicle preparations, consisting of phosphatidylcholine or phosphatidylethanolamine with increasing mole fractions of phosphatidylglycerol. In addition, we will attach a nitroxide spin label to DNA fragments. The spin label is expected to show reduced mobility when dendrimers are bound to the DNA; competitive removal of the bound dendrimer can be monitored by recovered mobility in the presence of anionic vesicles.

Lipid-Dendrimer Complexes

Dendritic polymers may serve as key building blocks in the construction of novel supramolecular assemblies with useful biomedical or material properties. Dendrimers with alkyl chain termini have been designed that self-assemble to form a well ordered, liquid crystalline cubic phase.⁴⁰ Well-defined supramolecular assemblies of dendrimers and surfactants may prove especially useful in biomedical applications, where uniformity is especially important. To explore the possibility of synthesizing new dendrimer-lipid assemblies, we will use established techniques in polyelectrolyte-surfactant complex formation and apply them to polyamidoamine dendritic polymers. In particular, dendrimers will be complexed with anionic surfactants and lipids in a 1:1 stoichiometry at low ionic strength. This procedure usually causes precipitation of the polyion-surfactant complex.⁴¹ To facilitate the formation of a well-packed lipid monolayer around the dendrimer, we will study H_{II} phase lipids, such as dioleoylphosphatidic acid.⁴² The structures of these complexes will be studied by small angle and wide angle X-ray diffraction, which will identify regular morphologies (e.g. hexagonal close packing, if present) and repeat dimensions.⁴³ Finally, mixtures of lipids will be used to develop "bilayer-coated" starburst dendrimers. These constructs should be rugged and resistant to osmotic stress, owing to their small size compared to liposomes; they may also exhibit novel properties for entrapment of aqueous solutes.

Summary

The research proposed herein will contribute to our understanding of an architecturally novel class of molecules, the polyamidoamine dendrimers. The research will focus on the study of the supramolecular complexes formed by dendrimers and DNA, and dendrimers and lipid bilayer membranes. These complexes are surely important in the biomedical application of dendrimers to DNA transfection, but the proposed research is fundamental in nature, and will lead to an improved understanding of the properties of these novel materials.

References

1. Tomalia, D. A. and P. R. Dvornic. 1996. Dendritic polymers: divergent synthesis. *In* Polymeric Materials Encyclopedia. J. C. Salamone, Ed. CRC Press, Boca Raton. 1814-1830.
2. Tomalia, D., A. Naylor and W. I. Goddard. 1990. Starburst dendrimers: molecular level control of size, shape, surface chemistry, and flexibility from atoms to macroscopic matter. *Angew. Chem. Int. Ed. Engl.* 29:138-175.
3. deGennes, P. G. and H. J. Hervet. 1983. Statistics of starburst polymers. *J. Phys. Lett. (Paris)* 44:L351-L360.
4. Bielinska, A., J. Kukowska-Latallo, L. T. Piehler, D. A. Tomalia, R. Spindler, Y. R. and J. R. J. Baker. 1995. STARBURST PAMAM dendrimers: a novel synthetic vector for the transfection of DNA into mammalian cells. *Polymeric Materials Science and Engineering* 73:273-274.

5. Boussif, O., F. Lezoualc'h, M. Zanta, M. Mergny, D. Scherman, B. Demeneix and J.-P. Behr. 1995. A versatile vector for gene and oligonucleotide transfer into cells in culture and in vivo: polyethyleneimine. *Proc. Natl. Acad. Sci. USA* 92:7297-7301.
6. Tang, M., C. Redemann and F. C. J. Szoka. 1996. In vitro gene delivery by degraded polyaminoamine dendrimers. *Bioconjugate Chem.* 7:703-714.
7. Kukowska-Latallo, J., A. Bielinska, J. Johnson, R. Spindler, D. Tomalia and J. J. Baker. 1996. Efficient transfer of genetic material into mammalian cells using Starburst polyamidoamine dendrimers. *Proc. Natl. Acad. Sci. USA* 93:4897-4902.
8. Haensler, J. and F. Szoka. 1993. Polyamidoamine cascade polymers mediate efficient transfection of cells in culture. *Bioconjugate Chem.* 4:372-379.
9. Miller, D. K., E. Griffiths, J. Lenard and R. A. Firestone. 1983. Cell killing by lysosomotropic detergents. *J. Cell Biol.* 97:1841-1851.
10. Hui, S.-W. 1997. Curvature stress and biomembrane function. *Curr. Topics Membr.* 44:541-563.
11. Raudino, A., F. Castelli and S. Gurrieri. 1990. Polymer-induced lateral phase separation in mixed lipid membranes: a theoretical model and calorimetric investigation. *J. Phys. Chem.* 94:1526-1535.
12. Lakowicz, J. R. 1983. Principles of fluorescence spectroscopy. Plenum, New York. 496 pp.
13. Schneider, D. J. and J. H. Freed. 1989. Calculating slow motional magnetic resonance spectra: A user's guide. In *Biological Magnetic Resonance. Spin Labeling. Theory and Applications*. L. J. Berliner and J. Ruben, Ed. Plenum Press, New York. 1-76.
14. Simpson, R. and P. Künzler. 1979. Chromatin and core particles from the inner histones and synthetic polydeoxyribonucleotides of defined sequence. *Nucl. Acids Res.* 6:1387-1393.
15. Nelson, H. C. M., J. Finch, B. Luisi and A. Klug. 1987. The structure of an oligo(dA)·oligo(dT) tract and its biological implications. *Nature (Lond.)* 330:221-225.
16. Waring, M. J. 1965. Complex formation between ethidium bromide and nucleic acids. *J. Mol. Biol.* 13:269-282.
17. Arndt-Jovin, D. and T. Jovin. 1989. Fluorescence labeling and microscopy of DNA. *Meth. Cell Biol.* 30:417-448.
18. McGhee, J. D. and P. H. von Hippel. 1974. Theoretical aspects of DNA-protein interactions: cooperative and non-cooperative binding of large ligands to a one-dimensional homogeneous lattice. *J. Mol. Biol.* 86:469-489.
19. LePecq, J.-B. and C. Paoletti. 1967. A fluorescent complex between ethidium bromide and nucleic acids. *J. Mol. Biol.* 27:87-106.
20. Bielinska, A., J. Kukowska-Latallo and J. Baker. 1997. The interaction of plasmid DNA with polyamidoamine dendrimers: mechanism of complex formation and analysis of alterations induced in nuclease sensitivity and transcriptional activity of the complexed DNA. *Biochim. Biophys. Acta* 1353:180-190.
21. McMurray, C. and K. E. van Holde. 1991. Binding of ethidium to the nucleosome core particle. 1. Binding and dissociation reactions. *Biochemistry* 30:5631-5643.

22. Lasic, D. D. 1994. Sterically stabilized vesicles. *Angew. Chem. Int. Ed. Engl.* 33:1685-1698.
23. Woodle, M. C. and D. D. Lasic. 1992. Sterically stabilized liposomes. *Biochim. Biophys. Acta* 1113:171-199.
24. Collins, D., J. Connor, H.-P. Ting-Beall and L. Huang. 1990. Proton and divalent cations induce synergistic but mechanistically different destabilizations of pH-sensitive liposomes composed of DOPE and oleic acid. *Chem. Phys. Lipids* 55:339-349.
25. Düzgünes, N., R. Straubinger, P. Baldwin, D. Friend and D. Papahadjopoulos. 1985. Proton-induced fusion of oleic acid-phosphatidylethanolamine liposomes. *Biochemistry* 24:3091-3098.
26. Lohman, T. M. and D. P. Mascotti. 1992. Nonspecific ligand-DNA equilibrium binding parameters determined by fluorescence methods. *Meth. Enzymology* 212:424-458.
27. Udenfriend, S., S. Stein, W. Dairman, W. Leimgruber and M. Weigle. 1972. Fluorescamine: A reagent for assay of amino acids, peptides, proteins, and primary amines in the picomolar range. *Science (Wash., D.C.)* 178:871-872.
28. Lohman, T. M. and D. P. Mascotti. 1992. Thermodynamics of ligand-nucleic acid interactions. *Meth. Enzymology* 212:400-424.
29. Jockusch, S., N. J. Turro and D. A. Tomalia. 1996. Aggregation of organic dyes on starburst dendrimers. *J. Info. Recording* 22:427-422.
30. Wong, I. and T. Lohman. 1993. A double filter method for nitrocellulose-filter binding: application to protein-nucleic acid interactions. *Proc. Natl. Acad. Sci. (USA)* 90:5428-5432.
31. Trifonov, E. N. 1985. Curved DNA. *CRC Crit. Rev. Biochem.* 19:89-106.
32. Ben-Tal, N., B. Honig, R. Peitzsch, G. Denisov and S. McLaughlin. 1996. Binding of small basic peptides to membranes containing acidic lipids: Theoretical models and experimental results. *Biophys. J.* 71:561-575.
33. Hope, M. J., M. B. Bally, G. Webb and P. R. Cullis. 1985. Production of large unilamellar vesicles by a rapid extrusion procedure. Characterization of size distribution, trapped volume, and ability to maintain a membrane potential. *Biochim. Biophys. Acta* 812:55-65.
34. MacDonald, R. C., R. I. MacDonald, B. P. M. Menco, K. Takeshita, N. K. Subbarao and L. Hu. 1991. Small-volume extrusion apparatus for preparation of large, unilamellar vesicles. *Biochim. Biophys. Acta* 1061:297-303.
35. Olson, F., C. A. Hunt, F. C. Szoka, W. J. Vail and D. Papahadjopoulos. 1979. Preparation of liposomes of defined size distribution by extrusion through polycarbonate membranes. *Biochim. et Biophys. Acta* 557:9-23.
36. Stewart, J. C. M. 1980. Colorimetric determination of phospholipids with ammonium ferrothiocyanate. *Anal. Biochem.* 104:10-14.
37. Israelachvili, J. N. 1985. Intermolecular and Surface Forces. Harcourt Brace Janovich, London. 296 pp.
38. Ladokhin, A., W. Wimley and S. H. White. 1995. Leakage of membrane vesicle contents: determination of mechanism using fluorescence quenching. *Biophys. J.* 69:1964-1971.
39. Mui, B. L.-S., P. Cullis, E. Evans and T. Madden. 1993. Osmotic properties of large unilamellar vesicles prepared by extrusion. *Biophys. J.* 64:443-453.

40. Balagurusamy, V., G. Ungar, V. Percec and G. Johansson. 1997. Rational design of the first spherical supramolecular dendrimers self-organized in a novel thermotropic cubic liquid-crystalline phase and the determination of their shape by X-ray analysis. *J. Am. Chem. Soc.* 119:1539-1555.
41. Goddard, E. D. 1993. Polymer and surfactant of opposite charge. *In* Interactions of surfactants with polymers and proteins. E. D. Goddard and K. P. Ananthapadmanabhan, Ed. CRC Press, Boca Raton. 171-202.
42. Gruner, S. M. 1992. Nonlamellar lipid phases. *In* Structural Biology of Membranes. P. L. Yeagle, Ed. CRC, Boca Raton, FL. 211-250.
43. Ponomarenko, E., D. A. Tirrell and W. J. MacKnight. 1998. Water-insoluble complexes of poly(L-lysine) with mixed alkyl sulfates: composition controlled solid state structures. *Macromolecules* 31:1584-1589.

silicon species (Si^+) and the nucleophilic are the combination of phenylsilane and bromine as the most suitable synthon of Si^+ . On the other hand, Si^+ is generated by the reaction between terminal silane and chlorosilane in the presence of platinum catalyst. Because the starburst polymers prepared by the divergent method have phenylsilane units at the exterior position, some functional groups can be easily introduced via the generation of Si^+ species.¹⁹ The convergent starburst polysiloxanes possess the cyano function in the beginning. One of the potential applications of the starburst polymers could be as drug carriers. Because of the harmless nature of polysiloxanes, the present starburst polysiloxanes could be considered as promising drug microcarriers directly injectable into the body.

REFERENCES

1. Buhleier, E.; Wehner, W.; Vogtle, F. *Synthesis*, **1978**, 155.
2. Tomalia, D. A.; Naylor, A. M.; Goddard, W. A. III. *Angew. Chem. Int. Ed. Engl.* **1990**, *29*, 138.
3. Morikawa, A.; Kakimoto, M.; Imai, Y. *Macromolecules* **1991**, *24*, 3469.
4. Birkofer, L.; Stuhl, O. *The Chemistry of Organic Silicon Compounds, Part 1*; Patai, S., Rappoport, Z. Ed.; John Wiley & Sons: New York, **1989**, p 724.
5. Gold, J. R.; Sommer, L. H.; Whitmore, F. C. *J. Am. Chem. Soc.* **1948**, *70*, 2874.
6. Sommer, L. H.; Tyler, L. J.; Whitmore, F. C. *J. Am. Chem. Soc.* **1948**, *70*, 2872.
7. Ojima, I.; Kumagai, M.; Miyazawa, Y. *Tetrahedron Lett.* **1977**, 1385.
8. Eaborn, C. *J. Chem. Soc.* **1949**, 2755.
9. McBride, J. J. Jr.; Beachell, H. C. *J. Am. Chem. Soc.*, **1952**, *74*, 5247.
10. Colvin, E. W. *Silicon in Organic Synthesis*, Butterworths: London, United Kingdom, **1981**.
11. Billmeyer, F. W. Jr. *Text Book of Polymer Science*, 3rd ed.; John Wiley & Sons: New York, **1984**, p 208.
12. Morikawa, A.; Kakimoto, M.; Imai, Y. *Macromolecules* **1992**, *25*, 3247.
13. Hawker, C. J.; Frechet, J. M. J. *J. Chem. Soc., Chem. Commun.* **1990**, 1010.
14. Hawker, C. J.; Frechet, J. M. J. *Macromolecules*, **1990**, *23*, 4726.
15. Hawker, C. J.; Frechet, J. M. J. *J. Am. Chem. Soc.* **1990**, *112*, 7638.
16. Wooley, K. L.; Hawker, C. J.; Frechet, J. M. J. *J. Am. Chem. Soc.* **1991**, *113*, 4252.
17. Speier, J. L.; Webster, J. A.; Barnes, G. H. *J. Am. Chem. Soc.* **1957**, *79*, 974.
18. Speier, J. L. *Homogeneous Catalysis of Hydrosilation by Transition Metals*, Advances in Organometallic Chemistry, Academic: New York, **1979**; Vol. 17.
19. Morikawa, A.; Kakimoto, M.; Imai, Y. *Polym. J.* **1992**, *24*, 573.

DENDRITIC POLYMERS, DIVERGENT SYNTHESIS (Starburst Polyamidoamine Dendrimers)

Donald A. Tomalia* and Peter R. Dvornic
Michigan Molecular Institute

Dendritic polymers represent the fourth and the most recently discovered class of macromolecular architecture. These polymers are distinguished from all other classical types by containing the ideal one branch juncture per repeating unit. They may be classified into two subgroups: single-trunked, branched arrays called dendrons and multidendron assemblies called dendrimers. Because dendrimers are composed of two or more dendrons, they represent an enhancement in structural complexity within this class of polymers.

The first successful preparation of a well-characterized dendritic polymer was reported in 1984 by one of us.¹⁻³ The term dendrimer was introduced at that time, coined from the Greek word for tree, *dendron*, and a suffix, *mer*, was added to denote the smallest structural repeating unit of a larger macromolecule.

Dendritic macromolecules, including dendrons and dendrimers, may be derived from at least four architectural components. They include initiator cores or focal points (see Figure 1); terminal surface groups, which may be chemically reactive or inert; interior branch junctures, possessing various branching characteristics or multiplicities that are equal to or larger than two; and connectors, di-valent segments that covalently connect neighboring branch junctures to provide scaffolding upon which terminal surface groups reside. These basic architectural components constitute the branch cells. They are assembled according to classical chemistry principles, which are determined by the nature of the contributing atoms and the chemical bonds or critical atomic design parameters (CADPs).^{4,5} These CADPs include the sizes of participating atoms and atomic groups, their valencies, directions, bond lengths, bond angles, and conformational bond flexibility (Figure 2A). The branch cells are in turn organized around the initiator core (I) according to mathematical principles (geometrically progressive). The resulting dendrimer is defined by a hierarchy of branch cells, including the core branch cell, internal branch cells, and surface branch cells (Figure 2B).

These three types of branch cells share one characteristic: they all contain a single-branch juncture point. They may be homogenous or differ in chemical structure or branching functionality (multiplicity). The surface branch cells may

*Author to whom correspondence should be addressed.

MAJOR MACROMOLECULAR ARCHITECTURES




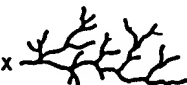



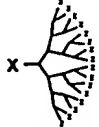






Linear	Branched	Cross-Linked	Dendritic
 Flexible Coil	 Random Short Branches	 Lightly Cross-Linked	 Hyper-Branched (Non-Ideal Dendron)
 Rigid Rod	 Random Long Branches	 Densely Cross-Linked	 Ideal Dendron
 Cyclic (Closed Linear)	 Regular Comb-Branched	 Interpenetrating Networks	 Dendrimer
 Polyrotaxane	 Regular Star-Branched		

FIGURE 1. The four types of macromolecular architecture. Note that structural complexity increases from top to bottom within each group.

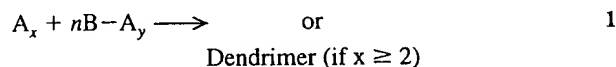
contain chemically reactive or passive functional groups. The chemically reactive surface groups may be used for further dendritic growth or for modification of the dendritic surfaces. The chemically passive groups may be used to physically modify the dendritic surfaces (e.g., adjusting hydrophobic-hydrophilic ratios).

PREPARATION

In theory, dendritic polymers may be prepared by two synthetic approaches: convergent and divergent. With the convergent approach (Figure 3A), the growth process begins from what will later become the dendron surface and progresses in a radial molecular direction, inward or toward the focal point (X).⁶⁻¹⁰ In contrast, the divergent approach (Figure 3B) involves dendritic growth from the initiator core or focal point and progresses outward in a radial direction from the core to the surface.^{1,2}

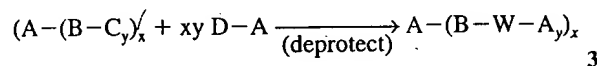
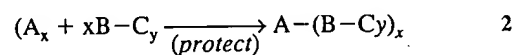
The divergent approach can be realized by three different synthetic methods: one-pot synthesis, the protect-deprotect method and the excess monomer method.^{1,2,7-29,49} In the one-pot synthesis, a dendritic polymer is prepared by a step growth polymerization reaction of a single B-A_y monomer, which is initiated by an A_x initiator. This reaction is shown in Equation 1, where *x* and *y* are functionalities of the reacting species. The integers may or may not be equal; *y* is equal to or larger than 2, and *n* is a large number:

Dendron (if *x* = 1)



An important practical advantage of the one-pot synthesis is its relative simplicity to perform. However, this method lacks reaction control, thus leading to more polydispersed products. It is essentially governed by statistical laws, and for that reason, it yields dendritic products with substantial amounts of structural irregularities (see Figure 1: non-ideal dendrons).

The protect-deprotect divergent method is represented by the reaction sequences shown in Equations 2 and 3:



where *x* and *y* have the same meaning as in Equation 1, C is a protective group that does not react with A under applied reaction conditions, D is a functional group that can react with C, and W is a nonreactive unit resulting from the reaction of C and D.¹⁷⁻¹⁹ Repeating this reaction sequence results in the formation of dendrons or dendrimers, as

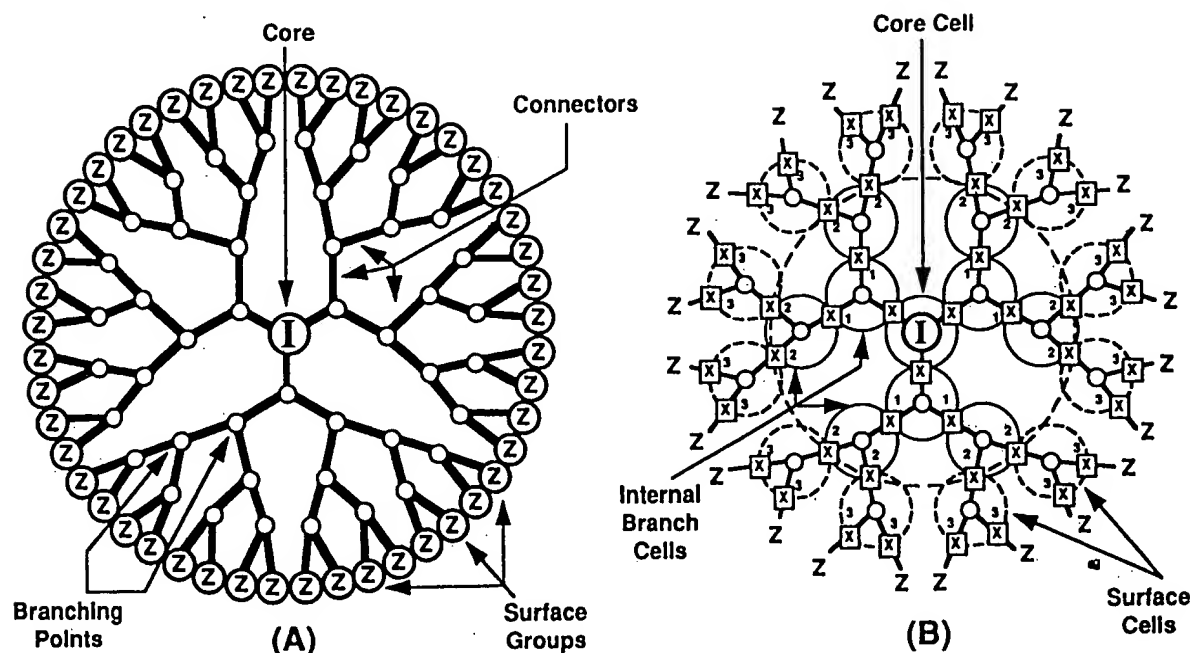
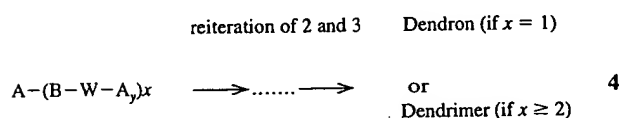


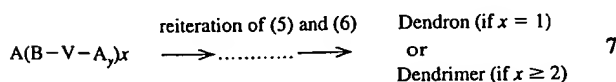
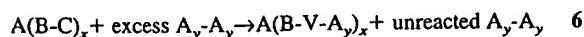
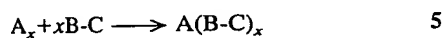
FIGURE 2. Dendritic molecular architecture: (A) basic structural elements and (B) fundamental branch cells.

shown by Equation 4.



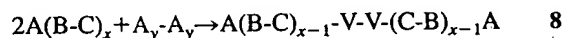
A characteristic feature of this method is that it provides almost complete control of the dendritic molecular growth process and can be used to produce monodispersed dendritic products. However, lower yields and product loss usually associated with protect-deprotect reaction protocol may severely reduce overall product yields to impractical values after only a few reiterations. In more severe cases, this problem may lead to early extinction of dendritic growth if the reiteration schemes are not nearly quantitative.³⁰

The excess monomer method for divergent dendritic synthesis is represented by Equations 5–7.^{1,2,20–29}



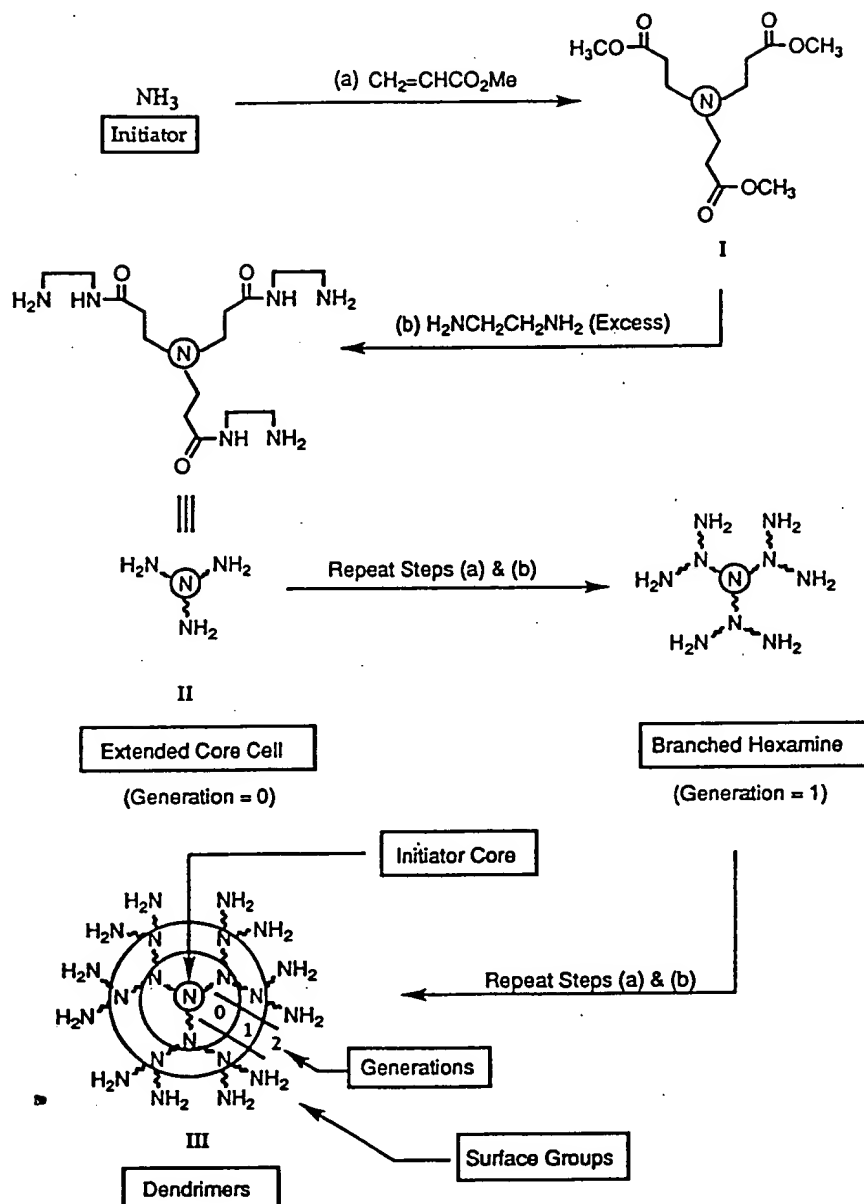
All symbols have the same meaning as in the previous equations. However, in this synthetic protocol, groups C react with groups A to yield the nonreactive unit V. Equations 5 and 6 represent the reaction sequence, and Equation 7 generalizes their subsequent reiteration.

The essential characteristic of this method is that it reduces the probability that reactive groups A will undergo Equation 6, while maximizing the probability that functional groups C will undergo that transformation. Thus, when the $y[A]/x[C]$ ratio is a very large number, the complete conversion of the C groups is accomplished, but the intermolecular reactions between C and A groups (Equation 8) are suppressed.



The net result is a favored formation of pure $(A(B-V-A_y))_x$ products (Equation 6) in almost quantitative yields relative to $A(B-C)_x$.

Thus, the excess monomer method combines the advantages of previous methods. It provides high yields of dendritic products (i.e., nearly quantitative, like the one-pot synthesis), which even after a large number of reiterations (up to 5–7), still contain high relative amounts of ideal structures (similar to the protect-deprotect method). For this reason, the excess monomer method currently offers the



9

NMR spectroscopy for structural characterization, and high-performance liquid chromatography (HPLC) or size exclusion chromatography (SEC) with capillary gel electrophoresis (CGE) to determine purity. A typical set of ES-MS and ^{13}C NMR spectra for **I** shows three major signals and four resonances, respectively. The ES-MS signals are found at m/z values of 276, 298, and 202 and are assigned to the protonated molecular ions of the triester **I** ($M_1 = 275$), $\text{I}-\text{H}^+$; its Na^+ analogue, $\text{I}-\text{Na}^+$; and to $\text{H}_2\text{C}=\text{N}^+[\text{CH}_2\text{CH}_2\text{C}(\text{O})\text{OCH}_3]_2$, respectively. The last compound is often formed as a rearranged product of $\text{I}-\text{H}^+$ in the spectrometer (there is no $\text{H}_2\text{C}=\text{N}^+$ signal in the corre-

sponding ^{13}C NMR), resulting from the collisions of these ions with argon gas and subsequent β -cleavage of the expected intermediate. The ^{13}C NMR signal assignments for **I** are as follows: $\delta = 32$ ppm ($=\text{N}-\text{CH}_2-\text{CH}_2-\text{C}(\text{O})-\text{OCH}_3$), $\delta = 49.5$ ppm ($=\text{N}-\text{CH}_2-$), $\delta = 51.4$ ppm ($=\text{O}-\text{CH}_3$), and $\delta = 172.7$ ppm ($=\text{C}(\text{O})-$), respectively, relative to tetramethylsilane (TMS). The absence of other signals in these spectra demonstrates the high degree of purity observed for **I** (usually between 97 and 100%; see Table 1).

The Michael addition reaction (Equation 9a) routinely yields generation -0.5 PAMAM triester, **I**, in practically quantitative yields, and is essentially free of possible

TABLE 1. Typical Yields and Purities of Full Generation Ammonia Core PAMAM Dendrimers^{a,b}

Generation	Series 1		Series 2		Series 3	
	yield (%)	purity (%)	yield (%)	purity (%)	yield (%)	purity (%)
0	100	—	—	92 ^c	100	92.1 ^c
1	100	95 ^c	100	89.8 ^c 98.5 ^d	—	85.3 ^c 96 ^d
2	—	99.2 ^c	—	95.9 ^c 99.5 ^d	—	92.6 ^c 98.4 ^d
3	100	—	100	97.6 ^c 100 ^d	—	93.4 ^c 100 ^d
4	100	99.2 ^c 96.3 ^d	—	95.8 ^c 96 ^d	—	95.8 ^c 94.3 ^d
5	100	— 98 ^d	—	91 ^c 98 ^d	—	87.3 ^c 94.7 ^d

^aYields of obtained full generation products relative to the amounts of the preceding half generation reactants used. For generation 0, yields are given relative to the amount of ammonia initiator core.

^bPurities as weight percent of a monodendrimer component in the reaction products.

^cBy capillary gel electrophoresis.

^dBy high-performance liquid chromatography.

^eEstimated from ¹³C NMR.

dimeric–oligomeric adducts. These two features of the alkylation step are critical for this divergent synthesis strategy to succeed. Simple removal of solvent and excess MA leads to a product (Equation 9a) that can be used directly as a reactant (template) for the subsequent amidation reaction (Equation 9b). Usually, there is no yield (mass) loss in the purification of "crude" I, which is often a negative feature in many multistage, protect-deprotect protocols.

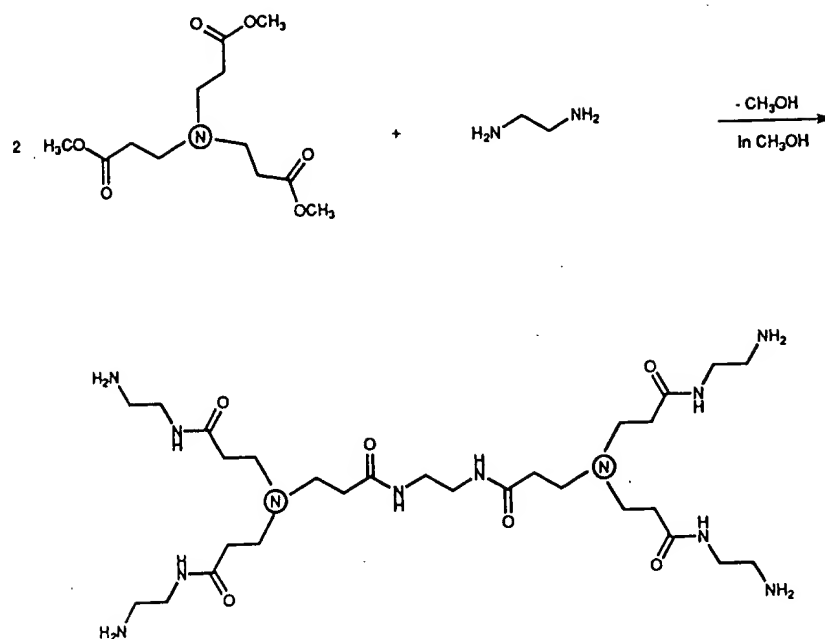
The next step (Equation 9b) in the first iteration reaction sequence leading to the synthesis of PAMAM dendrimers involves a reacting triester I with a large excess of EDA to produce generation 0 PAMAM triamine, II.^{31,32} Detailed investigation of this reaction showed that larger EDA excesses resulted in higher yields of ideal Structure II. Smaller excesses favored side reactions to give higher molecular weight by-products, such as dimers, trimers, or higher oligomers, resulting from intermolecular reactions like the one shown in Equation 10.

In practice, the amidation reaction is performed under inert nitrogen in methanol and requires about 48 h at 0 °C for completion. The resulting reaction mixture is heated for 30 min at 40 °C, followed by stripping of volatiles, which include methanol solvent and unreacted EDA. This procedure yields practically quantitative amounts of pure triamine II. A typical ¹³C NMR for this compound shows five well-defined signals that can be assigned to the expected structure as follows: $\delta = 32.6$ ppm (=N-CH₂CH₂-), $\delta = 39.6$ ppm (-CH₂-NH₂), $\delta = 41.6$ ppm (-C(O)-N(H)-CH₂-), $\delta = 48.5$ ppm (=N-CH₂-CH₂-), and $\delta = 174.8$ (-C(O)-), relative to TMS, respectively. Typical ES-MS exhibits four major signals with *m/z* values at 359 and 381, which can be assigned to H⁺ and Na⁺ derivatives of the ideal Structure II

in Equation 9. The signal at *m/z* = 659.5 can be assigned to dimer IV, and the signal at *m/z* = 246 to a two-armed product of incomplete amidation of I. Occasionally, a signal at *m/z* = 341 may be observed and can be assigned to an imidazoline species obtained from II by eliminating a molecule of water.

The product distribution within a crude reaction product II, as determined by ES-MS, depends on the conditions and the excesses of EDA monomer used for the synthesis. Therefore, at this amidation reaction stage, early deviations from ideal dendritic growth may occur, leading to the formation of imperfect dendritic by-products. Nevertheless, HPLC, SEC, and CGE, indicate that this procedure can be optimized to give triamine II in purities as high as 96–98% (see Table 1). Thus, structural defects can be substantially minimized while the yield of the ideal structure product can be kept nearly quantitative. Just as for the alkylation reaction, this feature enables the divergent synthesis to continue without extensive purification of intermediate II. Consequently, even after many reiterations of the reaction sequence, an important feature of the excess monomer method is that it allows the synthesis of high yields of regular dendritic products even at generations as high as 9 or 10.³³ The first serious deviations from the ideal structure are detected only at about generation 7 (Figure 4).

The preparation of triamine II (Equation 9b) completes the first full reiteration sequence employed in the divergent synthesis of PAMAM dendrimers. This reaction sequence is used for advancement to higher generation dendrimers.^{1,2,20–29,31,32} This advancement involves the synthesis of half and full generation intermediates (i.e., ester- and amine-terminated intermediates, respectively). For example, the second iteration of this sequence produces



10

generations 0.5 and 1, the hexaester and hexamine, respectively. The same reactions are performed in the same way as for generations -0.5 and 0. They yield essentially quantitative amounts of the generational products through generation 5. Typical yields and purities of these intermediates are listed in Table 1.³⁴

DIVERGENT SYNTHESIS

As Figure 3B shows, a divergent molecular growth process involves a series of geometrically progressive additions of branches upon branches. This growth produces a tethered arrangement of ordered, layered branch cells around a central core. As this process progresses from the core toward the outer surface, the dendrimer architecture is developed by the construction of the components that define a dendrimer hierarchy: core branch cells, interior branch cells, and surface branch cells. As Figure 2 shows, the presence of these three components represents the *conditio sine qua non* for any fully developed dendron-dendrimer structure. In other words, the components provide the minimal structural requirement to designate a molecular structure as either a dendron or dendrimer (Figure 1).

Some general features of a divergent growth process leading to a fully developed dendrimer structure can be seen in Figure 5.³⁵

Thus, the first component of a dendrimer structure to form during a divergent synthesis is the core cell (Structure A in Figure 5). In PAMAM dendrimer synthesis (Equation 9), this construction is completed after the ammonia initia-

tor core first reacts with methyl acrylate giving a core cell that remains unchanged during the subsequent dendritic growth process. Generally, the structure of the core cell is unique within a dendrimer molecule (i.e., different from either of the other two components yet to form).

The second fundamental component of dendritic architecture to form during the divergent growth process is the surface cells (Structure B in Figure 5). As Equation 9 and Figure 5 show, this construction phase is complete at the one-and-a-half iterative sequence stage (i.e., at generation 0.5). The surface branch cell structure differs from the core cell because one of its $-\text{[CH}_2\text{CH}_2\text{C(O)}\text{]}-$ groups is replaced by an ethyleneimino, $-\text{[N(H)CH}_2\text{CH}_2\text{]}-$, unit in the surface cells. In addition, the surface branch cells possess reactive functional groups such as $-\text{C(O)-OCH}_3$, or $-\text{NH}_2$ groups, for further extension of the divergent growth process.

Another distinction between the surface branch cells and the core branch cell is that there is usually only one core cell per dendrimer molecule, whereas the number of surface cells is in fact larger than the total number of all core and interior cells taken together. The total number increases from generation to generation according to a geometric progression law, which is represented by Equation 11:

$$Z' = N_c N_b^G / N_b \quad 11$$

where Z' is the number of surface branch cells, N_c is the multiplicity of the core, N_b is the multiplicity of the branch cells, and G is the generation number.^{4,5}

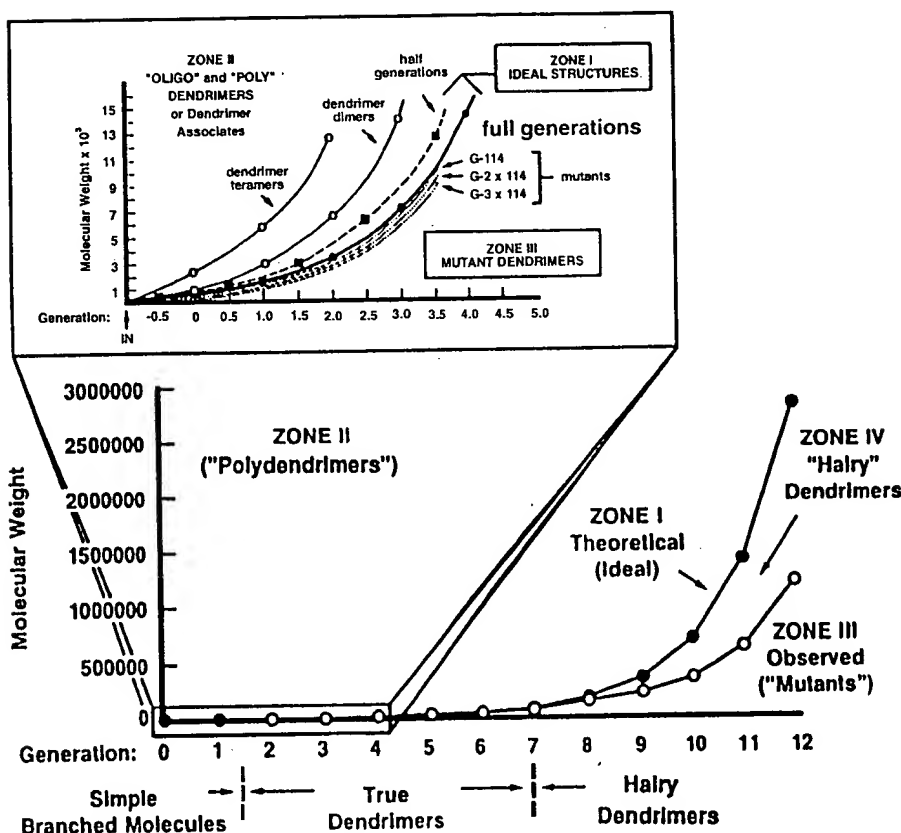


FIGURE 4. Theoretical versus observed molecular weight of polyamidoamine Starburst dendrimers. Zone I comprises ideal dendrimer structures, zone II contains oligo and poly dendrimers, and zone III comprises defective mono dendrimers (above generations 9 or 10 mostly hairy dendrimers).

Chronologically, the last three dendritic components to develop during the divergent growth process are the interior branch cells (Structure C of Figure 5). In a typical PAMAM dendrimer synthesis, these cells first appear at generation 1.5. They provide covalent connectivity in a radial direction from the core cell to the surface cells and are structurally similar to the surface cells. They possess an identical dendritic repeating unit, but the surface cells have additional surface groups that may or may not be reactive for further growth. Thus, for PAMAM dendrimers, the repeating unit common to the interior and surface cells is $-\{N(H)CH_2CH_2N[CH_2CH_2C(O)]_2\}$, and the reactive surface groups on the surface cells may be either ester or primary amine groups.

In contrast to the surface cells, interior cells are inert and less mobile. They may be found between the core cell and the surface cells, between other interior cells and the surface cells, or between two layers of interior cells, depending on a particular dendrimer generation number. Functionally, they provide an interior infrastructure (i.e., internal

scaffolding) for the entire dendrimer structure. In that respect, the interior cells represent the key component that connects and holds together the entire dendrimer molecule.

DENDRITIC BRANCHING

The three dendritic architectural components are formed chronologically during the divergent growth process (Figure 5). They develop along the central symmetry axes of each main monodendron. Thus, during a divergent dendritic growth process, each of these axes represents a main reaction coordinate that extends in space (i.e., from the core to the surface) and in time (i.e., from generation to subsequent generation).

When the first layer of branch cells develops around the initiator core, the resulting structures consist of the core cell and the N_c surface cells (generation B of Figure 5), where N_c represents the functionality of the core atom or atomic group. Clearly, this structure does not represent a fully developed dendrimer structure because it is missing one of

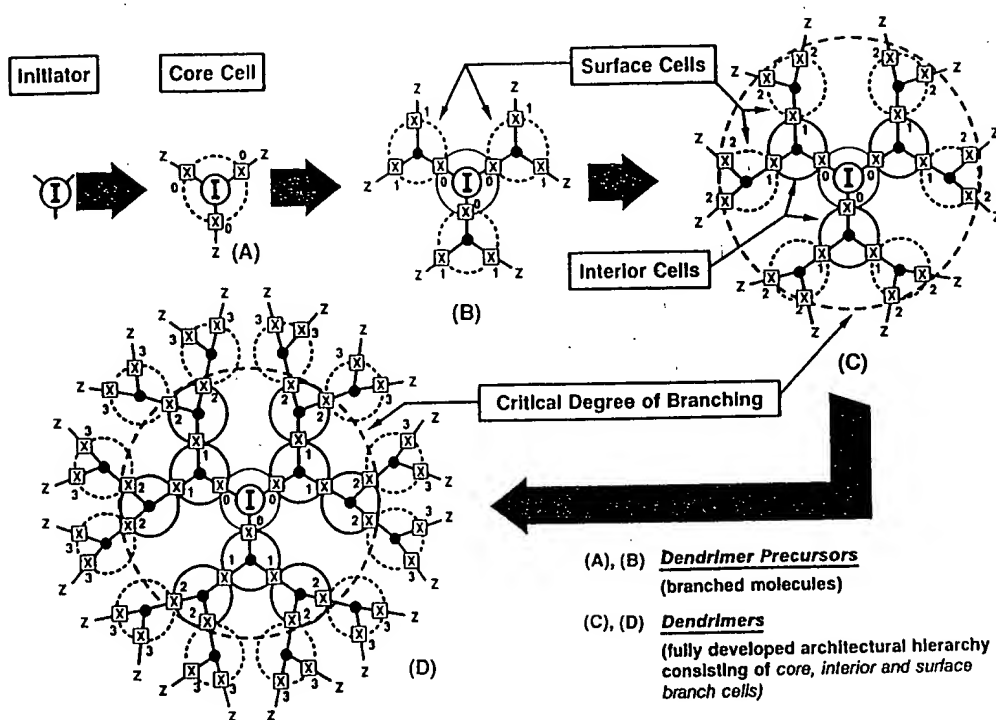


FIGURE 5. Divergent development of dendritic structure. (A and B) dendrimer precursors (i.e., simple branched molecules) (C and D) true dendrimers with fully developed architectural hierarchy consisting of core, interior, and surface branch cells. Note the critical stage of structural development in C.

the three fundamental components required, the interior cells. Therefore, this and other similarly branched structures (generation A of Figure 5) may be considered precursors to dendrimer structures but not dendrimers. The complete development of a dendrimer structure requires at least progression through generation 1.5 (Equation 9 and generation C of Figure 5).

Thus, a fully developed dendrimer structure first appears only after passing through the growth stage above. At that point, the lightly branched structures (generations A and B of Figure 5) transform into fully developed dendrimers that, in the genealogy of the synthesis, contain all three branch cell components (i.e., generation C of Figure 5). At this level of structural complexity, the transition from lightly branched to true dendrimer intermediates takes place. We refer to this transition as the critical degree of branching.³⁵

HIERARCHICAL ORDER OF STRUCTURE

Only after the critical branching stage (i.e., where core, interior, and surface branch cells form as shown in Figure 5) does the resulting product possess the level of structural complexity needed for a fully developed dendritic structure. Thus, within every family of branched compounds, this critical degree of branching represents an interface between

simple branched family members and their fully developed dendrimer counterparts. The former can be considered precursors to fully developed dendrimers. In addition, within every homologous series of dendritic compounds, there exists a hierarchical order of molecular complexity representing the functional dependence of molecular weight or generation number. This order is illustrated in Figure 6, which compares mono-dendrimers (Zone 1) to oligo poly-dendrimers (Zone 2) and defective (mutant) mono-dendrimers (Zone 3).

DE GENNES DENSE-PACKED STATE

Because of the geometrically progressive, growth pattern expressed by Equation 11, dendrons and dendrimers may be constructed in a precise manner. Therefore, such compounds are expected to have precise degrees of polymerization, exact molecular weights, and represent perfectly isomolecular macromolecules.^{4,5}

In such systems, the Z values ($Z = N_b \cdot Z'$ of Equation 11) represent saturation limits at which no additional monomer units can be added to the outer shell at a particular generation.^{3,4} Therefore, the surface shell's saturation at a particular generation renders that dendrimer surface inert toward further reactions with the reagent used to obtain that

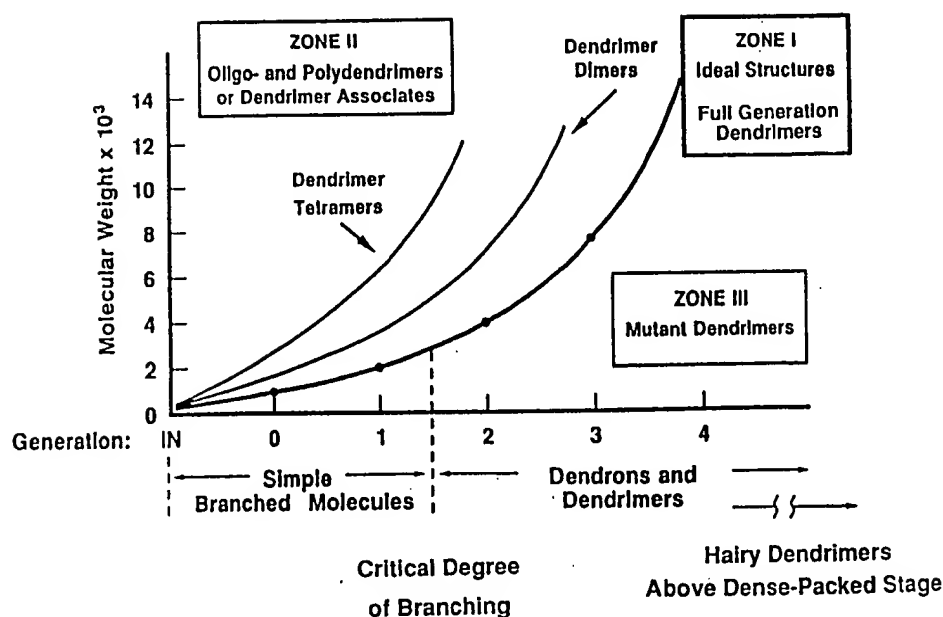


FIGURE 6. Hierarchical order of structural complexity in a homologous series of branched molecules: simple branched molecules, dendrimers, and hairy dendrimers. Note the critical degree of branching for the PAMAM family at generation 1.5.

generation. No additional increase in molecular weight is possible regardless of how large an excess of reactants is used. Divergent dendritic growth, which precisely obeys this mathematically directed growth pattern, is referred to as ideal dendritic growth. Dendrimers or dendrons resulting from such a growth are considered ideal or perfect dendritic structures.^{4,5} In such structures, the degree of polymerization and the corresponding molecular weights are related to N_c , N_b , and G values as Equations 12 and 13 indicate.

$$N_{RU} = N_c \left[\frac{N_b^{G+1} - 1}{N_b - 1} \right] \quad 12$$

$$M = M_c + N_c \left[M_{RU} \left(\frac{N_b^{G+1} - 1}{N_b - 1} \right) + M_t N_b^{G+1} \right] \quad 13$$

Because the radii of dendrimer molecules increase in a linear manner as a function of G , whereas the surface cells amplify from generation to generation according to a geometric progression (i.e., the branching law, $N_c N_b^{G-1}$), ideal dendritic growth cannot extend indefinitely. There will be a critical generation at which the reacting dendrimer surface will not have enough space to accommodate all of the mathematically required new units at that saturation

point. This stage in divergent dendritic growth is referred to as the de Gennes dense-packed state.³⁶ At this stage, these surfaces become so crowded with exterior groups that, although they are chemically reactive, they are sterically prohibited from participating further in ideal dendritic growth.⁴

Nevertheless, this handicap does not preclude dendritic growth beyond this point. As demonstrated by mass spectral studies, further increases in the molecular weight can occur beyond the de Gennes dense-packed stage (Figure 4). However, products resulting from dendritic growth continuing beyond the dense-packed stage are imperfect in structure because all surface groups in the precursor generation are sterically precluded from undergoing further reaction. Presumably, a sterically determined fraction of these groups will remain trapped under the newly formed dendrimer surface, yielding a new type of dendrimer product that contains either functionally mixed molecular surfaces, possessing two types of surface groups (i.e., carbomethoxy and amino units for PAMAM dendrimers) or monofunctional surfaces possessing only one type of surface groups in at least two generation levels.³⁷ In any case, the number of functional groups on the newly formed molecular surfaces will not correspond to the predictions of the geometric branching law (Equation 11) but will fall between the mathematically predicted value for that generation (Z_G) and the corresponding value for the precursor generation (Z_{G-1}).

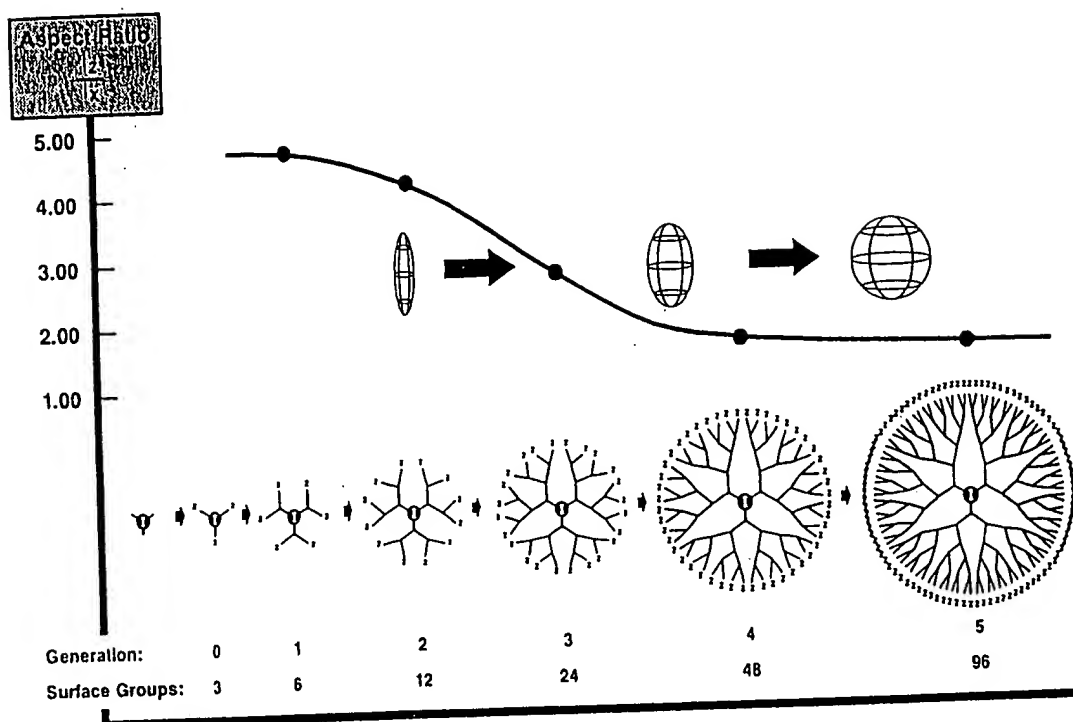


FIGURE 7. The shape change in ammonia core Starburst PAMAM dendrimer molecular topology. Aspect ratio (I_z/I_x) as a function of generation. Note the shape transition from generation 3 to generation 4.

This value yields defective dendrimer generations called hairy dendrimers (Figure 6). Their external surface groups can be envisioned to contain irregular dendron cusplike growths protruding from a bold, regular molecular surface.³⁷

PROPERTIES OF STARBURST

Computer-simulated modeling related to size and shape have been performed on PAMAM dendrimers. The molecular dynamics calculations based on the force field acting on all atoms in equilibrated structures showed that, with increasing generations, these dendrimers seem to develop by passing through a continuum of molecular shapes ranging from open extended structures to closed globular spheroids. This change in shape apparently occurs because tethered steric constraints are imposed on the developing branches. This explanation was determined by the change observed for the calculated aspect ratio of the corresponding longest and shortest principal moments (I_z/I_x) in these developing structures (Figure 7).³⁸

As Figure 7 shows, tridendron PAMAM dendrimers appear spherical after about generation 4. Within these spheres, the solvent accessible surface (SAS) seems to increase with generations so that the fraction of the internal molecular surface increases from about 29% of the total

SAS for generation 4, to 69% for generation 5, and 124% for generation 6. However, the molecular density (M/V) shows a clear minimum at about generation 4 (Figure 8), suggesting that fully developed PAMAM dendrimers have a great deal of accessible internal surface area in a solvent-filled intramolecular free volume, which may consist of internal cavities and channels.⁵

As Figure 9 shows, ^{13}C NMR measurements of spin-lattice relaxation times of specifically tagged PAMAM dendrimers (deuterated in either the surface layers or in the internal segments) appear to support this view. They showed considerably reduced mobility in the outer surface groups relative to that in the interior segments.³⁹⁻⁴¹ This behavior indicates a unimolecular encapsulation type topology in which a relatively soft or spongy interior is enclosed within a considerably harder outer molecular surface or crust. This hypothesis was recently supported by Dutch scientists who referred to this feature as a dendritic box.⁴³

Our recent rheological and differential scanning calorimetry (DSC) data also appears to support this model.⁴⁴ Thus, we discovered that PAMAM dendrimer solutions exhibited Newtonian behavior (Figures 10a and 10b) over a wide range of shear rates (from about 150 to about 750–1250 s^{-1}), temperature (from 15 to 40 $^{\circ}\text{C}$), molecular weights (500 to 29,000 or from $G = 0$ to $G = 5$), and concentrations

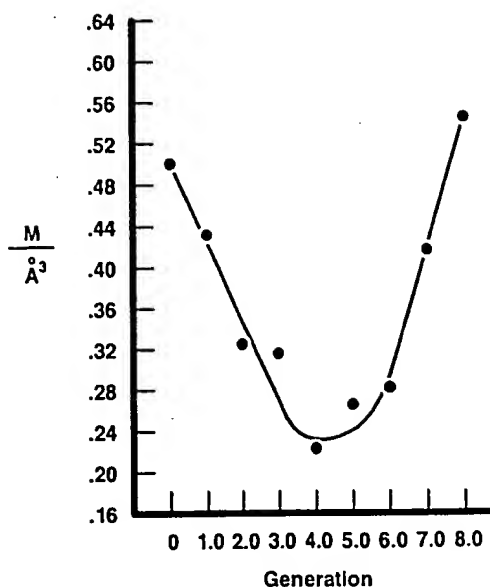


FIGURE 8. The molecular density of ammonia core Starburst® PAMAM dendrimers as a function of generation. Note the minimum at generation 4.

(30–75% by weight). In addition, neat dendrimers showed a linear increase in viscosity with molecular weight at temperatures from 90 to 115 °C.

Furthermore, DSC measurements on PAMAM dendrimers (from EDA and NH₃ cores) showed exponentially increasing glass transition temperatures with their increasing molecular weight reaching an asymptotic value at PAMAM generation 3 or 4 (Figure 11).⁴⁴

From these results, PAMAM dendrimers appear to possess outer surfaces that are substantially impenetrable to

¹³C NMR SPIN-LATTICE RELAXATION TIMES vs. GENERATION

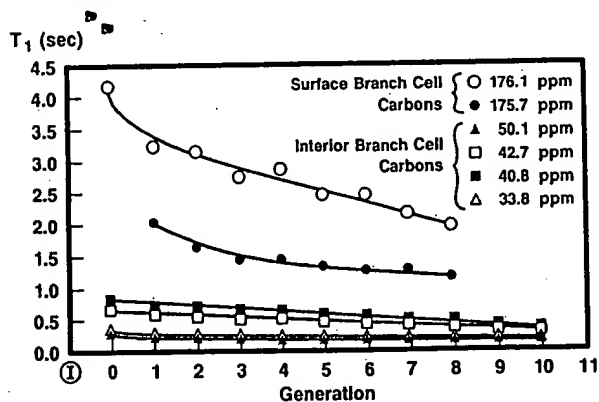
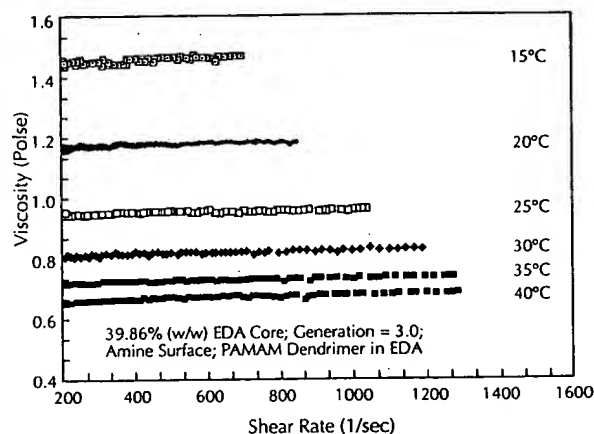
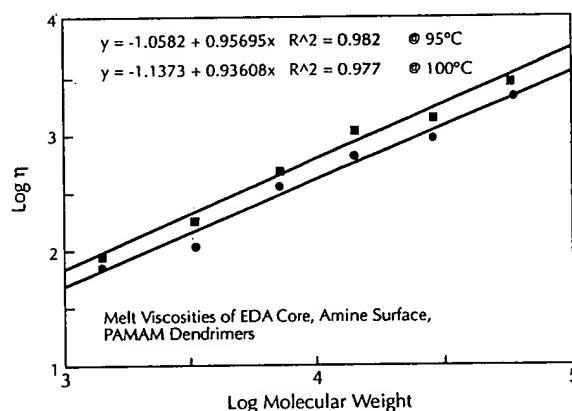


FIGURE 9. ¹³C NMR spin-lattice relaxation times (T₁) as a function of generation for surface branch cells and interior branch cells of ammonia core Starburst PAMAM dendrimers.



(a)



(b)

FIGURE 10. Rheological behavior of ethylene diamine core Starburst PAMAM dendrimers: (a) viscosity as a function of shear rate for a typical dendrimer and EDA solution; (b) viscosity as a function of molecular weight (i.e., generation) for neat dendrimer melts,

neighboring dendrimers (from the viscosity data), while retaining pronounced segmental mobility within the internal volume, possibly around the core and over the first two to three generations. The DSC results also suggest that at the fifth branch layer around the core (i.e., at generation 4), segmental motions responsible for the glass transition apparently reach their limiting values and cannot be extended any further. This limit is indicated by the sharp T_g increase from -11 °C for generation 0 to ~ 8 °C for generation 4 in Figure 11. In the case of higher generation dendrimers, T_g values are unaffected by further increases in molecular weight.

The molecular dimensions of PAMAM dendrimers have been examined by computer modeling and by size exclusion chromatography.^{4,5} In general, excellent agreement between calculated and experimental results was observed. These

GLASS TRANSITION TEMPERATURES OF PAMAM DENDRIMERS

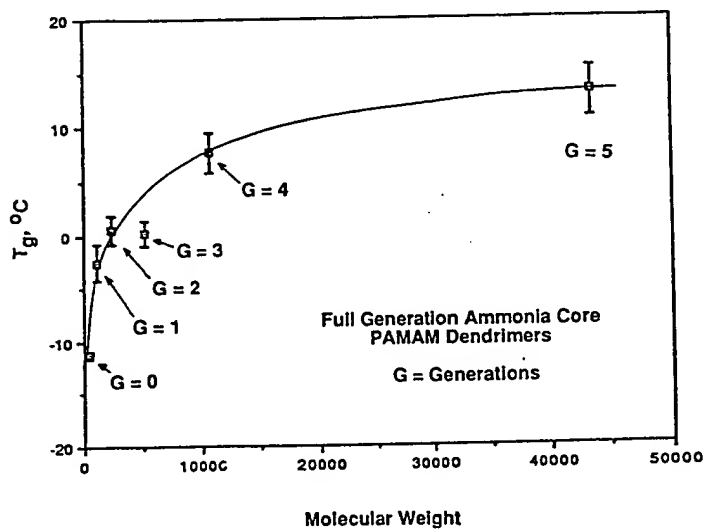
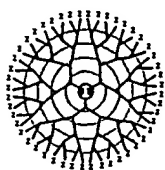


FIGURE 11. Glass transition temperature (T_g) as a function of molecular weight (i.e., generation) of full generation ammonia core Starburst PAMAM dendrimers. Note asymptotic leveling at generations 4 and 5.

ELECTROSPRAY MASS SPECTROSCOPY OF PAMAM DENDRIMERS



M.W. = 10632.96

Generation = 4.0

$N_c = 3$; $N_b = 2$

$\text{I} = \text{NH}_3$

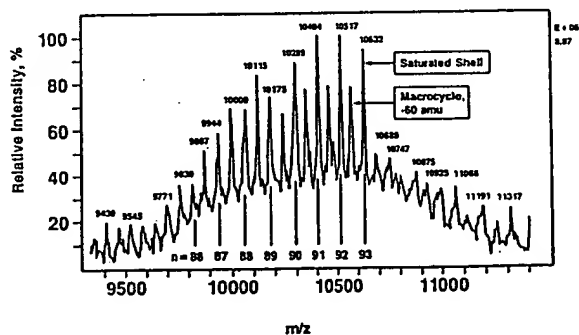


FIGURE 12. Typical electrospray mass spectrum of a generation 4 ammonia core Starburst PAMAM dendrimer. Note peaks corresponding to the missing arm and looped mutant structures.

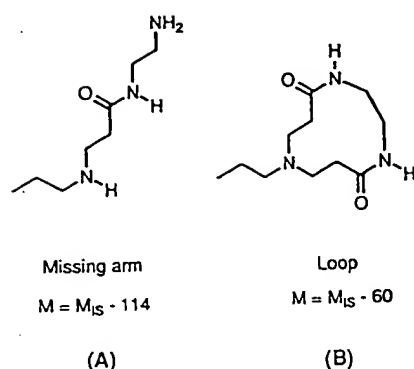


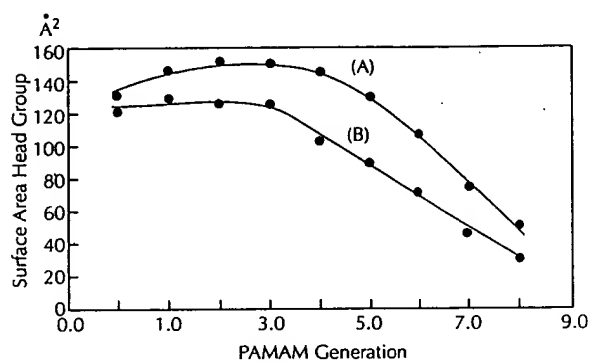
FIGURE 13. Structures of the missing arm and loop defects in the Starburst PAMAM dendrimers.

studies indicate diameters over a range of 1 to 10 nm from generation 0 to generation 8, respectively, with a linear enhancement of 0.7 and 1.2 nm per generation.^{4,5} At these nanoscopic dimensions, direct observation of single dendrimer molecules are possible with electron microscopy. These studies showed that dendrimers were observable as highly monodispersed spheroids.² For example, the sodium salt of generation 3.5 PAMAM dendrimer showed that almost 90% of all particles had diameters ranging within 10% of the average value determined by computer simulations. This feature seems to result directly from the control that a synthetic chemist has over critical molecular design parameters such as size, shape, surface chemistry, flexibility, and topology. The complexity of this dendritic architecture also reflects the extraordinary control provided by the excess monomer method. Analytical methods, such as ES-MS, allow the ideal construction to be examined in great detail.⁴⁵ For example, in generation 4 PAMAM (Figure 12) and in addition to the expected ideal structure ($M_{IS} = 10,632$), a series of the so-called missing arm (at $M = M_{IS} - \times 114$) and looped (at $M = M_{IS} - \times 60$) defects is also formed.^{46,47}

The missing arm defects (Figure 13A) correspond to products of incomplete alkylation, or retro-Michael reaction, leading to a mass defect of one or more units (i.e., $\times \cdot (-CH_2CH_2C(O)N(H)CH_2CH_2N)$ or $\times \cdot 114$ amu). However, loops (Figure 13B) result from intramolecular bridging of a neighboring carbomethoxy group by an amine-terminated functionality (i.e., $\times \cdot (NH_2CH_2CH_2NH_2)$ units or a mass defect of $\times \cdot 60$ amu).⁴⁵ Statistical treatments of these data show that despite these minor structural imperfections, the molecular weight distributions of the resulting dendrimers are narrow and are routinely observed to be as low as $\overline{M}_w / \overline{M}_n = 1.0003$ to 1.0005. Clearly, these results represent a significant step toward preparing perfectly isomolecular, high molecular weight polymers.

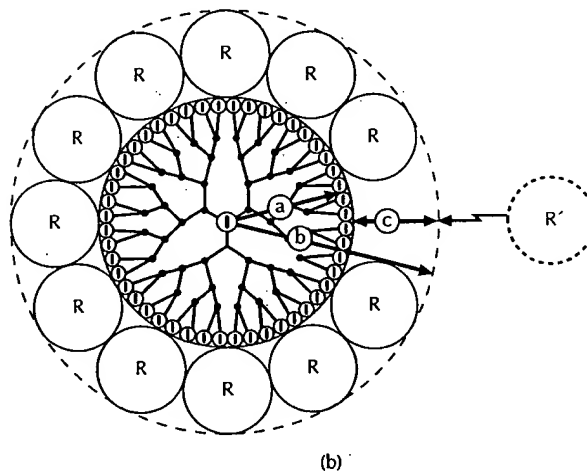
The dendrimer surface group reactivity changes little until the de Gennes dense-packed stage is approached. Within the PAMAM series, this stage occurs at about generation 7, above which the reactivity decreases significantly, indicating considerable constrictions in the surface area per terminal group as Figure 14 shows (compare also with Figure 4).⁵

Above generation 4, the surface area available per terminal group decreases dramatically. The surface area approaches the cross-sectional area of the amine-terminated



Curve (A): Assumes 95% of theoretical surface groups/generation
Curve (B): Assumes 100% of theoretical surface groups/generation

(a)



(b)

FIGURE 14. Sterically induced stoichiometry (SIS) in chemical reactions involving dendrimers as substrates: (a) plot of surface area per terminal group \bar{Z} as a function of generation for ammonia core Starburst PAMAM dendrimers, assuming 95% of the theoretical number of terminal groups are present. (b) schematic representation of sterical hindrances to the incoming reactant (R') to a terminal group above the critical dendrimer generation for SIS, assuming 100% of terminal groups are present.

branch segment (i.e., $\cong 33\text{\AA}$) at generation 8, leading to increased steric hindrance to approaching reagents (Figure 14B). Sterically induced stoichiometry (SIS) results.⁴ At higher generations (i.e., greater than $G = 7$ in PAMAM series), the rate constants and conversions on these dendrimer surfaces decrease substantially, resulting in longer reaction times and larger populations of imperfect structures.

Dendrimer interiors and surfaces can be readily modified to possess chemically reactive or passive functional groups. Currently, over thirty different interiors have been synthesized in our laboratory and elsewhere. Dendrimer interiors may contain carbon, nitrogen, oxygen, silicon, phosphorous, metals, or virtually any element found in the periodic table. Over 100 dendrimer surface modifications have been reported to date. A few of the functional groups integrated into PAMAM dendrimer surfaces are illustrated in Table 2

Generally, dendrimer surfaces can be modified to contain electrophilic or nucleophilic, hydrophobic or hydrophilic, and cationic or anionic moieties. Thus, dendrimer surface

modification allows virtually every known bonding mode to integrate onto the surface of these precisely controlled nanoscopic structures. As such, dendrimers possess highly reactive surfaces that may participate in either classical (sub-nanoscale chemistry) or novel nanoscopic conversions (Figure 15). In the latter, dendrimers have been validated as reactive nanoscopic building blocks suitable for constructing various megamolecular structures. These building blocks follow basic rules of chemical combination with nano-particles such as proteins, poly(nucleic acids), DNA, RNA, or other dendrimers to produce nanoscopic compounds, clusters, and assemblies.

Many of these new nanostructures exhibit commercial promise as gene transfection and drug delivery agents, immuno-diagnostic reagents, nano-catalysts, magnetic resonance imaging contrast agents, nano-reactors, and nanocalibrators.^{48,50-55} In conclusion, dendrimers should play a significant role in the systematic investigation of nanoscopic chemistry, architecture, and properties in biological and abiotic areas of interest.

TABLE 2. Dendrimer Surface Reactions with Various Electrophiles and Nucleophiles

A circular dendrimer structure with a central node labeled '1' and branching outwards. The surface is represented by a series of lines radiating from the center, ending in a group labeled $(X)_{N_c N_b^G}$.

$$(X)_{N_c N_b^G}$$

Reagent

A circular dendrimer structure with a central node labeled '1' and branching outwards. The surface is represented by a series of lines radiating from the center, ending in a group labeled $(Y)_{N_c N_b^G}$.

$$(Y)_{N_c N_b^G}$$

DENDRIMER
TYPE

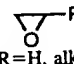
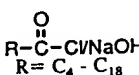
DENDRIMER
SURFACE, (X)

GENERATIONS

REAGENT

DENDRIMER
SURFACE, (Y)

ELECTROPHILIC REAGENTS

1.	PAMAM	-NH ₂	0-10	CH ₂ =CHCO ₂ Me	-N-(CH ₂ CH ₂ CO ₂ Me) ₂
2.	PAMAM	-NH ₂	0-4	BrCH ₂ CO ₂ Me	-N-(CH ₂ CO ₂ Me) ₂
3.	PAMAM	-NH ₂	0-10	 (R=H, alkyl, aryl)	-N-(CH ₂ CHOHR) ₂
4.	PAMAM	-NH ₂	0-6	 R = C ₄ - C ₁₈	-NHCOR
5.	PAMAM	-NH ₂	0-4	Aryl-CH ₂ -Cl	-NH-CH ₂ -Aryl

NUCLEOPHILIC REAGENTS

6.	PAMAM	-CO ₂ Me	0-10	H ₂ N(CH ₂) ₂ -NH ₂	-CONH(CH ₂) ₂ -NH ₂
7.	PAMAM	-CO ₂ Me	0-3	H ₂ N(CH ₂) ₆ -NH ₂	-CONH(CH ₂) ₆ -NH ₂
8.	PAMAM	-CO ₂ Me	0-3	N-(CH ₂ CH ₂ NH ₂) ₃	-CONH(CH ₂) ₂ -N((CH ₂) ₂ -NH ₂) ₂
9.	PAMAM	-CO ₂ Me	0-9	H ₂ NCH ₂ CH ₂ OH	-CONHCH ₂ CH ₂ OH
10.	PAMAM	-CO ₂ Me	0-4	H ₂ N-(CH ₂) ₂ -NH(CH ₂) ₂ -OH	-CONH(CH ₂) ₂ -NH(CH ₂) ₂ -OH

Classical (Sub-nanosopic) Chemistry

Nanosopic Chemistry

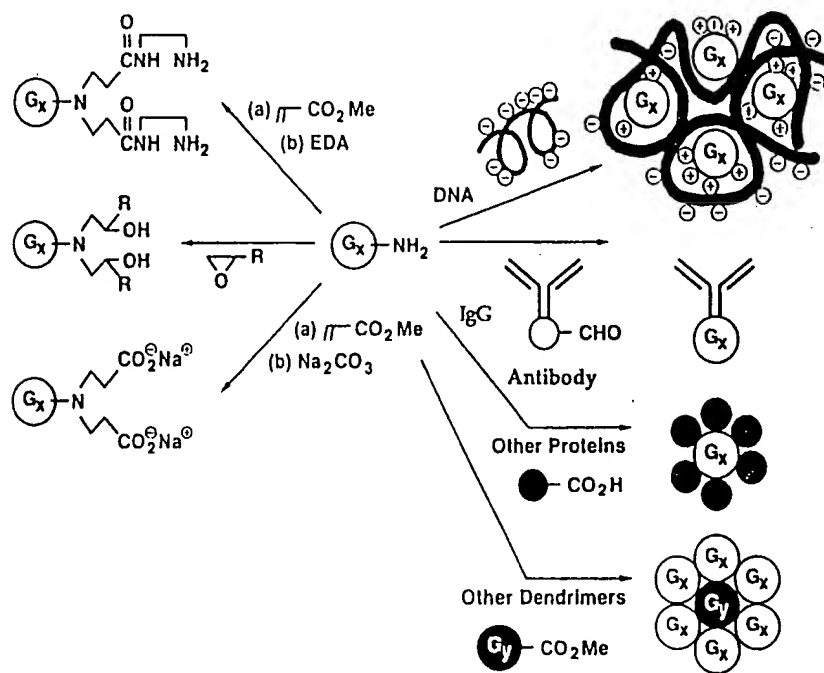


FIGURE 15. Sub-nanosopic and nanoscopic chemistry on dendrimer surfaces, where $G_x = G_y$ = generations 1–7.

REFERENCES

- Tomalia, D. A.; Dewald, J. R.; Hall, M. J. et al. *Preprints 1st Society Polymer Science Japan International Polymer Conference* Kyoto, Japan, 1984; 65.
- Tomalia, D. A.; Baker, H.; Dewald, J. R. et al. *Polymer J. (Tokyo)* **1985**, *17*, 117.
- Tomalia, D. A.; Baker, H.; Dewald, J. R. et al. *Macromolecules*, **1986**, *19*, 2466.
- Tomalia, D. A.; Naylor, A. M.; Goddard, W. A., III *Angew. Chem., Int. Ed. Engl.* **1990**, *29*, 138.
- Tomalia, D. A.; Durst, H. D. *Topics in Current Chemistry* Vol. 165: *Supramolecular Chemistry I—Directed Synthesis and Molecular Recognition*; Weber, E., Ed.; Springer Verlag: Berlin, 1993; p 193–313.
- Fréchet, J. M. J.; Jiang, Y.; Hawker, C. J. et al. In *Proceedings of IUPAC International Symposium on Macromolecules* Seoul, Korea, 1989.
- Hawker, C. J.; Fréchet, J. M. J. *J. Am. Chem. Soc.* **1990**, *112*, 7638.
- Hawker, C. J.; Fréchet, J. M. J. *J. Chem. Soc., Chem. Commun.* **1990**, 1010.
- Hawker, C. J.; Fréchet, J. M. J. *Macromolecules* **1990**, *23*, 4726.
- Miller, T. M.; Neenan, T. X. *Chem. Mater.* **1990**, *2*, 346.
- Bochkarev, M. N. *Organomet. Chem. USSR* **1988**, *1*, 115.
- Kim, Y. H.; Webster, O. W. *Polym. Prepr. Am. Chem. Soc.* **1988**, *29*, 310.
- Kim, Y. H.; Webster, O. H. *J. Am. Chem. Soc.* **1990**, *112*, 4592.
- Hawker, C. J.; Lee, R.; Fréchet, J. M. J. *J. Am. Chem. Soc.* **1991**, *113*, 4583.
- Mathias, L. J.; Carothers, T. W. *Polym. Prepr. Am. Chem. Soc.* **1991**, *32*, 633.
- Mathias, L. J.; Carothers, T. W. *J. Am. Chem. Soc.* **1991**, *113*, 4043.
- Denkewalter, R. G.; Kole, J. F.; Lukasavage, W. J. U.S. Patent 4 410 688, 1983; *Chem. Abstr.* **11**, 103907.
- Hall, H.; Padias, A.; McConnell, R. et al. *J. Org. Chem.* **1987**, *52*, 5305.
- Newkome, G. R.; Yao, Z.-Q.; Baker, G. R. et al. *J. Org. Chem.* **1985**, *50*, 2003.
- Tomalia, D. A.; Dewald, J. R. U.S. Patent 4 507 466, 1985.
- Tomalia, D. A.; Dewald, J. R. U.S. Patent 4 558 120, 1985.
- Tomalia, D. A.; Dewald, J. R. U.S. Patent 4 568 737, 1986.
- Tomalia, D. A.; Dewald, J. R. U.S. Patent 4 587 329, 1986.
- Tomalia, D. A.; Dewald, J. R. U.S. Patent 4 631 337, 1986.
- Tomalia, D. A.; Dewald, J. R. U.S. Patent 4 694 064, 1987.
- Tomalia, D. A.; Dewald, J. R. U.S. Patent 4 713 975, 1987.
- Tomalia, D. A.; Dewald, J. R. U.S. Patent 4 737 550, 1988.
- Tomalia, D. A.; Dewald, J. R. U.S. Patent 4 871 779, 1989.
- Tomalia, D. A.; Dewald, J. R. U.S. Patent 4 857 599, 1989.
- Buhleier, F.; Wehner, W.; Vogtle, F. *Synthesis* **1978**, 155.
- Tomalia, D. A.; Baker, H.; Dewald, J. R. et al. *Macromolecules* **1986**, *19*, 2466.
- Tomalia, D. A.; Swanson, D. R.; Klimash, J. W. et al. *Polym. Prepr., Am. Chem. Soc. Div. Polym. Chem.* **1993**, *34*(1), 52.
- Swanson, D. R.; Savickas, P.; Kallos, G. et al. unpublished results.

34. Swanson, D. R.; Brothers, H. M., II unpublished results.
35. Dvornic, P. R.; Tomalia, D. A. *Chem. Br.* 1994, 30, 641.
36. de Gennes, P. G.; Hervet, H. *J. Phys. Lett. (Paris)* 1983, 44, 351.
37. Dvornic, P. R.; Tomalia, D. A. *Macromol. Chem., Macromol. Symp.* 1994, 88, 123.
38. Naylor, A. M.; Goddard, W. A., III; Kiefer, G. E. et al. *J. Am. Chem. Soc.* 1989, 111, 2339.
39. Meltzer, A. D.; Tirrell, D. A.; Jones, A. A. et al. *Macromolecules* 1992, 25, 4549.
40. Ottaviani, M. F.; Bossmann, S.; Turro, N. J. et al. *J. Am. Chem. Soc.* 1994, 116, 661.
41. Gopidas, K. R.; Leheny, A. R.; Caminati, G. et al. *J. Am. Chem. Soc.* 1991, 113, 7335.
42. Tomalia, D. A. *Proceedings of SFC 91, 4e Congres de la Societe Française de Chimie* Strasbourg, France, 1991; p 31.
43. Jansen, J. F. G. A.; de Brabander-van den Berg, E. M. M.; Meijer, E. W. *Science* 1994, 266, 1226.
44. Uppuluri, S.; Dvornic, P. R.; Tomalia, D. A. unpublished results.
45. Dvornic, P. R.; Tomalia, D. A. *Macromol. Chem., Macromol. Symp.* in press.
46. Tomalia, D. A.; Hedstrand, D. M. Presented at The Taniguchi Conference on Precision Polymer Synthesis Preprints; Kyoto, Japan, May, 1991.
47. Kallos, G. J.; Tomalia, D. A.; Hedstrand, D. M. et al. *Rap. Commun. Mass Spec.* 1991, 5, 383.
48. Haensler, J.; Szoka, F. C., Jr. *Bioconjugate Chem.* 1993, 4, 372.
49. Smith, P. B.; Martin, S. J.; Hall, M. J. et al. In *Applied Polymer Analysis and Characterization*; Mitchell, J., Jr., Ed.; Hanser: München/New York, 1987; p 357.
50. Singh, P.; Moll, F., III; Lin, S. H. et al. *Clin. Chem.* 1994, 40, 1845.
51. Knapen, J. W. J.; van der Made, A. W.; de Wilde, J. C. et al. *Nature* 1994, 372, 659.
52. Tomalia, D. A.; Dvornic, P. R. *Nature* 1994, 372, 617.
53. Wiener, E. C.; Brechbiel, M. W.; Brothers, H. et al. *Magnetic Resonance in Medicine* 1994, 31, 1.
54. Turro, N. J.; Barton, J. K.; Tomalia, D. A. *Acc. Chem. Res.* 1991, 24, 332.
55. Dandliker, P. J.; Diederich, F.; Gross, M. et al. *Angew. Chem. Int. Ed. Engl.* 1994, 33, 1739.

DENDRITIC POLYRADICALS

Suchada Rajca and Andrzej Rajca*
 Department of Chemistry
 University of Nebraska

Synthesis of highly branched, dendritic macromolecules underwent a rapid development in the 1980s.¹⁻³ Elegant methodologies that merge the repetitive reactions of polymer chemistry with stepwise execution of synthetic organic chemistry allow for synthesis of monodisperse macromol-

ecules with MW on the order of 10^4 in good yield, typically after only a few synthetic steps.¹ In the convergent syntheses,⁴⁻⁷ where rigorous purification can be carried out after each synthetic step, not only monodisperse but pure macromolecules are obtained. Furthermore, a high degree of branching in dendrimers shows promise for control of molecular shape.⁸⁻¹¹

Properly designed dendritic macromolecules may be viewed as finite fragments of Bethe lattice, which is one of the important models for phenomena related to condensed matter physics and materials science (Figure 1).¹² For example, functionalization with ferromagnetically coupled "unpaired" electrons would allow us to examine some fundamental questions concerning magnetic phenomena in nanometer-size magnetic particles.¹³⁻¹⁶ 1,3-Connected triarylmethyl-based polyradicals, which are derived from almost century-old Gomberg triphenylmethyl radical and homologous Schlenk hydrocarbon diradical,¹⁷⁻¹⁹ were selected as the building blocks. Our earlier studies established that an intramolecular ferromagnetic coupling was maintained in a series of polyradicals with up to 10 "unpaired" electrons (e.g., high-spin ground state with spin, $S = 5$ for a decaradical) and polyradicals could be handled in solution at low temperature and inert atmosphere.²⁰⁻²⁹

Here we summarize the synthesis leading to the dendritic polyradical with 31 triarylmethyl sites for "unpaired" electrons (Figures 1 and 2).¹⁵

PREPARATION

Synthesis of Polyethers

Preparation of 1,3-connected polyarylmethyl polyethers is based upon a convergent synthetic route, in which branched polymeric arms are built "inward" toward the central core.^{6,15,30} We employ three steps: (a) Br/Li exchange, (b) addition of aryllithium to carbonyl compound, and (c) conversion of the alcohol to the corresponding methyl ether. Sequential iterations of steps (a)–(c) yield dendritic polyethers (Figure 3).^{15,30}

The intermediates and products after steps (b) and (c) are isolated and purified; that is, the alternating polarity in the alcohol/ether/alcohol/ether/...sequence of isolated compounds greatly aids purification by chromatography. Further advantage in purification is gained from the convergent character of the synthesis, which implies that the molecular weight after step (b) is approximately doubled and the amount of the side products with molecular weights similar to the product is minimized. General procedure for each synthetic step is described below:

Step (a): Aryllithium is obtained by monolithiation of bromobenzene derivative in ether (distilled from sodium-benzophenone in a nitrogen atmosphere), at low tempera-

*Author to whom correspondence should be addressed.

POLYMERIC MATERIALS ENCYCLOPEDIA

Editor-in-Chief
JOSEPH C. SALAMONE
Professor Emeritus
University of Massachusetts, Lowell

VOLUME
3
—
D — E



CRC Press
Boca Raton New York London Tokyo

Acquiring Editor: *Joel Claypool*
Senior Project Editor: *Andrea Demby*
Editorial Assistant: *Maureen Aller*
Marketing Manager: *Greg Daurelle*
Marketing Manager Direct Reponse: *Arline Massey*
Cover Designer: *Denise Craig*
Interior Designer: *Jonathan Pennell*
Manufacturing Assistant: *Sheri Schwartz*
Compositor: *RTIS*

TP1110
P65
1996
vol. 3
COPY 2

Library of Congress Cataloging-in-Publication Data

Polymeric materials encyclopedia / editor-in-chief Joseph C. Salamone.

p. cm.

Includes bibliographical references and index.

ISBN 0-8493-2470-X

1. Plastics—Encyclopedia. 2. Polymers—Encyclopedia

I. Salamone, Joseph C., 1939—

TP1110.P65 1996

668.9'03—dc20

96-12181
CIP

This book contains information obtained from authentic and highly regarded sources. Reprinted material is quoted with permission, and sources are indicated. A wide variety of references are listed. Reasonable efforts have been made to publish reliable data and information, but the author and the publisher cannot assume responsibility for the validity of all materials or for the consequences of their use.

Neither this book nor any part may be reproduced or transmitted in any form or by any means, electronic or mechanical, including photocopying, microfilming, and recording, or by any information storage or retrieval system, without prior permission in writing from the publisher.

All rights reserved. Authorization to photocopy items for internal or personal use, or the personal or internal use of specific clients, may be granted by CRC Press, Inc., provided that \$.50 per page photocopied is paid directly to Copyright Clearance Center, 27 Congress Street, Salem, MA 01970 USA. The fee code for users of the Transactional Reporting Service is ISBN 0-8493-2470-X/96/\$0.00+.50. The fee is subject to change without notice. For organizations that have been granted a photocopy license by the CCC, a separate system of payment has been arranged.

The consent of CRC Press does not extend to copying for general distribution, for promotion, for creating new works, or for resale. Specific permission must be obtained in writing from CRC Press for such copying.

Direct all inquiries to CRC Press, Inc., 2000 Corporate Blvd., N.W., Boca Raton, Florida 33431.

Trademark Notice: Product or corporate names may be trademarks or registered trademarks, and are used only for identification and explanation, without intent to infringe.

© 1996 by CRC Press, Inc.

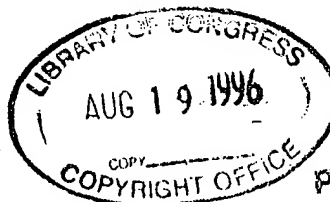
No claim to original U.S. Government works

International Standard Book Number 0-8493-2470-X

Library of Congress Card Number 96-12181

Printed in the United States of America 1 2 3 4 5 6 7 8 9 0

Printed on acid-free paper

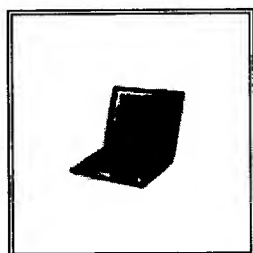




Merriam-Webster's COLLEGIATE® DICTIONARY

- ▶ Home
- ▶ Word of the Day
- ▶ Word Games
- ▶ Word for the Wise
- ▶ Books and CDs
- ▶ Company Info
- ▶ Customer Service
- ▶ Network Options
- ▶ Language Zone
- ▶ The Lighter Side
- ▶ Site Map

Survey America's rich
literary tradition!



Collegiate® Dictionary

Collegiate® Thesaurus

Help

Click on the Collegiate Thesaurus tab to look up the current word in the thesaurus.

20 entries found for **complex**.

To select an entry, click on it. (Click 'Go' if nothing happens.)

complex[1,noun]
complex[2,adjective]
complex[3,transitive verb]
AIDS-related complex
B complex
complex fraction



Main Entry: **¹com·plex**

Pronunciation: 'käm-"pleks

Function: *noun*

Etymology: Late Latin *complexus* totality, from Latin, embrace, from *complecti*

Date: 1643

1 : a whole made up of complicated or interrelated parts <a *complex* of university buildings> <a *complex* of welfare programs> <the military-industrial *complex*>

2 a : a group of culture traits relating to a single activity (as hunting), process (as use of flint), or culture unit **b (1)** : a group of repressed desires and memories that exerts a dominating influence upon the personality **(2)** : an exaggerated reaction to a subject or situation **c** : a group of obviously related units of which the degree and nature of the relationship is imperfectly known

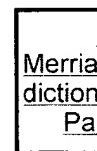
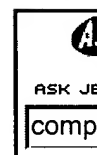
3 : a chemical association of two or more species (as ions or molecules) joined usually by weak electrostatic bonds rather than covalent bonds

Get the **Top 10 Most Popular Sites for "complex"**

Get the **Word of the Day** e-mailed every morning. It's free! Click here.

- ▶ **En garde! Prepare to cross words with Richard Lederer**
Accept the challenge of 50 all-new wordplay-themed crossword puzzles.
- ▶ **Accolades for Merriam-Webster's Collegiate Encyclopedia**
"Proudly stands out as the most affordable, authoritative, and comprehensive one-volume encyclopedia available today."

Audio pr
on-line! V
this red a
to an en
click on
word p



—American Reference Books Annual 2001

Pronunciation Symbols

\&\ as a and u in abut	\e\ as e in bet	\o\ as aw in law
\&\ as e in kitten	\E\ as ea in easy	\oi\ as oy in boy
\&r\ as ur/er in further	\g\ as g in go	\th\ as th in thin
\a\ as a in ash	\i\ as i in hit	\[th]\ as th in the
\A\ as a in ace	\I\ as i in ice	\u\ as oo in loot
\d\ as o in mop	\j\ as j in job	\u\ as oo in foot
\au\ as ou in out	\ng]\ as ng in sing	\y\ as y in yet
\ch\ as ch in chin	\O\ as o in go	\zh\ as si in vision

For more information see the [Guide To Pronunciation](#).

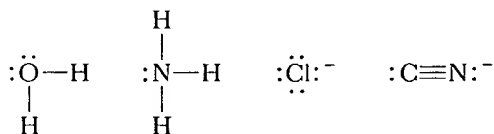
[Home](#)[Link to Us](#)[Advertising Info](#)[Customer Service](#)[Company Info](#)[Contact Us](#)

© 2001 by Merriam-Webster, Incorporated
[Merriam-Webster Privacy Policy](#)



In earlier chapters we noted that metallic elements are characterized by a tendency to lose electrons in their chemical reactions. For this reason, positively charged metal ions play a primary role in the chemical behavior of metals. Of course, metal ions do not exist in isolation. In the first place they are accompanied by anions that serve to maintain charge balance. In addition, metal ions act as Lewis acids (Section 17.8). Neutral molecules or anions with unshared pairs of electrons may be bound to the metal center. On several occasions we have discussed compounds in which a metal ion is surrounded by a group of anions or neutral molecules. Examples include $[\text{Au}(\text{CN})_2]^-$, discussed in connection with metallurgy in Section 24.4; hemoglobin, discussed in connection with the oxygen-carrying capacities of the blood in Section 14.4; $[\text{Cu}(\text{CN})_4]^{2-}$ and $[\text{Ag}(\text{NH}_3)_2]^+$, encountered in our discussion of equilibria in Section 18.5. Such species are known as **complex ions** or merely **complexes**. Compounds containing them are called **coordination compounds**.

The molecules or ions that surround a metal ion in a complex are known as **ligands** (from the Latin word *ligare*, meaning "to bind"). Ligands are normally either anions or polar molecules. Furthermore, they have at least one unshared pair of valence electrons, as illustrated in the following examples:



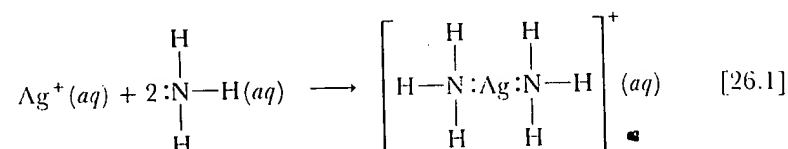
We will see that for most purposes it is adequate to think of the bonding between a metal ion and its ligands as an electrostatic interaction between the positive cation and the surrounding negative ions or dipoles oriented with their negative ends toward the metal ion. The ability of metal ions to form complexes normally increases as the positive charge of the cation increases and its size decreases. The weakest complexes are formed by the alkali metal ions, such as Na^+ and K^+ . Conversely, the +2 and +3 ions of the transition elements generally excel in complex formation. In fact, many of the transition metal ions form complexes more readily than their charge and size would suggest. For example, on the basis of size alone we might expect that Al^{3+} ($r = 0.45 \text{ \AA}$) would form complexes more readily than the larger Cr^{3+} ion ($r = 0.62 \text{ \AA}$).

CONTENTS

- 26.1 The Structure of Complexes
- 26.2 Chelates
- 26.3 Nomenclature
- 26.4 Isomerism
- 26.5 Ligand Exchange Rates
- 26.6 Structure and Isomerism: A Historical View
- 26.7 Color and Magnetism
- 26.8 Crystal-Field Theory

26.1 THE STRUCTURE OF COMPLEXES

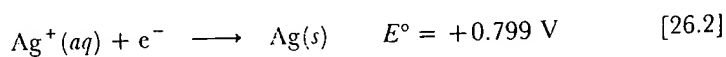
However, with most ligands Cr^{3+} forms much more stable complexes than does Al^{3+} . Thus the bonding in these complexes cannot be explained entirely on the basis of electrostatic attraction between metal ion and ligands. To account for some of the observed differences in complexes, we must assume that there is some degree of covalent character in the metal-ligand bond. Because metal ions have empty valence orbitals, they can act as Lewis acids (electron-pair acceptors). Because ligands have unshared pairs of electrons, they can function as Lewis bases (electron-pair donors). We can picture the bond between metal and ligand as the result of their sharing a pair of electrons that was initially on the ligand:



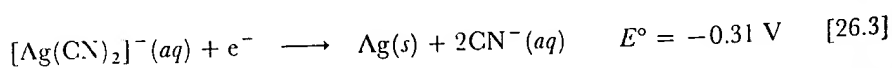
We shall examine the bonding in complexes more closely in Section 26.8.

In forming a complex, the ligands are said to coordinate to the metal or to complex the metal. The central metal and the ligands bound to it constitute the **coordination sphere**. In writing the chemical formula for a coordination compound, we use square brackets to set off the groups within the coordination sphere from other parts of the compound. For example, the formula $[\text{Cu}(\text{NH}_3)_4]\text{SO}_4$ represents a coordination compound consisting of the $[\text{Cu}(\text{NH}_3)_4]^{2+}$ ion and the SO_4^{2-} ion. The four ammonia groups in the compound are bound directly to the copper(II) ion.

As you might expect, a metal complex has different properties from either the metal ion or ligands from which it is derived. We are normally most interested in the effects of complex formation on the properties of the metal ion. The ease of oxidation or reduction of the metal ion may be drastically changed by complex formation. For example, Ag^+ is readily reduced in water:



By contrast, the $[\text{Ag}(\text{CN})_2]^-$ ion is not at all readily reduced, because formation of the cyano complex stabilizes silver in the +1 oxidation state:



Solubility properties may be dramatically different in the presence of complexing agents. For example, CrBr_3 is insoluble in water, but the complex $[\text{Cr}(\text{H}_2\text{O})_6]\text{Br}_3$ is very soluble. Colors may be different. CrBr_3 is a deep green-black, but $[\text{Cr}(\text{H}_2\text{O})_6]\text{Br}_3$ is violet. These differences in properties, illustrated in Figure 26.1, occur because the metal ion plus its surrounding ligands is a distinct species in its own right and so has characteristic physical and chemical properties.

The charge of a complex is the sum of the charges on the central metal and on its surrounding ligands. In $[\text{Cu}(\text{NH}_3)_4]\text{SO}_4$ we can deduce the charge on the complex if we first recognize SO_4 as being the sulfate ion

FIGURE 26.1 The colors of CrBr_3 and $[\text{Cr}(\text{H}_2\text{O})_6]\text{Br}_3$ are different because the immediate surroundings of the metal ion are different in the two compounds. (Donald Clegg and Roxy Wilson)



A Powerful Nonviral Vector for *In Vivo* Gene Transfer into the Adult Mammalian Brain: Polyethylenimine

BASSIMA ABDALLAH, AHMED HASSAN, CORINNE BENOIST, DANIEL GOULA, JEAN PAUL BEHR,¹
and BARBARA A. DEMENEIX

ABSTRACT

Nonviral gene transfer into the central nervous system (CNS) offers the prospect of providing safe therapies for neurological disorders and manipulating gene expression for studying neuronal function. However, results reported so far have been disappointing. We show that the cationic polymer polyethylenimine (PEI) provides unprecedentedly high levels of transgene expression in the mature mouse brain. Three different preparations of PEI (25-, 50-, and 800-kD) were compared for their transfection efficiencies in the brains of adult mice. The highest levels of transfection were obtained with the 25-kD polymer. With this preparation, DNA/PEI complexes bearing mean ionic charge ratios closest to neutrality gave the best results. Under such conditions, and using a cytomegalovirus (CMV)-luciferase construction, we obtained up to 0.4×10^6 RLU/ μ g DNA (equivalent to 0.4 ng of luciferase), which is close to the values obtained using PEI to transfect neuronal cultures and the more easily transfected newborn mouse brain (10^6 RLU/ μ g DNA). Widespread expression (over 6 mm³) of marker (luciferase) or functional genes (*bcl2*) was obtained in neurons and glia after injection into the cerebral cortex, hippocampus, and hypothalamus. Transgene expression was found more than 3 months post-injection in cortical neurons. No morbidity was observed with any of the preparations used. Thus, PEI, a low-toxicity vector, appears to have potential for fundamental research and genetic therapy of the brain.

OVERVIEW SUMMARY

Nonviral gene transfer into the adult mammalian brain offers the prospects of safe therapies and new experimental possibilities. However, results reported so far have been disappointing. We show that the cationic polymer polyethylenimine (PEI) provides high levels of transgene expression in the mature mouse brain. We used polymer preparations of low mean molecular weight and a polymer/DNA charge ratio near neutrality. Widespread expression (over 6 mm³) of marker (luciferase) or functional genes (*bcl2*) was obtained in neurons and glia after injection into the cerebral cortex, hippocampus, and hypothalamus. Transgene expression was found more than 3 months post-injection in cortical neurons. Thus, PEI, a low-toxicity vector, appears to have potential for fundamental research and genetic therapy of the brain.

INTRODUCTION

GENE TRANSFER INTO THE CENTRAL NERVOUS SYSTEM (CNS) offers the prospect of manipulating gene expression for studying neuronal function and eventually for treating neurological disorders. Much effort is currently directed toward the development of vectors suitable for delivering genes into the brain, which has two characteristics that make DNA delivery difficult. First, the blood-brain barrier tends to preclude vascular delivery. Second, the principally postmitotic neuronal population prevents the use of retroviruses. Thus, to date, the only significant successes in the mature brain have come from studies employing direct injection of viral vectors based upon DNA viruses such as adenoviruses (Akli *et al.*, 1993; Bajocchi *et al.*, 1993; Davidson *et al.*, 1993; Le Gal La Salle *et al.*, 1993), herpes-derived vectors (Boviatsis *et al.*, 1994; Pakzaban *et al.*, 1994; Wood *et al.*, 1994), and adeno-associated virus (Kaplit

Laboratoire de Physiologie Générale et Comparée, U.R.A. 90 CNRS, Muséum National d'Histoire Naturelle, F-75231, Paris Cedex 5, France.
¹Laboratoire de Chimie Génétique, URA 1386, Faculté de Pharmacie, Université Louis Pasteur, Strasbourg, France.

et al., 1994). Most recently, a retroviral system based on the human immunodeficiency virus (HIV) has been used to mediate stable transduction of neurons in the rat brain (Naldini *et al.*, 1996). Other applications of viral delivery in the CNS include treatment of brain tumors by retrovirus-producing cells (Culver *et al.*, 1992; Barba *et al.*, 1994) and by direct use of attenuated herpes simplex viruses (Chambers *et al.*, 1995; Kesari *et al.*, 1995). Also, retrovirally transformed cell lines have been used to produce therapeutic proteins to correct a lysosomal disorder affecting the brain (Snyder *et al.*, 1995).

Although most efforts have been directed to viral vectors, the application of nonviral techniques could provide promising and versatile alternatives. Compared to viruses, chemical DNA carriers have numerous advantages. They are of greater flexibility in use and are simpler to prepare, purify, and store. Safety and toxicity data are easily monitored. They can be employed with any kind of DNA, thus allowing accommodation of large sequences associated with the vector plasmids. Moreover, in terms of gene therapy, the risk of pathogenic and immunological complications is reduced. Given these potential benefits and conveniences, it is not surprising that many routes to nonviral gene transfer are currently being pioneered, although until now none have been shown to be as effective as their viral counterparts in the same context.

Amongst nonviral vectors two main classes of molecules can be broadly distinguished: cationic lipids like DOGS (dioctadecylamido glycyispermene, or Transfectam; Behr *et al.*, 1989) or Lipofectin (Felgner *et al.*, 1987) and polymeric DNA-binding cations such as poly-L-lysine (PLL), protamine, cationized albumin, and polyethylenimine (PEI; Boussif *et al.*, 1995). The efficiency of these highly charged molecules in transfecting numerous cell types *in vitro* has been described, but their potential usefulness for the more stringent *in vivo* situations has not been extensively assessed. Recently, we showed that the newborn mouse brain is amenable to gene transfer both with the cationic lipid DOGS mixed with a neutral lipid DOPE (dioleoyl phosphatidylethanolamine (Schwartz *et al.*, 1995) and to transfection with PEI (Boussif *et al.*, 1995). However, the adult brain proved to be impervious to DOGS/DOPE-based transfection, free DNA often giving better results than DNA complexed to the lipids (Schwartz *et al.*, 1996).

This led us to examine whether PEI (a highly branched organic polymer produced by polymerizing aziridine, in which every third atom is a protonable amino nitrogen) could be used for gene transfer into the adult brain. We obtained luciferase reporter gene activities that were close (in terms of light units per microgram of DNA used) to those found in neuronal cultures and in the newborn brain. Moreover, expression continued over 3 months and in the short term was found to be spread over large areas in thousands of cells that included both neurons and glia.

MATERIALS AND METHODS

Cationic polymers

PEIs of 800 kD (Fluka), 50 kD (Sigma), and 25 kD (Aldrich) were used as a 0.1 M stock solutions. To prepare 0.1 M solutions, 45 mg of the 25-kD preparation or 90 mg of the 800- and

50-kD preparations (these latter preparations are 50% wt/vol aqueous solutions) are diluted into 8 ml of dH₂O, adjusted to pH 7 with 1 N HCl, brought to 10 ml with dH₂O and filtered (0.2 μ m, Millipore). Solutions are stable and no special storage precautions required.

Expression plasmids

The *pCMV-luc* expression vector used contains the cytomegalovirus (CMV) promoter inserted upstream of the coding sequence of the firefly (*Photinus pyralis*) luciferase.

The *pCMV-EB2* expression vector (Garcia *et al.*, 1992) contains the CMV promoter inserted upstream of the coding sequence of human bcl-2.

The NSE-bcl-2 (*pEB2*) expression vector (Garcia *et al.*, 1992) contains the human bcl-2 coding region under the control of the rat neuron-specific enolase (NSE) promoter.

The β -actin-luc expression vector was prepared in the laboratory. A luciferase-poly(A) signal cassette was isolated from plasmid pGL2 basic by *Hind* III and *Sal* I digestion, and was inserted into *Hind* III-*Sal* I-digested β -actinBS⁺II plasmid (kindly provided by Pr. P. Charnay, ENS, Paris).

Plasmids were prepared by alkaline lysis followed by PEG precipitation (Ausubel *et al.*, 1994) and then resuspended in Tris-HCl pH 8, 1 mM, EDTA 0.1 mM and stocked as aliquots at -20°C till used.

Lipopolysaccharide assay

Lipopolysaccharide (LPS) quantification was carried out using EndoLAL kits (Chromogenix, Mölndal, Sweden) according to the manufacturers' instructions.

Preparation of PEI/DNA complexes

Plasmid DNA is diluted in 5% glucose to the chosen concentration (usually 0.5–2 μ g/ μ l). After vortexing, the appropriate amount of a 0.1 M PEI solution is added and the solution revortexed. The required amount of PEI, according to DNA concentration and number of equivalents needed, is calculated by taking into account that 1 μ g DNA is 3 nmol of phosphate and that 1 μ l 0.1 M PEI is 100 nmol of amine nitrogen. So, to complex 10 μ g of DNA (30 nmol phosphate) with 5 eq PEI, one needs 150 nmol of PEI (1.5 μ l of a 0.1 M solution).

Animals and injection procedures

Adult (8 weeks old) OF1 female or male mice (Iffa Credo, l'Abresle, France) were anesthetized by injection (i.p.) of sodium pentobarbital (60 mg/kg b.w.). Intracerebral injections were performed using a stereotaxic apparatus. To target the cerebral cortex and hippocampus, injections were made at approximately 1.0–2.0 mm lateral to the sagittal suture and 2.0–2.3 mm anterior to lambda and at a depth of 1.5–2 mm from the skull. To target the hypothalamus, injections were made at 2.5–3.0 mm anterior to lambda and 0.5–1 mm lateral to the median suture and at a depth of approximately 4 mm from the skull (Lehmann, 1974). The injections were made using a 10 μ l Hamilton syringe held by a micromanipulator. Five microliters of a 5% glucose solution containing 2.5 μ g of plasmid complexed with PEI were injected per site over 2–5 min; then the syringe was left in place for 5 min to limit the diffusion of the injected DNA away from

the site of release owing to the backflow pressure. Control brains were injected with either PEI/glucose or 5% glucose. Skin incisions were closed by interrupted sutures, and the animals were kept warm until recovered.

Tissue preparation

The animals were deeply anesthetized and perfused transcardially by saline solution (20–30 ml) followed by ice-cold 2% paraformaldehyde (50–70 ml) in 0.1 M phosphate-buffer pH 7.4 containing 0.05% glutaraldehyde. Brains were then cryoprotected in 30% sucrose, embedded on O.C.T (tissue freezing medium,

Miles Inc. USA), frozen on dry ice, and kept at -80°C until sectioning. Cryostat serial sections (10–12 μm) at the site of injection were cut, mounted onto two sets of gelatine-subbed glass slides, air-dried, and then processed for immunostaining or histological examination with hematoxylin/eosin or cresyl violet staining.

Immunofluorescence procedure

Double-labeling immunofluorescence for exogenous protein and cell-type markers was carried out on cryostat sections using labeled secondary antibodies. The brain sections were prein-

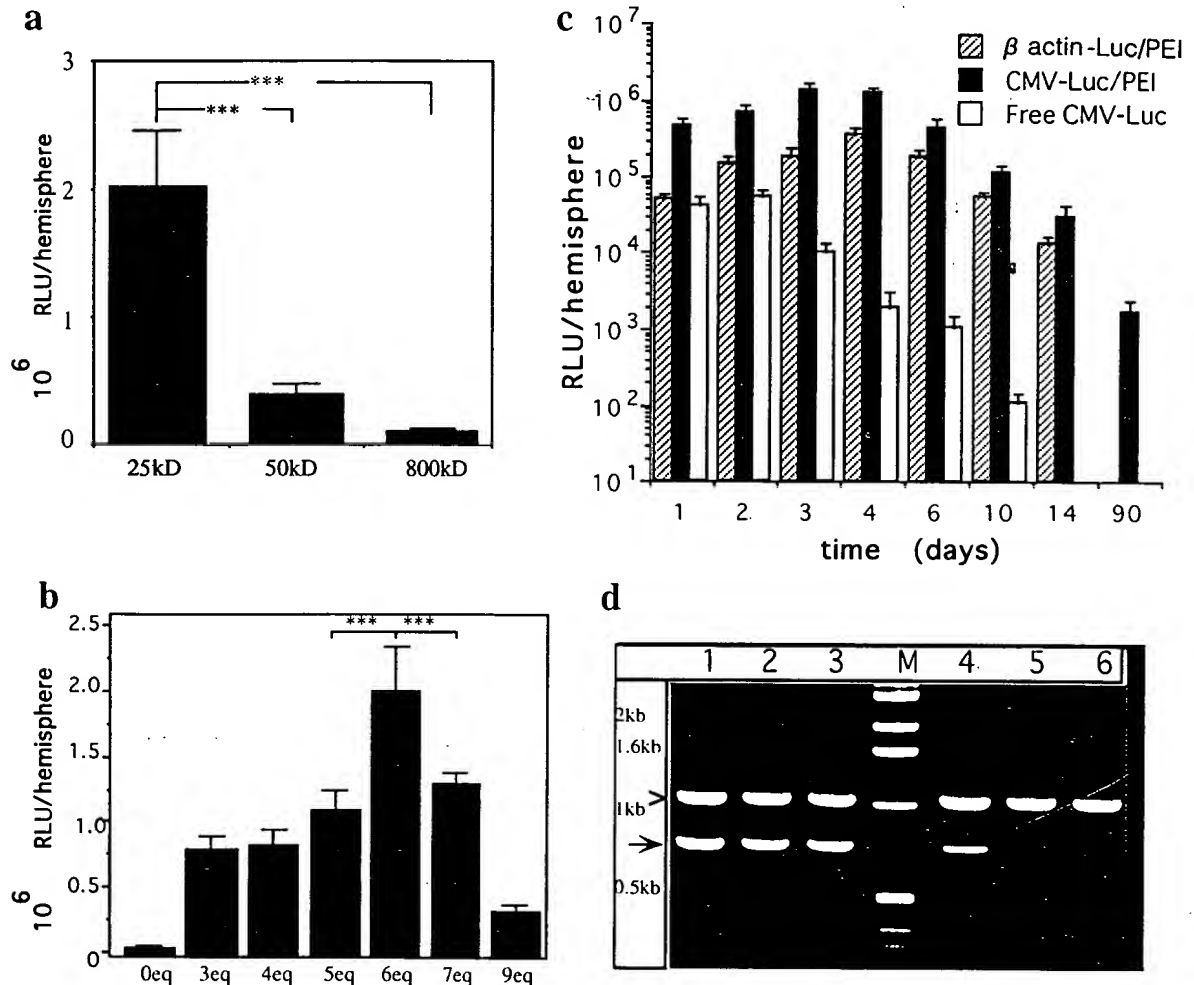


FIG. 1. a. Comparison of luciferase expression in adult mouse brains using pCMV-Luc complexed with PEI preparations of different mean molecular weights. Two injections (5 μl) of 0.5 $\mu\text{g}/\mu\text{l}$ pCMV-Luc with 6 eq of PEI 25, 50, or 800 kD were made into the brains of adult mice. In this experiment and those shown in b and c, mice were sacrificed 2 days post-injection and luciferase activity in the homogenized brains was measured. b. Transfection efficiency varies as a function of the equivalents of PEI nitrogen per DNA phosphate. Mice were injected with 5 μl of a 0.5 $\mu\text{g}/\mu\text{l}$ pCMV-Luc complexed with various ratios of PEI 25k. (N.B. 0 eq is free DNA.) c. Time course of transgene expression in the brain. Two injections (5 μl) with 0.5 $\mu\text{g}/\mu\text{l}$ of pCMV-Luc or β -actin-Luc complexes with 6 eq PEI 25 kD or free pCMV-Luc were made into the brains of adult mice. Animals were sacrificed at 1, 2, 4, 6, 10, 14, and 90 days post injection. d. Detection of pCMV-Luc by PCR on DNA extracted from different brain regions of 3 and 90 days p.i. The DNA extracted (1 μg) was amplified by PCR, using synthetic primers specific for pCMV-Luc vector or EF1 α . Lanes 1 and 4, Cortex, 3 and 90 days p.i., respectively; lanes 2 and 5, hippocampus, 3 and 90 days p.i., respectively; lanes 3 and 6, hypothalamus, 3 and 90 days p.i., respectively; M, marker, containing DNA fragments of known sizes. Arrowhead and whole arrows indicate EF1 α and pCMV-luc PCR amplification products respectively. In a and b. *** indicate statistical differences where $p < 0.001$.

cubated in a blocking solution containing 20% normal goat serum, 0.1% bovine serum albumin (BSA), and 0.3% Triton X-100 in 0.1 M phosphate-buffered saline (PBS, pH 7.4) for 1 hr at room temperature, followed by overnight incubation (at 4°C) in the primary antisera.

For luciferase immunofluorescence, two sets of serially cut sections were used. Cocktails contained rabbit polyclonal anti-luciferase antibody (Cortex, Biochem, USA) at a dilution of 1:250 with either a mouse monoclonal anti-neurofilament 160-kD antibody (Boehringer, Germany) at a dilution of 10 µg/µl in PBS pH 7.4 or a mouse monoclonal anti-glial fibrillary acidic protein (GFAP, Boehringer, Germany) at a dilution of 4 µg/µl in PBS. A rabbit anti-human bcl-2 polyclonal antibody (Clinisciences, USA) at a dilution of 1:1,500 in PBS was employed for bcl-2 detection. Control brain sections were incubated as above, but the primary antisera were omitted. Sections were washed three times in PBS and incubated in the secondary antibody as follows: goat anti-mouse IgG-Fluorescein (Sigma, France) at a dilution of 1:60 in PBS for 1 hr at room temperature with mild agitation, washed three times in PBS then incubated with goat anti-rabbit IgG-Texas Red (Sigma, France) diluted 1:60 in PBS for 1 hr at room temperature. Sections were rinsed in PBS and mounted in Vectashield (Vector Laboratories, Burlingame, CA) and examined under a fluorescent microscope. Four animals were treated for each area and each time point examined. A representative result is shown in each of the figures.

Luciferase assay

Animals were sacrificed by cervical dislocation and luciferase quantification was carried out employing a luciferase assay kit (Promega, France) as described previously (Schwartz *et al.*, 1995).

Detection of pCMV-Luc plasmid by PCR

DNA of pCMV-Luc was extracted from different regions (cortex, hippocampus, and hypothalamus) of 3 days and 90 days p.i. brains (Sambrook *et al.*, 1989). Two animals were killed for each time point. DNA was prepared separately for each hemisphere and each region of the 2 animals, thus giving $n = 4$ for each point. A typical gel is shown in Fig. 1d. The full-length CMV promoter was amplified using the GL-primers 1 and 2 (Promega), the corresponding sequences of which are inserted, respectively, clockwise and counterclockwise either side of the CMV promoter. The PCR reaction was performed in a total volume of 50 µl of 10 mM Tris pH 8.4, 50 mM KCl, 1.5 mM MgCl₂, 200 µM dNTPs, 30 pmol of 5' and 3' primers, 2.5 units of *Taq* polymerase (Perkin-Elmer), and 100 ng of DNA. Amplification was arrested after 30 cycles (94°C × 1 min, 50°C × 1 min and 72°C × 1 min). Aliquots (0.1 vol) of the amplification products were analyzed by 2% agarose gel electrophoresis, stained with ethidium bromide.

Statistical analysis of results

Results are expressed as relative light units (RLU) mean ± SEM for the whole injected organ (brain hemisphere), 10³ RLU representing about 10 fmol (10 pg) of luciferase. Results are expressed per group (4–8 animals). After ANOVA analysis where appropriate, Student's *t*-test was used to analyze differences between groups.

RESULTS

We compared the transfection efficiencies of three commercialized PEI preparations (25-, 50- and 800-kD) in the brains of adult mice. Transfecting pCMV-luc with the 25-kD polymer gave $2.1 \times 10^6 \pm 0.4 \times 10^6$ RLU/hemisphere (mean ± SEM, for 5 µg of DNA injected; Fig. 1a) at 4 days post-injection (p.i.). This was significantly greater ($p < 0.001$) than values obtained with 50 kD PEI ($3.10^5 \pm 0.77 \times 10^5$ RLU/hemisphere) and the 800 kD, which gave very low transfection levels. No morbidity was observed with any of the preparations used with the amounts of DNA indicated over the time course of the experiments (>3 months).

Given the deleterious effects of lipopolysaccharide (LPS) on gene transfer *in vitro* (Cotten *et al.*, 1994), we quantified the LPS in our plasmid preparations. Even though LPS levels ranged through 0.003 to 3–6 ng/µg DNA, transgene expression at 4 days p.i. was not correlated with LPS content. For instance, in the same experiment the plasmid with the highest value (3–6 ng of LPS/µg of DNA) produced $1.7 \pm 0.13 \times 10^6$ RLU, versus $1.2 \pm 0.24 \times 10^6$ RLU for the plasmid containing <3 pg LPS/µg of DNA. These luciferase values were not different ($p = 0.16$).

Next, transfection efficiencies resulting from different ratios of PEI nitrogen to DNA phosphate were tested using the 25-kD PEI preparation. As seen in Fig. 1b when working with between 0 and 9 nitrogens per phosphate (0–9 eqs), transfection efficiency was greatest at a 6 eq. Calculating values in RLU/µg of DNA injected and comparing complexed and naked DNA (0 eq PEI), in this experiment we find that 6 eq of PEI produces 4×10^5 RLU/µg DNA (equivalent to 0.4 ng of luciferase) which is 40 times greater than free DNA (10^4 RLU/µg) (Schwartz *et al.*, 1996) and close to the values obtained using PEI to transfect neuronal cultures and newborn mouse brains (10^6 RLU/µg of DNA) (Boussif *et al.*, 1995).

We next examined expression over 3 months p.i. from 5 µg of pCMV-luc or pβactin-luc complexed with 6 eq of PEI, or the same amount of free pCMV-luc. pCMV-luc complexed with PEI gave the highest expression at all time points. Profiles of expression of PEI-complexed βactin-luc and pCMV-luc were similar (Fig. 1c); in each case expression peaked around day 4. At each time point, expression from free pCMV-luc DNA was between 1 and 3 orders of magnitude lower than PEI-complexed pCMV-luc (Fig. 1c), and the differences were always significant (e.g., for day 1 $F = 33.3$, $p < 0.001$). Immunocytochemistry showed large groups of luciferase-positive cells in each brain area injected with CMV-luc: cortex, hippocampus, and hypothalamus (Fig. 2). Three months later, luciferase activity from PEI/PCMV-luc was low, but still measurable, in homogenates (Fig. 1c) and luciferase-positive neurons were still found in the cortex (Fig. 3). To assess whether promoter silencing or loss of plasmid DNA was the cause of signal extinction, we carried out PCR analysis at 3 days and 3 months p.i. on the three areas targeted. For pCMV-luc DNA, all regions gave high signals at 3 days p.i., but at 3 months the only signal detected was in the cortex (Fig. 1d), and here levels were much reduced as compared to 3 days p.i. However, for EF-1α DNA, which was used as an internal control for the PCR, levels were equivalent in all tissues at all time points (Fig. 1d).

Spatial expression of the transgene was analyzed using

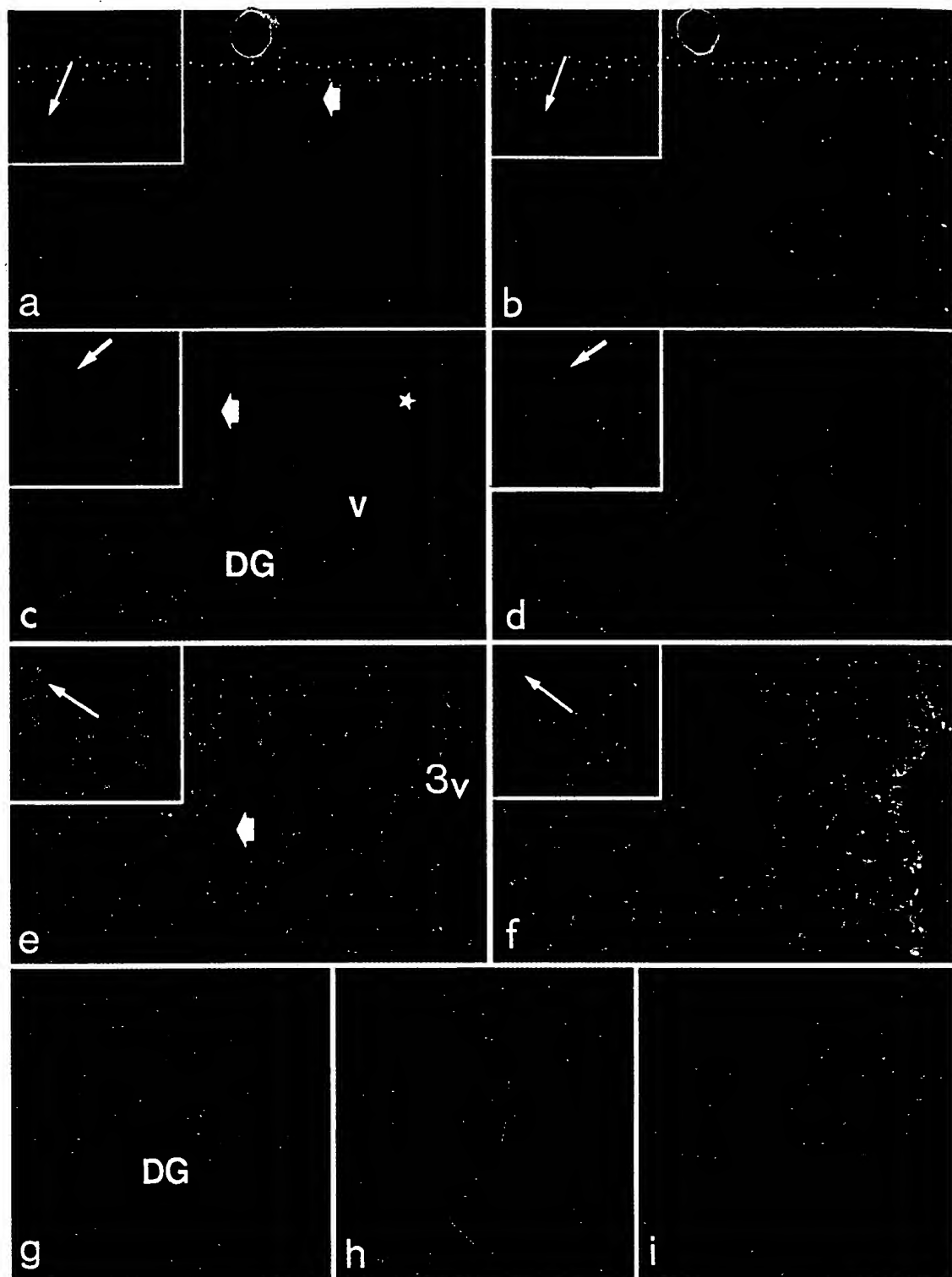


FIG. 2. PEI transfection produces widespread expression in large numbers of neurons and glia in the cerebral cortex, hippocampus, and hypothalamus at 4 days post-injection. For sections a–f, mice were injected with 5 μ l of a 0.5 μ g/ μ l pCMV–Luc complexed with 6 eq PEI 25k. a and b. Section of cerebral cortex double-labeled for luciferase (a) and NF (b). c and d. Hippocampus stained with luciferase (c) and NF (d). The site of injection is indicated by the star. e and f. Paraventricular hypothalamic nucleus stained with luciferase (e) and GFAP (f). In the insets of a–f, the longer, thinner arrows indicate cells that are positive for one marker but not for the other, whereas the shorter, thicker arrows denote cells positive for both labels. g. Representative tissue section of the hippocampus at site of injection transfected with PEI–glucose and showing no specific luciferase stain. h. Representative section of hypothalamic PVN showing no specific stain after omission of luciferase antisera. i. Representative tissue section of the hippocampus of a mouse injected with 5 μ l of a 5 μ g/ μ l pCMV–luc solution (free DNA, 0 eq PEI) and sacrificed 48 hr post-injection. At this concentration (10 \times that used with PEI complexation) and at this time point, which gives maximum expression (Schwartz *et al.*, 1996), some luciferase-positive cells are found. Magnification, 750 \times in a, b, c, d, g, h; 1,500 \times in e, f, i. Insets in a–f are three-fold magnifications of regions identified by the short fat arrows in the main image. DG, Dentate gyrus.

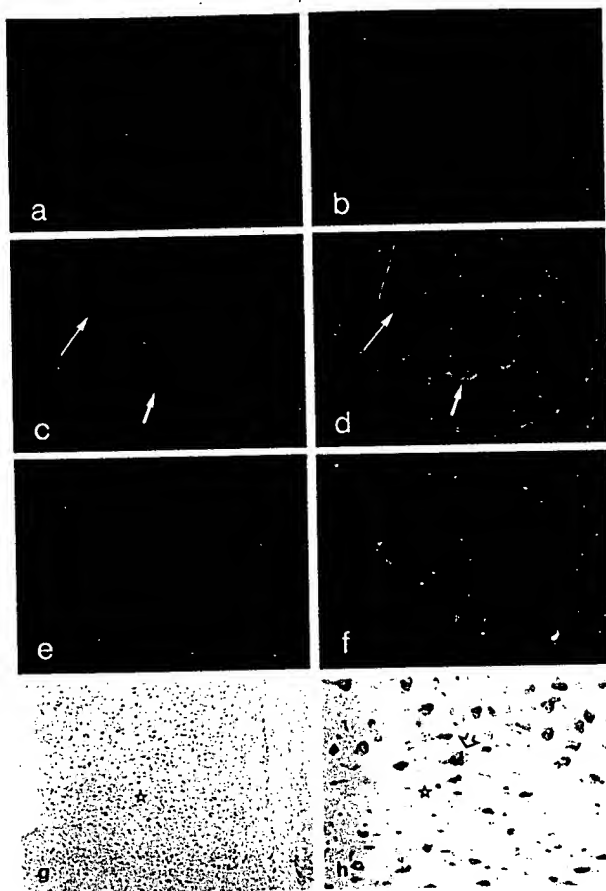


FIG. 3. PEI transfection produces strong expression in the cerebral cortex at 3 months post-injection. **a.** Immunofluorescent labeling of mouse cerebral cortex showing the distribution of luciferase-labeled cortical cells. **b.** Representative section of cerebral cortex showing no specific stain after omission of luciferase antisera. Sections of cortex showing luciferase-positive cells (**c,e**), doubled-labeled with either NF (**d**) or GFAP (**f**). Long arrows indicate cells that are positive for one marker but not for the other, whereas short arrows denote cells positive for both labels. **f,g.** Tissue section of the cerebral cortex at the site of injection (star) stained with hematoxylin and eosin. **h.** Higher magnification of the cerebral cortex stained with cresyl violet, showing typical neuronal morphology (arrow) at the site of injection (star). Magnification, = 500 \times in **a, b, g**; 5,000 \times in **c-f**.

pCMV-luc. Immunofluorescent double labeling at 4 days p.i. showed luciferase expressing cells in both neurofilament (NF)-positive and glial fibrillary acidic protein (GFAP)-positive populations within the cortex, hippocampus, and the paraventricular nucleus of the hypothalamus (Fig. 2a-f). The specificities of the reactions are confirmed by the observation that certain cells positive for one of the cell-specific markers may or may not be positive for the exogenous reporter protein, by control reactions where primary antibodies were omitted (Fig. 2g), and by immunofluorescence carried out on sections from injected with PEI and no DNA (Fig. 2h). Luciferase expression was

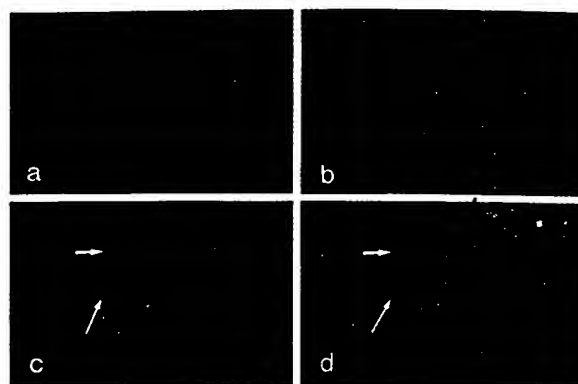


FIG. 4. Expression of bcl-2 at 2 days p.i. **a.** Immunofluorescence showing extensive distribution of bcl-2 expression in the hippocampus following transfection with 2.5 μ g pCMV-bcl-2 complexed with 6 eq 25 kD PEI. **b.** Control section from which the anti-bcl-2 antibody was omitted, showing absence of specific stain. **c** and **d.** Cell specificity of bcl-2 expression in the hippocampus. Double-immunofluorescence was used to reveal human bcl-2 protein expression (**c**) and NF-positive cells (**d**) following transfection with 2.5 μ g of NSE-bcl-2. Magnification, 80 \times in **a** and **b** or 400 \times in **c** and **d**.

found over 200 sections showing that complexes distribute through ≤ 2 mm around the site of injection. As seen in Fig. 2, more than 100 cells per section may express the transgene. Extrapolating from this and the 200 sections showing labeled cells, several thousand cells are expressing the transgene. Brains injected with 20 μ g pCMV-luc without PEI (0 eq) showed some positive cells (Fig. 2i), but expression was limited and more fleeting than with PEI-complexed DNA (Fig. 1c).

In the longer term, at 3 months p.i., expression is found in cortex (Fig. 3), but is not detectable in the hippocampus or hypothalamus. In the cortex, luciferase immunoreactivity is found in neurons (Fig. 3b,c) but not in glia (Fig. 3c,d). For histological examination, sections were stained with hematoxylin/eosin or cresyl violet. At 4 days p.i. the injection site showed some damage (see Fig. 2b,c) often with glial infiltration (data not shown), whereas at 3 months p.i., the site was hardly visible (Fig. 3g) and filled with glia alongside a typical neuronal morphology (Fig. 3h).

We also examined the expression (at 2 days p.i.) in the hippocampus of a functional gene, bcl-2, that is implicated in survival of numerous cell types including neurons (Garcia *et al.*, 1992). Two constructs expressing human bcl-2 were used: one with a pCMV promoter (pCMV-bcl-2) and one with a neuron-specific promoter, neuron-specific enolase (NSE-bcl-2). Both gave high levels of expression (Fig. 4). Figure 4a shows a low-power view of a brain following injection of 2.5 μ g of pCMV-bcl-2 into the right hippocampal area. bcl-2 expression is seen in the right, dorsal hippocampal area, with some diffusion into the left hemisphere. Double labeling with neuronal and glia-specific markers showed bcl-2 expression in both cell types after transfection with pCMV-bcl2 (data not shown) but, using the neuron-specific promoter (NSE-bcl-2) expression was limited to some neurons (Fig. 4c,d).

DISCUSSION

The data show that PEI can provide high levels of transgene expression in the mature mammalian CNS. The number of cells transfected (several thousand) is within the same range as reported for adenoviral gene transfer (Akli *et al.*, 1993) and orders of magnitude greater than levels (a few cells) obtained with the HIV-derived vector (Naldini *et al.*, 1996) and all nonviral reports so far. Three groups have published some histological data in the adult rat brain showing low rates of transfection (a few dozen cells) with chloramphenicol acetyl transferase (CAT) or β -galactosidase (β -Gal)-expressing constructs complexed with cationic lipid (Ono *et al.*, 1990; Zhang *et al.*, 1992; Roessler and Davidson, 1994). To evaluate and optimize PEI-based gene transfer into the nervous system, we chose to use a luciferase-expressing vector because this reporter gene has a greater dynamic range of measure than the other reporter systems commonly used, CAT and β -Gal.

The highest level of transfection was found with low amounts of PEI: ≤ 6 eq nitrogens per DNA phosphate, which gives a effective mean charge ratio (R) of cations to anions of about 1.2 (one in five PEI amines being protonated at physiological pH). Charge ratios of around 1.8 (9 PEI eqs per phosphate) give the best results *in vitro* and in the developing brain (Boussif *et al.*, 1995). The results presented here show that in the mature brain, a more compact tissue than the newborn brain, particles bearing a net ionic charge near neutrality provide the best transfection results. It is possible that using PEI/DNA complexes of neutral mean ionic charge allows the complexes to distribute widely through the tissue. After injection of 5 μ l transfection solution containing particles with a charge ratio near neutrality, one finds labeled cells distributed through >2 mm around the site of injection. This means that the technique could be adjusted by modifying either the injection volume and/or the overall charge ratio to deliver therapeutic genes into a precise, limited brain structure (such as a tyrosine hydroxylase-related gene into the substantia nigra for therapy of Parkinson's disease) or, alternatively, larger volumes can be used for reprogramming of widespread neuronal populations. An example of such use would be expressing transgenes in spinal motoneurons in motoneuronal diseases or striatal neurons in Huntington's chorea.

The duration of expression of PEI-mediated luciferase activity that we observe in the brain is in the same order of magnitude as that described with viral vectors in the rat brain, whether using adenoviral (Davidson *et al.*, 1993; Le Gal La Salle *et al.*, 1993) or adeno-associated viral vectors (Kaplitt *et al.*, 1994). As in each of these studies, we found some transgene-expressing cells up to 3 months post-injection, although this was limited to one of the three areas tested.

Some factors that could be influencing transgene expression over time include loss of transgene sequences, either linked or not to normal cell turnover, and alterations in the level of transcription associated with the promoter used. PCR analysis showed that the only tissue to retain any plasmid DNA at 3 months p.i. was the cortex, thus corroborating the immunocytochemical results and suggesting that loss of transgene sequences, rather than promoter silencing, was occurring. This hypothesis is bolstered from the results obtained using the β -actin promoter. We tested this endogenous,

'housekeeping' promoter to see if loss of activity seen with CMV might be related to the strong viral promoter interfering with normal cell function by overloading the transcriptional/translational machinery. This might be particularly damaging in neurons that display high metabolic activities. Indeed, in contrast, when expressed in skeletal muscle the CMV promoter supports transgene production for several months (Davis *et al.*, 1993; Manthorpe *et al.*, 1993). However, we found lower levels of gene expression from the β -actin promoter at all time points examined. One factor shown to affect gene expression in other systems is the LPS content of the plasmid preparation used (Cotten *et al.*, 1994). Although we saw no effect of LPS content on expression in the short term (<3 days), it is possible that using preparations completely free of LPS could improve long-term expression.

We then chose to express a functional gene *bcl-2*, the product of which is implicated in cell survival. Plasmid constructs containing the human *bcl-2* sequence under the control of the ubiquitously expressed CMV promoter or the neuronal promoter NSE were used. When double-labeling with neuronal and glial cell-specific markers was performed on brains transfected with the NSE-*bcl-2* construct, we found the gene product to be expressed principally in neurons. Thus, the use of cell-specific promoters can be a first step toward the targeting of genes to subpopulations of cells in the brain, the tissue with the greatest diversity of cell types (Mckay, 1989).

In conclusion, we show that the cationic polymer PEI can be used to introduce genes into the mature mammalian brain *in vivo*. In terms of number of cells transfected and duration of expression, the method provides results that are much higher than any nonviral method so far reported and that are within the range of those obtained with viral vectors. Applications of this technique will be found in the study of the CNS function and in therapies of inherited or acquired brain disease.

ACKNOWLEDGMENTS

We thank Dr. Martinou (GLAXO, Geneva) for generously providing the *bcl2* expression plasmids and I. Seugnet for preparing plasmids.

This work was supported by grants from the Association Française contre les Myopathies, the Association pour la Recherche contre le Cancer and Rhône-Poulenc Rorer (programme Bioavenir).

REFERENCES

- AKLI, S., CAILLAUD, C., VIGNE, E., STRATFORD-PERRICAUDET, L.D., POENARU, L., PERRICAUDET, M., KAHN, A., and PESCHANSKI, M.R. (1993). Transfer of a foreign gene into the brain using adenovirus vectors. *Nature Genet.* 3, 224-228.
- AUSUBEL, F.M., BRENT, R., KINGSTON, R.E., MOORE, D.D., SEIDMAN, J.G., SMITH, J.A., and STRUHL, K. (1994). Plasmid DNA purification by PEG precipitation. In *Current Protocols in Molecular Biology*, vol. 1. (John Wiley & Sons, Inc.) pp. 1.7.9-1.8.
- BAJOCCHI, G., FELDMAN, S.H., CRYSTAL, R.G., and MASTRANGELI, A. (1993). Direct *in vivo* gene transfer to ependymal cells in the central nervous system using recombinant adenovirus vectors. *Nature Genet.* 3, 229-234.

- BARBA, D., HARDIN, J., SADELAIN, M., and GAGE, F.H. (1994). Development of anti-tumor immunity following thymidine kinase-mediated killing of experimental brain tumors. *Proc. Natl. Acad. Sci. USA* **91**, 4348-4352.
- BEHR, J., DEMENEIX, B., LOEFFLER, J., and PEREZ-MUTUL, J. (1989). Efficient gene transfer into mammalian primary endocrine cells with lipopolyamine-coated DNA. *Proc. Natl. Acad. Sci. USA* **86**, 6982-6986.
- BOUSSIF, O., LEZOUALC'H, F., ZANTA, M.A., MERGNY, M., SCHERMAN, D., DEMENEIX, B., and BEHR, J.-P. (1995). A novel, versatile vector for gene and oligonucleotide transfer into cells in culture and in vivo: Polyethylenimine. *Proc. Natl. Acad. Sci. USA* **92**, 7297-7303.
- BOVIATIS, E.J., CHASE, M., WEI, M.X., TAMIYA, T., HURFORD, R.K., KOWALL, N.W., TEPPER, R.I., BREAKFIELD, X.O., and CHIOCCA, E.A. (1994). Gene transfer into experimental brain tumors mediated by adenovirus, herpes simplex virus and retrovirus vectors. *Hum. Gene Ther.* **5**, 183-191.
- CHAMBERS, R., GILLESPIE, G.Y., SOROCEANU, L., ANDREANSKY, S., CHATTERJEE, S., CHOU, J., ROIZMAN, B., and WHITLEY, R.J. (1995). Comparison of genetically engineered herpes simplex viruses for the treatment of brain tumors in a solid mouse model of human malignant glioma. *Proc. Natl. Acad. Sci. USA* **92**, 1411-1415.
- COTTEN, M., BAKER, A., SALTIK, M., WAGNER, E., and BUSCHLE, M. (1994). Lipopolysaccharide is a frequent contaminant of plasmid DNA preparations and can be toxic to primary human cells in the presence of adenovirus. *Gene Ther.* **1**, 239.
- CULVER, K.W., RAM, Z., WALLBRIDGE, S., ISHII, H., OLDFIELD, E.H., and BLAISE, R.M. (1992). *In vivo* gene transfer with retroviral vector-producer cells for treatment of experimental brain tumors. *Science* **256**, 1550-1552.
- DAVIDSON, B.L., ALLEN, E.D., KOZARSKY, K.F., WILSON, J.M., and ROESSLER, B.J. (1993). A model system for *in vivo* gene transfer into the central nervous system using an adenoviral vector. *Nature Genet.* **3**, 219-223.
- DAVIS, H.L., WHALEN, R.G., and DEMENEIX, B.A. (1993). Direct gene transfer into skeletal muscle *in vivo*: Factors affecting efficiency of transfer and stability of expression. *Hum. Gene Ther.* **4**, 151-159.
- FELGNER, P.L., GADEK, T.R., HOLM, M., ROMAN, R., CHAN, H.W., WENZ, M., NORTHROP, J.P., RINGOLD, G.M., and DANIELSEN, M. (1987). Lipofection: a highly efficient, lipid-mediated DNA-transfection procedure. *Proc. Natl. Acad. Sci. USA* **84**, 7413-7417.
- GARCIA, I., MARTINOU, I., YOSHIHIDE, T., and MARTINOU, J.C. (1992). Prevention of programmed cell death of sympathetic neurons by the bcl-2 proto-oncogene. *Science* **258**, 302-304.
- KAPLITT, M.G., LEONE, P., SALMUSKI, R., XIAO, X., PFAFF, D.W., O'MALLEY, K.L., and DURING, M.J. (1994). Long-term gene expression and phenotypic correction using adeno-associated virus vectors in the mammalian brain. *Nature Genet.* **8**, 148-153.
- KESARI, S., RANDAZZO, B.P., VALYI-NAGY, T., HUANG, Q.S., BROWN, S.M., MACLEAN, A.R., LEE, V.M., TROJANOWSKI, J.Q., and FRASER, N.W. (1995). Therapy of experimental human brain tumors using a neuroattenuated herpes simplex virus mutant. *Lab. Invest.* **73**, 636-648.
- LE GAL LA SALLE, G., ROBERT, J.J., BERRARD, S., RIDOUX, V., STRADFORD-PERRICAUDET, L.D., PERRICAUDET, M., and MALLET, J. (1993). An adenovirus vector for gene transfer into neurons and glia in the brain. *Science* **259**, 988-990.
- LEHMANN, A. (1974). *Atlas stéréotaxique du cerveau de la souris*. (Editions du CNRS, Paris).
- MANTHORPE, M., CORNEFERT-JENSEN, F., HARTIKKA, J., FELGNER, P.L., RUNDELL, A., MARGALITH, M., and DWARKI, V. (1993). Gene therapy by intramuscular injection of plasmid DNA: studies on firefly luciferase gene expression in mice. *Hum. Gene Ther.* **4**, 419-431.
- MCKAY, R.D.G. (1989). The origins of cellular diversity in the mammalian central nervous system. *Cell* **58**, 815-851.
- NALDINI, L., BLOMER, U., GALLAY, P., ORY, D., MULLIGAN, R., GAGE, F.H., VERMA, I.M., and TRONO, D. (1996). *In vivo* gene delivery and stable transduction of nondividing cells by a lentiviral vector. *Science* **272**, 263-267.
- ONO, T., FUJINO, Y., TSUCHIYA, T., and TSUDA, M. (1990). Plasmid DNAs directly injected into mouse brain with lipofectin can be incorporated and expressed by brain cells. *Neurosci. Lett.* **117**, 259-263.
- PAKZABAN, P., GELLER, A.I., and ISACSON, O. (1994). Effect of exogenous nerve growth factor on neurotoxicity of and neuronal gene delivery by a Herpes simplex amplicon vector in the rat brain. *Hum. Gene Ther.* **5**, 987-995.
- ROESSLER, B.J., and DAVIDSON, B.L. (1994). Direct plasmid-mediated transfection of adult murine brain cells *in vivo* using cationic liposomes. *Neurosci. Lett.* **167**, 5-10.
- SAMBROOK, J., FRITSCH, E.F., and MANIATIS, T. (1989). *Molecular Cloning: A Laboratory Manual*. (Cold Spring Harbor Laboratory Press, Cold Spring Harbor, NY).
- SCHWARTZ, B., BENOIST, C., ABDALLAH, B., SCHERMAN, D., BEHR, J.P., and DEMENEIX, B.A. (1995). Lipospermine-based gene transfer into the newborn mouse brain is optimized by a low lipospermine/DNA charge ratio. *Hum. Gene Ther.* **6**, 1515-1524.
- SCHWARTZ, B., ABDALLAH, B., BENOIST, C., RANGARA, R., HASSAN, A., SCHERMAN, D., and DEMENEIX, B. (1996). Gene transfer by naked DNA into adult mouse brain. *Gene Ther.* **3**, 405-411.
- SNYDER, E.Y., TAYLOR, R.M., and WOLFE, J.H. (1995). Neural progenitor cell engraftment corrects lysosomal storage throughout the MPS VII mouse brain. *Nature* **374**, 367-370.
- WOOD, M.J., BYRNES, A.P., PFAFF, D.W., RABKIN, S.D., and CHARLTON, H.M. (1994). Inflammatory effects of gene transfer into the CNS with defective HSV-1 vectors. *Gene Ther.* **1**, 283-291.
- ZHANG, L.X., WU, M., and HAN, J.S. (1992). Suppression of audiogenic epileptic seizures by intracerebral injection of a CCK gene vector. *NeuroReport* **3**, 700-702.

Address reprint requests to:

Dr. Barbara A. Demeneix

Laboratoire de Physiologie Générale et Comparée

U.R.A. 90 CNRS

Muséum Nationale d'Histoire Naturelle

F-75231, Paris Cedex 5, France

Received for publication April 22, 1996; accepted after revision August 1, 1996.

HUMAN GENE THERAPY

Editor-in-Chief
W. FRENCH ANDERSON, M.D.

Associate Editors
MALCOLM K. BRENNER, M.D., Ph.D.
A. DUSTY MILLER, Ph.D.
JAMES M. WILSON, M.D., Ph.D.

European Editors
CLAUDIO BORDIGNON, M.D.
JEAN MICHEL HEARD, Ph.D.

Mary Ann Liebert, Inc. publishers

18 ISSUES IN 1996
Original Articles
Clinical Protocol

#17

IN THE UNITED STATES PATENT AND TRADEMARK OFFICE



In re application of:

WAGNER *et al.*

Appl. No. 09/446,317

§ 371 Date: April 17, 2000

For: **Complexes for Transporting
Nucleic Acid into Eukaryotic
Higher-Cells**

Art Unit: 1614

Examiner: Schnizer, R.

Atty. Docket: 0652.2010000/EKS/PSC

Declaration of Manfred Ogris Under 37 C.F.R. § 1.132

Assistant Commissioner for Patents
Washington, D.C. 20231

Sir:

1. I, Manfred Ogris, hereby declare and state as follows:
2. I am a named inventor of the captioned application, which is assigned to Boehringer Ingelheim International GmbH, a corporation of Germany, which has a principle place of business at Binger Strasse 173, Ingelheim am Rhein D-55216, Germany.
3. I received my Ph.D in **Biotechnology** from **Universität für Bodenkultur** in 1999.
4. Polymers such as polyethyleneimine (PEI) can take the form of several macromolecular structures including linear, branched, cross-linked and dendritic. *See Tomalia, et al., Polymeric Materials Encyclopedia, Vol. 3, page 1815, Figure 1 (1996) (Exhibit 1).* Within the branched category of macromolecular structures, polymers such as PEI can take the form of random short branched, random long branched, regular comb-branched and regular star branched polymers. (*Id.*)

- 2 -

WAGNER *et al.*
Appl. No. 09/446,317

5. One of ordinary skill in the art would recognize the term "PEI," when used alone and without any modifying adjective to mean random branched PEI, and not the more unusual forms of PEI such as linear PEI, dendritic PEI or hyper-comb branched PEI. For example, Coll *et al.*, *Hum. Gen. Therapy* 10:1659-66 (1999) (Exhibit 2), performing transfection studies using linear PEI, refer to PEI as "L-PEI" or "linear polyethyleneimine" and describe the gene delivery vectors as "L-PEI/DNA complexes." In addition, Tomalia *et al.*, U.S. Patent No. 5,714,166, disclosing dense star PEI are careful to indicate that they are employing "STARBURST™ polyethyleneimines." (Column 13, lines 61-62.) Yin *et al.*, U.S. Patent No. 5,919,442 are also careful to indicate that they are employing "hyper comb-branched" PEI in their studies. They indicate that their invention is a "strikingly different type of macromolecule" in relation to branched polyethyleneimine (PEI). (Column 12-32.) Godbey *et al.*, *J. Controlled Release* 60:149-160 (1999) (Exhibit 3) state that "[t]he branched form of PEI has yielded significantly greater success in terms of cell transfection, and is therefore the standard form of PEI that is used for gene delivery . . . [u]nless otherwise noted, all references to PEI ascribe to the branched form of the molecule." *Id.* at 150. Figure 1 of Godbey *et al.* shows that the branched PEI being referred to is random branched PEI. Klotz *et al.*, *Biochemistry* 8:4752-56 (1969) (Exhibit 4) teach that PEI is a "highly branched water-soluble polymer." *Id.* at 4753. The schematic representation of the polymer provided by Klotz *et al.* indicates that the "PEI" described by Klotz *et al.* is random branched PEI. *Id.*

6. The exemplary teachings in the art described in paragraph 5 show that one of ordinary skill in the art would use an adjective (e.g., hyper-comb branched or STARBURST™) or other modifying term (e.g., L-PEI) to identify the more unusual forms of PEI and that one of ordinary skill in the art would recognize the term "PEI" without a modifying adjective to mean random branched PEI.

- 3 -

WAGNER *et al.*
Appl. No. 09/446,317

7. All the examples of PEI listed in the specification of the captioned-application (page 6, lines 1-10 and Example 1, lines 19-20) (PEI 700D, PEI 2000 D, PEI 25000 D, PEI 750000 D (Aldrich), PEI 50000 D(Sigma), PEI 800000 D (Fluka) and LUPASOL® FG: 800D, LUPASOL® G20 anhydrous: 1300 D, LUPASOL® WF: 25000 D, LUPASOL® G 20: 1300 D, LUPASOL® G 35: 2000 D, LUPASOL® P: 750000 D, LUPASOL® PS: 750000 D, and LUPASOL® SK: 2000000 D) are random branched PEI.

8. I hereby declare that all statements made herein of my own knowledge are true and that all statements made on information and belief are believed to be true; and further that these statements were made with the knowledge that willful false statements and the like so made are punishable by fine or imprisonment, or both, under § 1001 of Title 18 of the United States Code, and that such willful false statements may jeopardize the validity of the application or any patents issued thereupon.

28. August 2001
Date


Manfred Ogris

an electrophilic silicon species (Si^+) and the nucleophilic silanols, where the combination of phenylsilane and bromine acts as the most suitable synthon of Si^+ . On the other hand, Si^+ is generated by the reaction between terminal olefins and chlorosilane in the presence of platinum catalyst.

Because the starburst polymers prepared by the divergent method have phenylsilane units at the exterior position, some functional groups can be easily introduced via the generation of Si^+ species.¹⁹ The convergent starburst polysiloxanes possess the cyano function in the beginning. One of the potential applications of the starburst polymers could be as drug carriers. Because of the harmless nature of polysiloxanes, the present starburst polysiloxanes could be considered as promising drug microcarriers directly injectable into the body.

REFERENCES

- Buhleier, E.; Wehner, W.; Vogtle, F. *Synthesis*, **1978**, 155.
- Tomalia, D. A.; Naylor, A. M.; Goddard, W. A. III. *Angew. Chem. Int. Ed. Engl.* **1990**, *29*, 138.
- Morikawa, A.; Kakimoto, M.; Imai, Y. *Macromolecules* **1991**, *24*, 3469.
- Birkofer, L.; Stuhl, O. *The Chemistry of Organic Silicon Compounds, Part 1*; Patai, S., Rappoport, Z. Ed.; John Wiley & Sons: New York, 1989, p 724.
- Gold, J. R.; Sommer, L. H.; Whitmore, F. C. *J. Am. Chem. Soc.* **1948**, *70*, 2874.
- Sommer, L. H.; Tyler, L. J.; Whitmore, F. C. *J. Am. Chem. Soc.* **1948**, *70*, 2872.
- Ojima, I.; Kumagai, M.; Miyazawa, Y. *Tetrahedron Lett.* **1977**, 1385.
- Eaborn, C. *J. Chem. Soc.* **1949**, 2755.
- McBride, J. J. Jr.; Beachell, H. C. *J. Am. Chem. Soc.*, **1952**, *74*, 5247.
- Colvin, E. W. *Silicon in Organic Synthesis*, Butterworths: London, United Kingdom, 1981.
- Billmeyer, F. W. Jr. *Text Book of Polymer Science*, 3rd ed.; John Wiley & Sons: New York, 1984, p 208.
- Morikawa, A.; Kakimoto, M.; Imai, Y. *Macromolecules* **1992**, *25*, 3247.
- Hawker, C. J.; Frechet, J. M. J. *J. Chem. Soc., Chem. Commun.* **1990**, 1010.
- Hawker, C. J.; Frechet, J. M. J. *Macromolecules*, **1990**, *23*, 4726.
- Hawker, C. J.; Frechet, J. M. J. *J. Am. Chem. Soc.* **1990**, *112*, 7638.
- Wooley, K. L.; Hawker, C. J.; Frechet, J. M. J. *J. Am. Chem. Soc.* **1991**, *113*, 4252.
- Speier, J. L.; Webster, J. A.; Barnes, G. H. *J. Am. Chem. Soc.* **1957**, *79*, 974.
- Speier, J. L. *Homogeneous Catalysis of Hydrosilation by Transition Metals*, Advances in Organometallic Chemistry, Academic: New York, 1979; Vol. 17.
- Morikawa, A.; Kakimoto, M.; Imai, Y. *Polym. J.* **1992**, *24*, 573.

DENDRITIC POLYMERS, DIVERGENT SYNTHESIS (Starburst Polyamidoamine Dendrimers)

Donald A. Tomalia* and Peter R. Dvornic
Michigan Molecular Institute

Dendritic polymers represent the fourth and the most recently discovered class of macromolecular architecture. These polymers are distinguished from all other classical types by containing the ideal one branch juncture per repeating unit. They may be classified into two subgroups: single-trunked, branched arrays called dendrons and multi-dendron assemblies called dendrimers. Because dendrimers are composed of two or more dendrons, they represent an enhancement in structural complexity within this class of polymers.

The first successful preparation of a well-characterized dendritic polymer was reported in 1984 by one of us.¹⁻³ The term dendrimer was introduced at that time, coined from the Greek word for tree, *dendron*, and a suffix, *mer*, was added to denote the smallest structural repeating unit of a larger macromolecule.

Dendritic macromolecules, including dendrons and dendrimers, may be derived from at least four architectural components. They include initiator cores or focal points (see **Figure 1**); terminal surface groups, which may be chemically reactive or inert; interior branch junctures, possessing various branching characteristics or multiplicities that are equal to or larger than two; and connectors, di-valent segments that covalently connect neighboring branch junctures to provide scaffolding upon which terminal surface groups reside. These basic architectural components constitute the branch cells. They are assembled according to classical chemistry principles, which are determined by the nature of the contributing atoms and the chemical bonds or critical atomic design parameters (CADPs).^{4,5} These CADPs include the sizes of participating atoms and atomic groups, their valencies, directions, bond lengths, bond angles, and conformational bond flexibility (**Figure 2A**). The branch cells are in turn organized around the initiator core (I) according to mathematical principles (geometrically progressive). The resulting dendrimer is defined by a hierarchy of branch cells, including the core branch cell, internal branch cells, and surface branch cells (**Figure 2B**).

These three types of branch cells share one characteristic: they all contain a single-branch juncture point. They may be homogenous or differ in chemical structure or branching functionality (multiplicity). The surface branch cells may

*Author to whom correspondence should be addressed.

MAJOR MACROMOLECULAR ARCHITECTURES








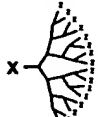



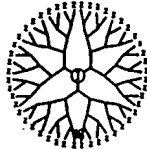


Linear	Branched	Cross-Linked	Dendritic
 Flexible Coil	 Random Short Branches	 Lightly Cross-Linked	 Hyper-Branching (Non-Ideal Dendron)
 Rigid Rod	 Random Long Branches	 Densely Cross-Linked	 Ideal Dendron
 Cyclic (Closed Linear)	 Regular Comb-Branched	 Interpenetrating Networks	 Dendrimer
 Polyrotaxane	 Regular Star-Branched		

FIGURE 1. The four types of macromolecular architecture. Note that structural complexity increases from top to bottom within each group.

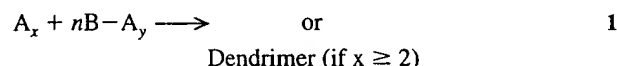
contain chemically reactive or passive functional groups. The chemically reactive surface groups may be used for further dendritic growth or for modification of the dendritic surfaces. The chemically passive groups may be used to physically modify the dendritic surfaces (e.g., adjusting hydrophobic-hydrophilic ratios).

PREPARATION

In theory, dendritic polymers may be prepared by two synthetic approaches: convergent and divergent. With the convergent approach (Figure 3A), the growth process begins from what will later become the dendron surface and progresses in a radial molecular direction, inward or toward the focal point (X).⁶⁻¹⁰ In contrast, the divergent approach (Figure 3B) involves dendritic growth from the initiator core or focal point and progresses outward in a radial direction from the core to the surface.^{1,2}

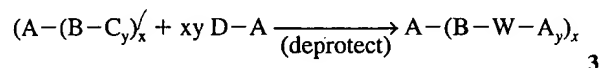
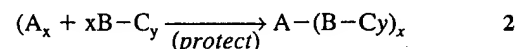
The divergent approach can be realized by three different synthetic methods: one-pot synthesis, the protect-deprotect method and the excess monomer method.^{1,2,7-29,49} In the one-pot synthesis, a dendritic polymer is prepared by a step growth polymerization reaction of a single B-A_y monomer, which is initiated by an A_x initiator. This reaction is shown in Equation 1, where *x* and *y* are functionalities of the reacting species. The integers may or may not be equal; *y* is equal to or larger than 2, and *n* is a large number:

Dendron (if *x* = 1)



An important practical advantage of the one-pot synthesis is its relative simplicity to perform. However, this method lacks reaction control, thus leading to more polydispersed products. It is essentially governed by statistical laws, and for that reason, it yields dendritic products with substantial amounts of structural irregularities (see Figure 1: non-ideal dendrons).

The protect-deprotect divergent method is represented by the reaction sequences shown in Equations 2 and 3:



where *x* and *y* have the same meaning as in Equation 1, C is a protective group that does not react with A under applied reaction conditions, D is a functional group that can react with C, and W is a nonreactive unit resulting from the reaction of C and D.¹⁷⁻¹⁹ Repeating this reaction sequence results in the formation of dendrons or dendrimers, as

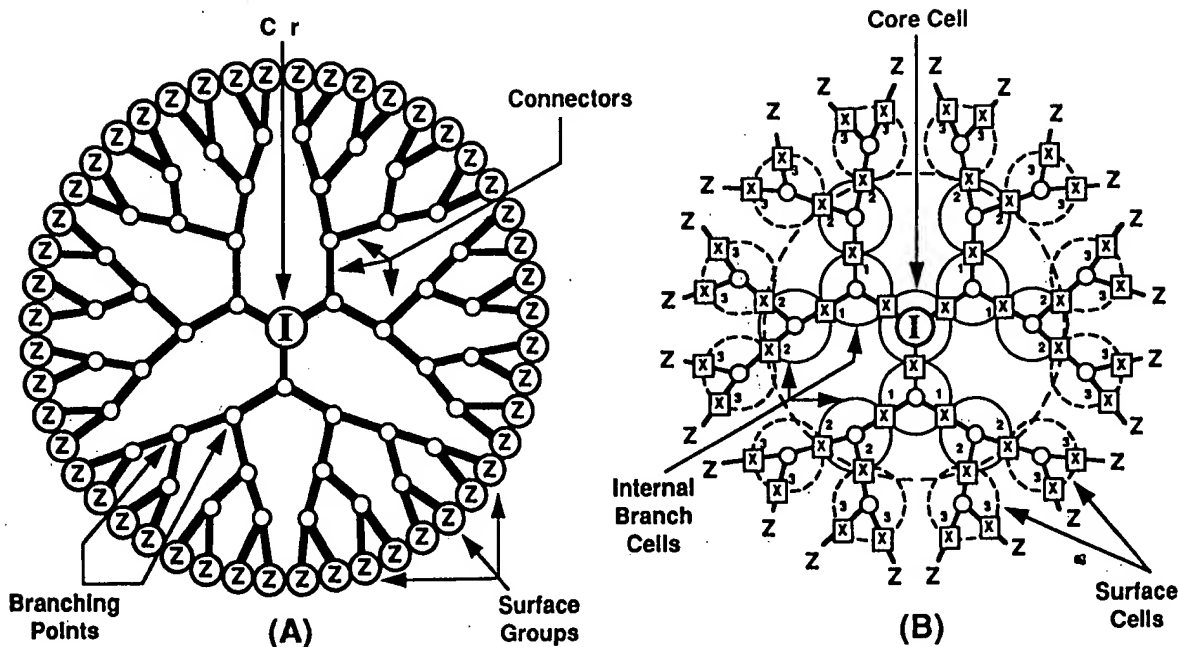
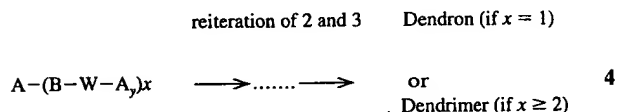


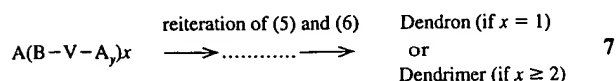
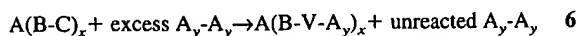
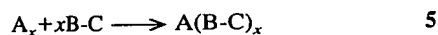
FIGURE 2. Dendritic molecular architecture: (A) basic structural elements and (B) fundamental branch cells.

shown by Equation 4.



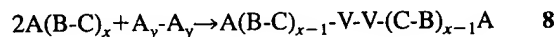
A characteristic feature of this method is that it provides almost complete control of the dendritic molecular growth process and can be used to produce monodispersed dendritic products. However, lower yields and product loss usually associated with protect-deprotect reaction protocol may severely reduce overall product yields to impractical values after only a few reiterations. In more severe cases, this problem may lead to early extinction of dendritic growth if the reiteration schemes are not nearly quantitative.³⁰

The excess monomer method for divergent dendritic synthesis is represented by Equations 5–7.^{1,2,20–29}



All symbols have the same meaning as in the previous equations. However, in this synthetic protocol, groups C react with groups A to yield the nonreactive unit V. Equations 5 and 6 represent the reaction sequence, and Equation 7 generalizes their subsequent reiteration.

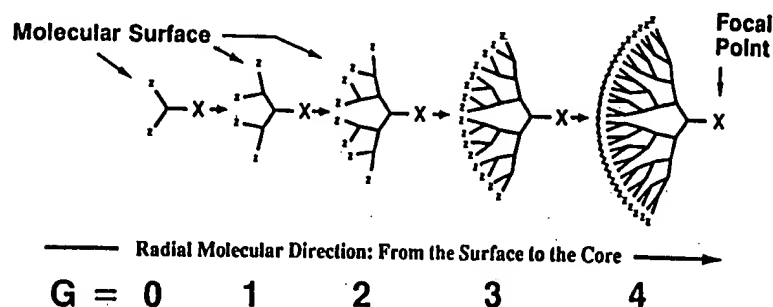
The essential characteristic of this method is that it reduces the probability that reactive groups A will undergo Equation 6, while maximizing the probability that functional groups C will undergo that transformation. Thus, when the $y[A]/x[C]$ ratio is a very large number, the complete conversion of the C groups is accomplished, but the intermolecular reactions between C and A groups (Equation 8) are suppressed.



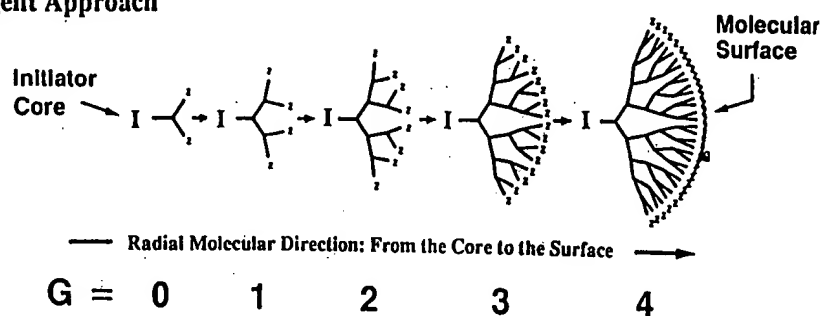
The net result is a favored formation of pure $(A(B-V-A_y))_x$ products (Equation 6) in almost quantitative yields relative to $A(B-C)_x$.

Thus, the excess monomer method combines the advantages of previous methods. It provides high yields of dendritic products (i.e., nearly quantitative, like the one-pot synthesis), which even after a large number of reiterations (up to 5–7), still contain high relative amounts of ideal structures (similar to the protect-deprotect method). For this reason, the excess monomer method currently offers the

(A) Convergent Approach



(B) Divergent Approach



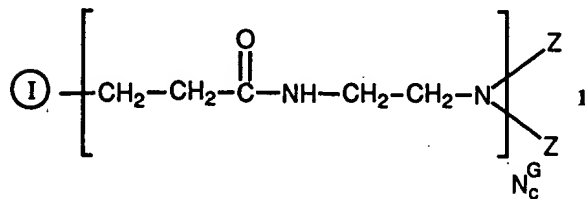
G = Dendritic Generations; Z = Surface Groups

FIGURE 3. Two principal synthetic approaches for preparing dendritic polymers. The divergent approach directly yields dendrimers.

most promising commercial route to dendrimers with well-defined macromolecular architecture.

PREPARATION OF STARBURST

Starburst® polyamidoamine (PAMAM) dendrimers are represented by **Structure 1**:

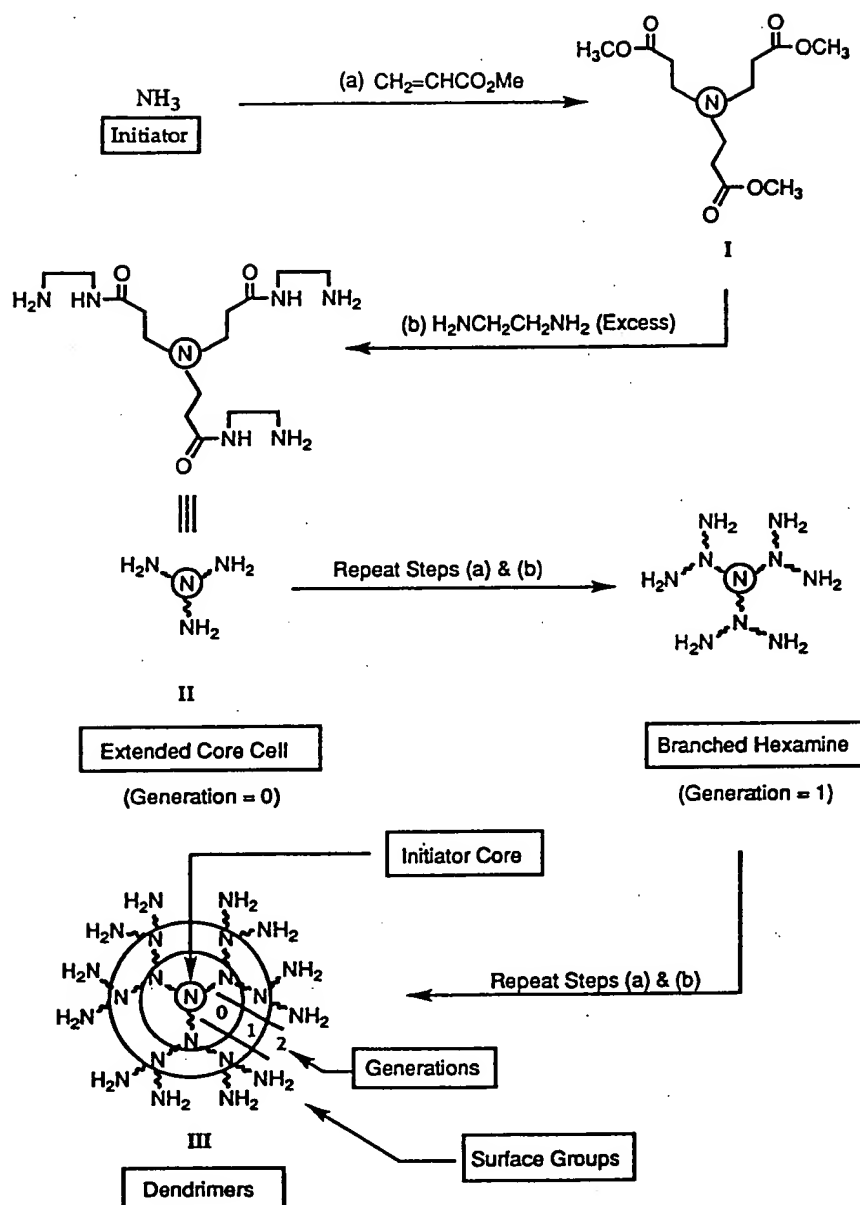


where I is the initiator core, which can be N , or $\text{N}(\text{CH}_2)_x$ with $x = 2, 4, \dots$, or some other suitable amino compound.^{1,2} The functionality of I, N_c is 3 if I is N or 4 if

I is $\text{N}(\text{CH}_2)_x$, whereas G is the number of generations surrounding the initiator core and containing the repeating units $[\text{CH}_2\text{CH}_2\text{C}(\text{O})\text{N}(\text{H})\text{CH}_2\text{CH}_2\text{N}]$. Z represents the terminal groups, which for PAMAM dendrimers are hydrogen atoms.

The preparation of PAMAM dendrimers involves a typical divergent synthesis as shown in **Equation 9**.^{1,2,20-29} It proceeds via a two-step growth sequence that consists of two reiterating reactions: the Michael addition of amino groups to the double bond of methyl acrylate (MA) followed by the amidation of the resulting terminal carbomethoxy, $\text{C}(\text{O})\text{OCH}_3$, with ethylene diamine (EDA). When ammonia is used as the initiator, the synthesis may be represented by the following reaction scheme in **Equation 9**.^{1,2}

In the first step of this process, methanolic ammonia is allowed to react under an inert nitrogen atmosphere with a three-fold molar amount of MA at 25 °C for about 48 h. The resulting triester, **I**, is obtained in nearly quantitative yield (see **Table 1**).^{31,32} This compound is referred to as generation -0.5 PAMAM triester. Its structure and purity are easily verified by various analytical methods. Such methods include electrospray mass spectroscopy (ES-MS) and ^{13}C



9

NMR spectroscopy for structural characterization, and high-performance liquid chromatography (HPLC) or size exclusion chromatography (SEC) with capillary gel electrophoresis (CGE) to determine purity. A typical set of ES-MS and ^{13}C NMR spectra for **I** shows three major signals and four resonances, respectively. The ES-MS signals are found at m/z values of 276, 298, and 202 and are assigned to the protonated molecular ions of the triester **I** ($M_1 = 275$), $\text{I} - \text{H}^+$; its Na^+ analogue, $\text{I} - \text{Na}^+$; and to $\text{H}_2\text{C}=\text{N}^+[\text{CH}_2\text{CH}_2\text{C}(\text{O})\text{OCH}_3]_2$, respectively. The last compound is often formed as a rearranged product of $\text{I} - \text{H}^+$ in the spectrometer (there is no $\text{H}_2\text{C}=\text{N}^+$ signal in the corre-

sponding ^{13}C NMR), resulting from the collisions of these ions with argon gas and subsequent β -cleavage of the expected intermediate. The ^{13}C NMR signal assignments for **I** are as follows: $\delta = 32$ ppm ($=\text{N}-\text{CH}_2-\text{CH}_2-\text{C}(\text{O})-\text{OCH}_3$), $\delta = 49.5$ ppm ($=\text{N}-\text{CH}_2-$), $\delta = 51.4$ ppm ($-\text{O}-\text{CH}_3$), and $\delta = 172.7$ ppm ($-\text{C}(\text{O})-$), respectively, relative to tetramethylsilane (TMS). The absence of other signals in these spectra demonstrates the high degree of purity observed for **I** (usually between 97 and 100%; see Table 1).

The Michael addition reaction (Equation 9a) routinely yields generation -0.5 PAMAM triester, **I**, in practically quantitative yields, and is essentially free of possible

TABLE 1. Typical Yields and Purities of Full Generation Ammonia Core PAMAM Dendrimers^{a,b}

Generation	Series 1		Series 2		Series 3	
	yield (%)	purity (%)	yield (%)	purity (%)	yield (%)	purity (%)
0	100	—	—	92 ^c	100	92.1 ^c
1	100	95 ^c	100	89.8 ^c 98.5 ^d	—	85.3 ^c 96 ^d
2	—	99.2 ^c	—	95.9 ^c 99.5 ^d	—	92.6 ^c 98.4 ^d
3	100	—	100	97.6 ^c 100 ^d	—	93.4 ^c 100 ^d
4	100	99.2 ^c 96.3 ^d	—	95.8 ^c 96 ^d	—	95.8 ^c 94.3 ^d
5	100	— 98 ^d	—	91 ^c 98 ^d	—	87.3 ^c 94.7 ^d

^aYields of obtained full generation products relative to the amounts of the preceding half generation reactants used. For generation 0, yields are given relative to the amount of ammonia initiator core.

^bPurities as weight percent of a monodendrimer component in the reaction products.

^cBy capillary gel electrophoresis.

^dBy high-performance liquid chromatography.

^eEstimated from ¹³C NMR.

dimeric-oligomeric adducts. These two features of the alkylation step are critical for this divergent synthesis strategy to succeed. Simple removal of solvent and excess MA leads to a product (Equation 9a) that can be used directly as a reactant (template) for the subsequent amidation reaction (Equation 9b). Usually, there is no yield (mass) loss in the purification of "crude" I, which is often a negative feature in many multistage, protect-deprotect protocols.

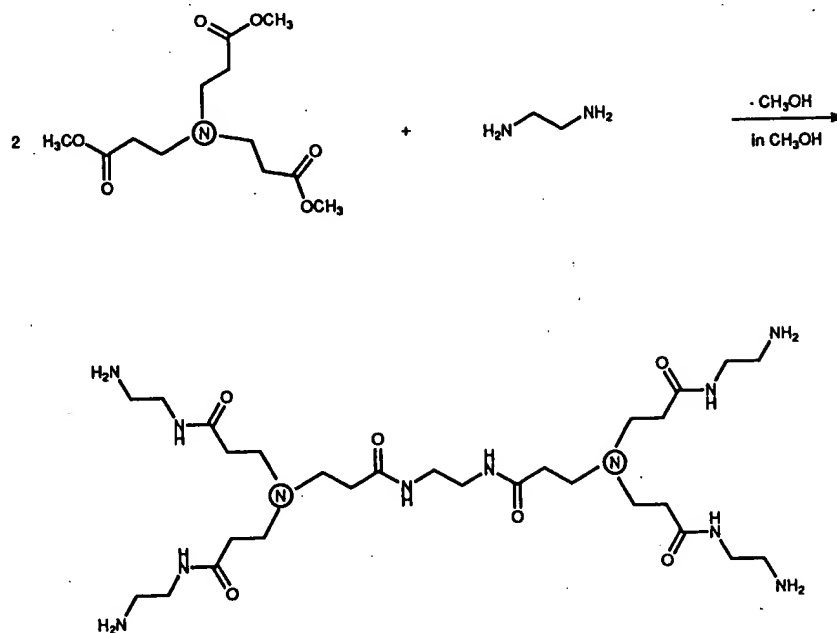
The next step (Equation 9b) in the first iteration reaction sequence leading to the synthesis of PAMAM dendrimers involves a reacting triester I with a large excess of EDA to produce generation 0 PAMAM triamine, II.^{31,32} Detailed investigation of this reaction showed that larger EDA excesses resulted in higher yields of ideal Structure II. Smaller excesses favored side reactions to give higher molecular weight by-products, such as dimers, trimers, or higher oligomers, resulting from intermolecular reactions like the one shown in Equation 10.

In practice, the amidation reaction is performed under inert nitrogen in methanol and requires about 48 h at 0 °C for completion. The resulting reaction mixture is heated for 30 min at 40 °C, followed by stripping of volatiles, which include methanol solvent and unreacted EDA. This procedure yields practically quantitative amounts of pure triamine II. A typical ¹³C NMR for this compound shows five well-defined signals that can be assigned to the expected structure as follows: $\delta = 32.6$ ppm (=N-CH₂-CH₂-), $\delta = 39.6$ ppm (-CH₂-NH₂), $\delta = 41.6$ ppm (-C(O)-N(H)-CH₂-), $\delta = 48.5$ ppm (=N-CH₂-CH₂-), and $\delta = 174.8$ (-C(O)-), relative to TMS, respectively. Typical ES-MS exhibits four major signals with *m/z* values at 359 and 381, which can be assigned to H⁺ and Na⁺ derivatives of the ideal Structure II

in Equation 9. The signal at *m/z* = 659.5 can be assigned to dimer IV, and the signal at *m/z* = 246 to a two-armed product of incomplete amidation of I. Occasionally, a signal at *m/z* = 341 may be observed and can be assigned to an imidazoline species obtained from II by eliminating a molecule of water.

The product distribution within a crude reaction product II, as determined by ES-MS, depends on the conditions and the excesses of EDA monomer used for the synthesis. Therefore, at this amidation reaction stage, early deviations from ideal dendritic growth may occur, leading to the formation of imperfect dendritic by-products. Nevertheless, HPLC, SEC, and CGE, indicate that this procedure can be optimized to give triamine II in purities as high as 96–98% (see Table 1). Thus, structural defects can be substantially minimized while the yield of the ideal structure product can be kept nearly quantitative. Just as for the alkylation reaction, this feature enables the divergent synthesis to continue without extensive purification of intermediate II. Consequently, even after many reiterations of the reaction sequence, an important feature of the excess monomer method is that it allows the synthesis of high yields of regular dendritic products even at generations as high as 9 or 10.³³ The first serious deviations from the ideal structure are detected only at about generation 7 (Figure 4).

The preparation of triamine II (Equation 9b) completes the first full reiteration sequence employed in the divergent synthesis of PAMAM dendrimers. This reaction sequence is used for advancement to higher generation dendrimers.^{1,2,20–29,31,32} This advancement involves the synthesis of half and full generation intermediates (i.e., ester- and amine-terminated intermediates, respectively). For example, the second iteration of this sequence produces



10

generations 0.5 and 1, the hexaester and hexaamine, respectively. The same reactions are performed in the same way as for generations -0.5 and 0. They yield essentially quantitative amounts of the generational products through generation 5. Typical yields and purities of these intermediates are listed in Table 1.³⁴

DIVERGENT SYNTHESIS

As Figure 3B shows, a divergent molecular growth process involves a series of geometrically progressive additions of branches upon branches. This growth produces a tethered arrangement of ordered, layered branch cells around a central core. As this process progresses from the core toward the outer surface, the dendrimer architecture is developed by the construction of the components that define a dendrimer hierarchy: core branch cells, interior branch cells, and surface branch cells. As Figure 2 shows, the presence of these three components represents the *conditio sine qua non* for any fully developed dendron-dendrimer structure. In other words, the components provide the minimal structural requirement to designate a molecular structure as either a dendron or dendrimer (Figure 1).

Some general features of a divergent growth process leading to a fully developed dendrimer structure can be seen in Figure 5.³⁵

Thus, the first component of a dendrimer structure to form during a divergent synthesis is the core cell (Structure A in Figure 5). In PAMAM dendrimer synthesis (Equation 9), this construction is completed after the ammonia initia-

tor core first reacts with methyl acrylate giving a core cell that remains unchanged during the subsequent dendritic growth process. Generally, the structure of the core cell is unique within a dendrimer molecule (i.e., different from either of the other two components yet to form).

The second fundamental component of dendritic architecture to form during the divergent growth process is the surface cells (Structure B in Figure 5). As Equation 9 and Figure 5 show, this construction phase is complete at the one-and-a-half iterative sequence stage (i.e., at generation 0.5). The surface branch cell structure differs from the core cell because one of its $-\text{[CH}_2\text{CH}_2\text{C(O)}\text{]}-$ groups is replaced by an ethyleneimino, $-\text{[N(H)CH}_2\text{CH}_2\text{]}-$, unit in the surface cells. In addition, the surface branch cells possess reactive functional groups such as $-\text{C(O)-OCH}_3$, or $-\text{NH}_2$ groups, for further extension of the divergent growth process.

Another distinction between the surface branch cells and the core branch cell is that there is usually only one core cell per dendrimer molecule, whereas the number of surface cells is in fact larger than the total number of all core and interior cells taken together. The total number increases from generation to generation according to a geometric progression law, which is represented by Equation 11:

$$Z' = N_c N_b^G / N_b \quad 11$$

where Z' is the number of surface branch cells, N_c is the multiplicity of the core, N_b is the multiplicity of the branch cells, and G is the generation number.^{4,5}

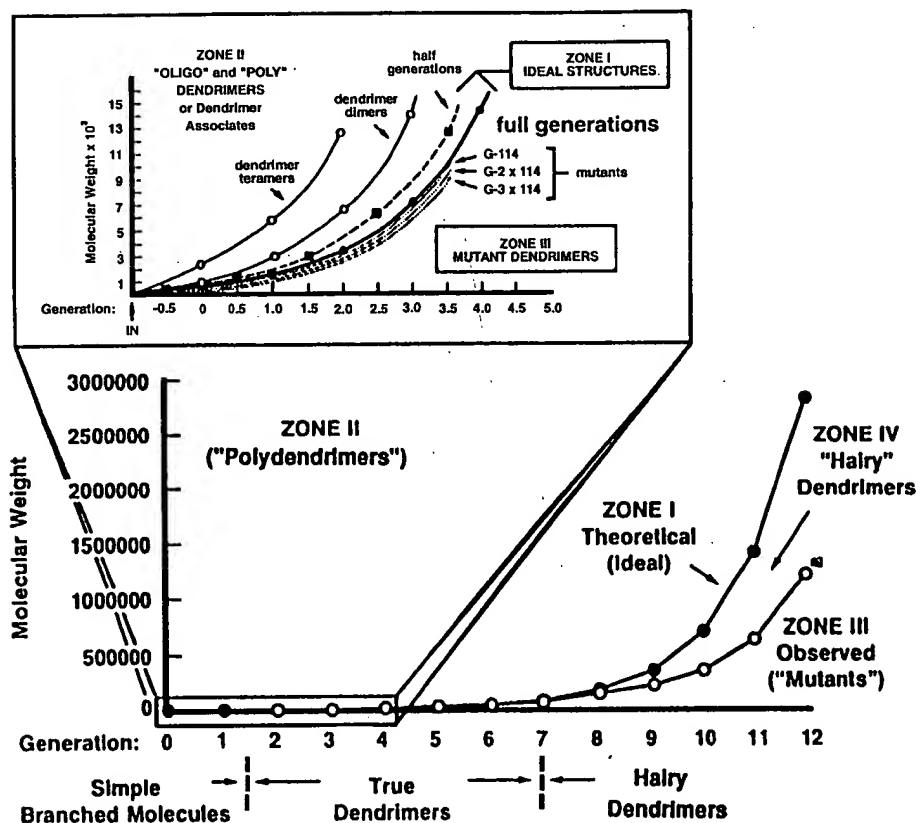


FIGURE 4. Theoretical versus observed molecular weight of polyamidoamine Starburst dendrimers. Zone I comprises ideal dendrimer structures, zone II contains oligo and poly dendrimers, and zone III comprises defective mono dendrimers (above generations 9 or 10 mostly hairy dendrimers).

Chronologically, the last three dendritic components to develop during the divergent growth process are the interior branch cells (Structure C of Figure 5). In a typical PAMAM dendrimer synthesis, these cells first appear at generation 1.5. They provide covalent connectivity in a radial direction from the core cell to the surface cells and are structurally similar to the surface cells. They possess an identical dendritic repeating unit, but the surface cells have additional surface groups that may or may not be reactive for further growth. Thus, for PAMAM dendrimers, the repeating unit common to the interior and surface cells is $-[N(H)CH_2CH_2N[CH_2CH_2C(O)]_2]$, and the reactive surface groups on the surface cells may be either ester or primary amine groups.

In contrast to the surface cells, interior cells are inert and less mobile. They may be found between the core cell and the surface cells, between other interior cells and the surface cells, or between two layers of interior cells, depending on a particular dendrimer generation number. Functionally, they provide an interior infrastructure (i.e., internal

scaffolding) for the entire dendrimer structure. In that respect, the interior cells represent the key component that connects and holds together the entire dendrimer molecule.

DENDRITIC BRANCHING

The three dendritic architectural components are formed chronologically during the divergent growth process (Figure 5). They develop along the central symmetry axes of each main monodendron. Thus, during a divergent dendritic growth process, each of these axes represents a main reaction coordinate that extends in space (i.e., from the core to the surface) and in time (i.e., from generation to subsequent generation).

When the first layer of branch cells develops around the initiator core, the resulting structures consist of the core cell and the N_c surface cells (generation B of Figure 5), where N_c represents the functionality of the core atom or atomic group. Clearly, this structure does not represent a fully developed dendrimer structure because it is missing one of

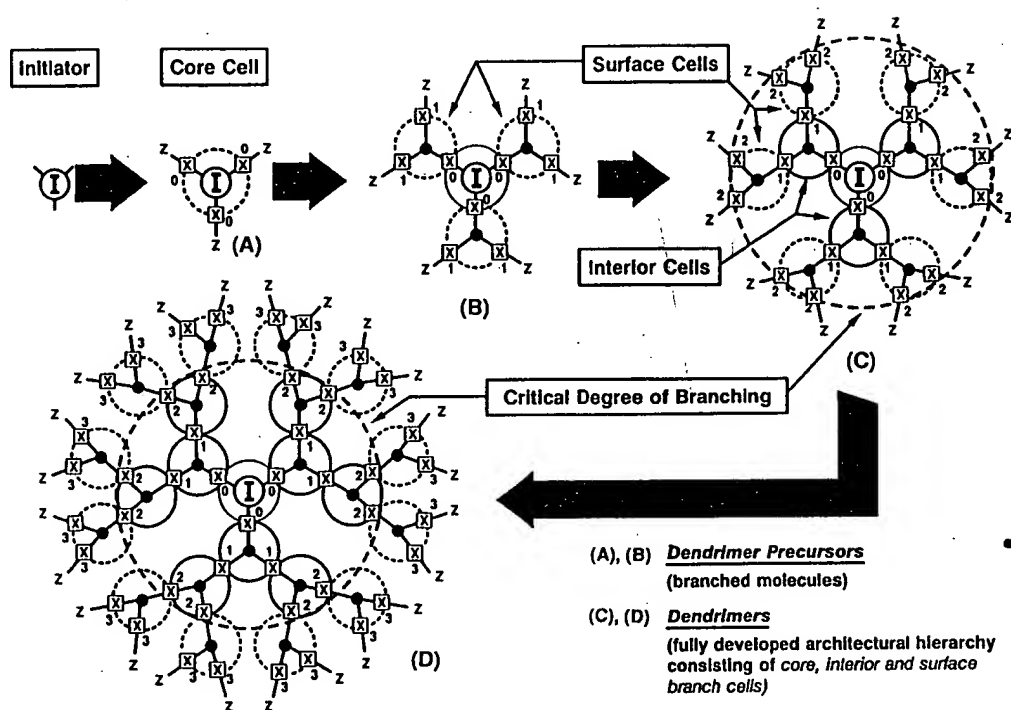


FIGURE 5. Divergent development of dendritic structure. (A and B) dendrimer precursors (i.e., simple branched molecules) (C and D) true dendrimers with fully developed architectural hierarchy consisting of core, interior, and surface branch cells. Note the critical stage of structural development in C.

the three fundamental components required, the interior cells. Therefore, this and other similarly branched structures (generation A of Figure 5) may be considered precursors to dendrimer structures but not dendrimers. The complete development of a dendrimer structure requires at least progression through generation 1.5 (Equation 9 and generation C of Figure 5).

Thus, a fully developed dendrimer structure first appears only after passing through the growth stage above. At that point, the lightly branched structures (generations A and B of Figure 5) transform into fully developed dendrimers that, in the genealogy of the synthesis, contain all three branch cell components (i.e., generation C of Figure 5). At this level of structural complexity, the transition from lightly branched to true dendrimer intermediates takes place. We refer to this transition as the critical degree of branching.³⁵

HIERARCHICAL ORDER OF STRUCTURE

Only after the critical branching stage (i.e., where core, interior, and surface branch cells form as shown in Figure 5) does the resulting product possess the level of structural complexity needed for a fully developed dendritic structure. Thus, within every family of branched compounds, this critical degree of branching represents an interface between

simple branched family members and their fully developed dendrimer counterparts. The former can be considered precursors to fully developed dendrimers. In addition, within every homologous series of dendritic compounds, there exists a hierarchical order of molecular complexity representing the functional dependence of molecular weight or generation number. This order is illustrated in Figure 6, which compares mono-dendrimers (Zone 1) to oligo poly-dendrimers (Zone 2) and defective (mutant) mono-dendrimers (Zone 3).

DE GENNES DENSE-PACKED STATE

Because of the geometrically progressive, growth pattern expressed by Equation 11, dendrons and dendrimers may be constructed in a precise manner. Therefore, such compounds are expected to have precise degrees of polymerization, exact molecular weights, and represent perfectly isomolecular macromolecules.^{4,5}

In such systems, the Z values ($Z = N_b \cdot Z'$ of Equation 11) represent saturation limits at which no additional monomer units can be added to the outer shell at a particular generation.^{3,4} Therefore, the surface shell's saturation at a particular generation renders that dendrimer surface inert toward further reactions with the reagent used to obtain that

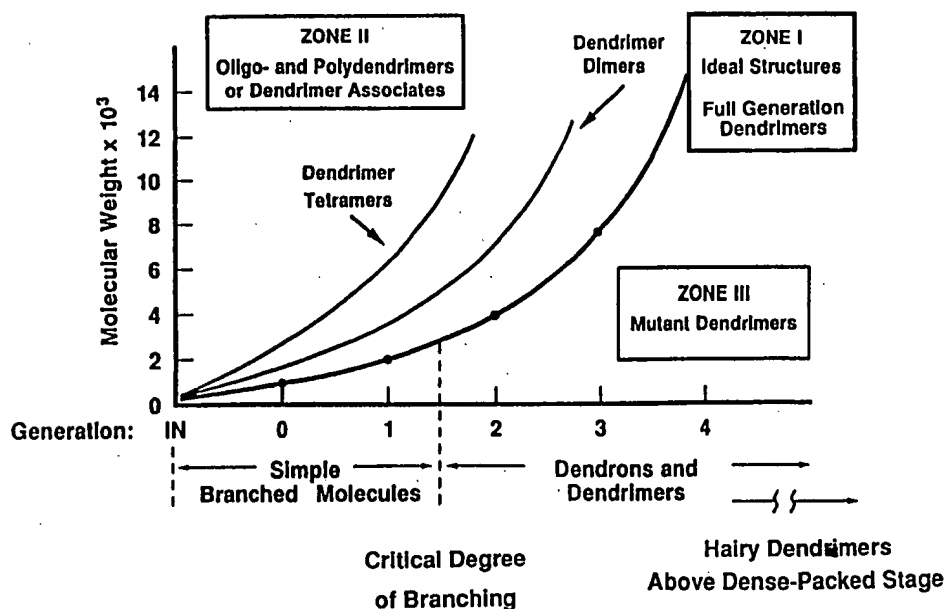


FIGURE 6. Hierarchical order of structural complexity in a homologous series of branched molecules: simple branched molecules, dendrimers, and hairy dendrimers. Note the critical degree of branching for the PAMAM family at generation 1.5.

generation. No additional increase in molecular weight is possible regardless of how large an excess of reactants is used. Divergent dendritic growth, which precisely obeys this mathematically directed growth pattern, is referred to as ideal dendritic growth. Dendrimers or dendrons resulting from such a growth are considered ideal or perfect dendritic structures.^{4,5} In such structures, the degree of polymerization and the corresponding molecular weights are related to N_c , N_b , and G values as Equations 12 and 13 indicate.

$$N_{RU} = N_c \left[\frac{N_b^{G+1} - 1}{N_b - 1} \right] \quad 12$$

$$M = M_c + N_c \left[M_{RU} \left(\frac{N_b^{G+1} - 1}{N_b - 1} \right) + M_t N_b^{G+1} \right] \quad 13$$

Because the radii of dendrimer molecules increase in a linear manner as a function of G , whereas the surface cells amplify from generation to generation according to a geometric progression (i.e., the branching law, $N_c N_b^{G-1}$), ideal dendritic growth cannot extend indefinitely. There will be a critical generation at which the reacting dendrimer surface will not have enough space to accommodate all of the mathematically required new units at that saturation

point. This stage in divergent dendritic growth is referred to as the de Gennes dense-packed state.³⁶ At this stage, these surfaces become so crowded with exterior groups that, although they are chemically reactive, they are sterically prohibited from participating further in ideal dendritic growth.⁴

Nevertheless, this handicap does not preclude dendritic growth beyond this point. As demonstrated by mass spectral studies, further increases in the molecular weight can occur beyond the de Gennes dense-packed stage (Figure 4). However, products resulting from dendritic growth continuing beyond the dense-packed stage are imperfect in structure because all surface groups in the precursor generation are sterically precluded from undergoing further reaction. Presumably, a sterically determined fraction of these groups will remain trapped under the newly formed dendrimer surface, yielding a new type of dendrimer product that contains either functionally mixed molecular surfaces, possessing two types of surface groups (i.e., carbomethoxy and amino units for PAMAM dendrimers) or monofunctional surfaces possessing only one type of surface groups in at least two generation levels.³⁷ In any case, the number of functional groups on the newly formed molecular surfaces will not correspond to the predictions of the geometric branching law (Equation 11) but will fall between the mathematically predicted value for that generation (Z_G) and the corresponding value for the precursor generation (Z_{G-1}).

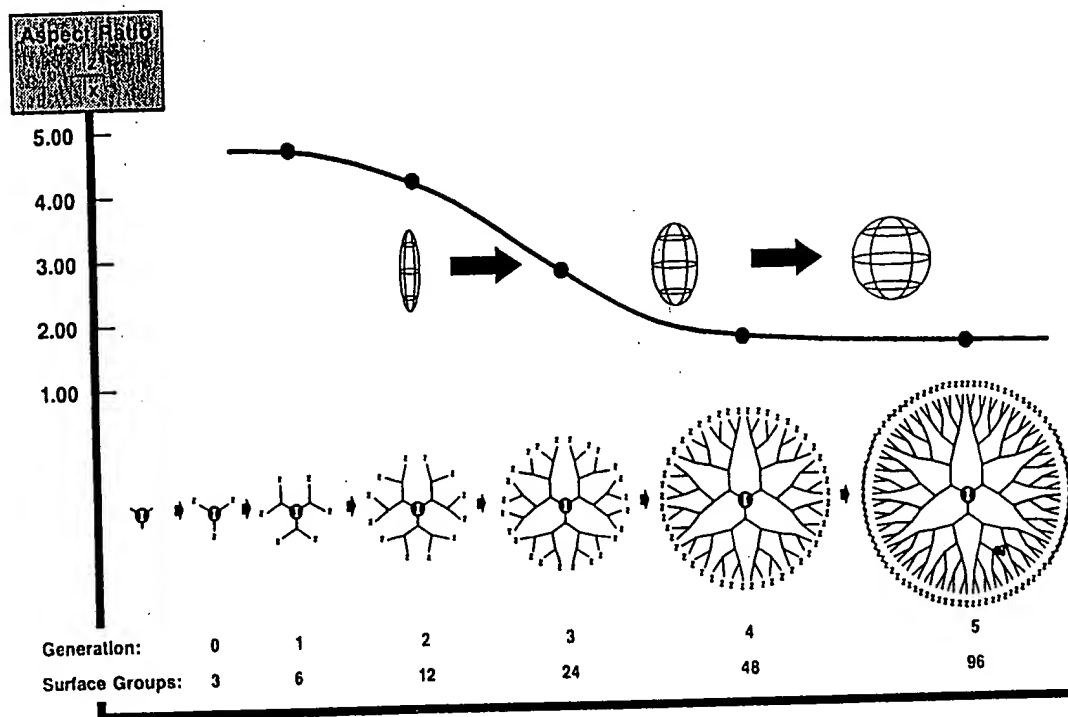


FIGURE 7. The shape change in ammonia core Starburst PAMAM dendrimer molecular topology. Aspect ratio (I_z/I_x) as a function of generation. Note the shape transition from generation 3 to generation 4.

This value yields defective dendrimer generations called hairy dendrimers (Figure 6). Their external surface groups can be envisioned to contain irregular dendron cusplike growths protruding from a bold, regular molecular surface.³⁷

PROPERTIES OF STARBURST

Computer-simulated modeling related to size and shape have been performed on PAMAM dendrimers. The molecular dynamics calculations based on the force field acting on all atoms in equilibrated structures showed that, with increasing generations, these dendrimers seem to develop by passing through a continuum of molecular shapes ranging from open extended structures to closed globular spheroids. This change in shape apparently occurs because tethered steric constraints are imposed on the developing branches. This explanation was determined by the change observed for the calculated aspect ratio of the corresponding longest and shortest principal moments (I_z/I_x) in these developing structures (Figure 7).³⁸

As Figure 7 shows, tridendron PAMAM dendrimers appear spherical after about generation 4. Within these spheres, the solvent accessible surface (SAS) seems to increase with generations so that the fraction of the internal molecular surface increases from about 29% of the total

SAS for generation 4, to 69% for generation 5, and 124% for generation 6. However, the molecular density (M/V) shows a clear minimum at about generation 4 (Figure 8), suggesting that fully developed PAMAM dendrimers have a great deal of accessible internal surface area in a solvent-filled intramolecular free volume, which may consist of internal cavities and channels.⁵

As Figure 9 shows, ^{13}C NMR measurements of spin-lattice relaxation times of specifically tagged PAMAM dendrimers (deuterated in either the surface layers or in the internal segments) appear to support this view. They showed considerably reduced mobility in the outer surface groups relative to that in the interior segments.³⁹⁻⁴¹ This behavior indicates a unimolecular encapsulation type topology in which a relatively soft or spongy interior is enclosed within a considerably harder outer molecular surface or crust.^{4,42} This hypothesis was recently supported by Dutch scientists who referred to this feature as a dendritic box.⁴³

Our recent rheological and differential scanning calorimetry (DSC) data also appears to support this model.⁴⁴ Thus, we discovered that PAMAM dendrimer solutions exhibited Newtonian behavior (Figures 10a and 10b) over a wide range of shear rates (from about 150 to about 750–1250 s^{-1}), temperature (from 15 to 40 $^{\circ}\text{C}$), molecular weights (500 to 29,000 or from $G = 0$ to $G = 5$), and concentrations

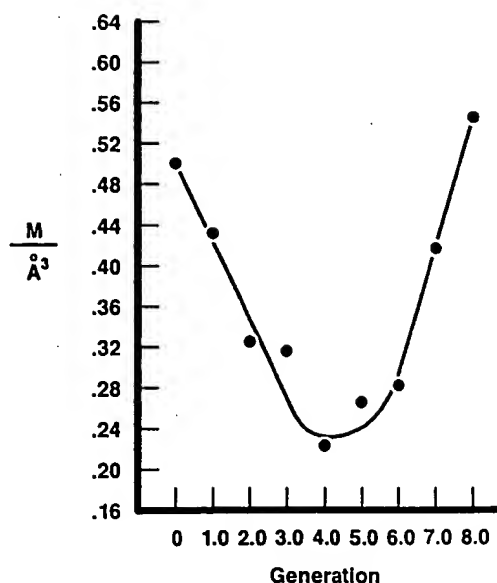


FIGURE 8. The molecular density of ammonia core Starburst® PAMAM dendrimers as a function of generation. Note the minimum at generation 4.

(30–75% by weight). In addition, neat dendrimers showed a linear increase in viscosity with molecular weight at temperatures from 90 to 115 °C.

Furthermore, DSC measurements on PAMAM dendrimers (from EDA and NH₃ cores) showed exponentially increasing glass transition temperatures with their increasing molecular weight reaching an asymptotic value at PAMAM generation 3 or 4 (Figure 11).⁴⁴

From these results, PAMAM dendrimers appear to possess outer surfaces that are substantially impenetrable to

¹³C NMR SPIN-LATTICE RELAXATION TIMES VS. GENERATION

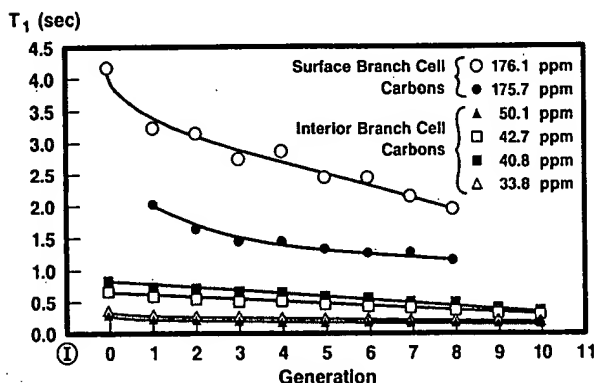


FIGURE 9. ¹³C NMR spin-lattice relaxation times (T₁) as a function of generation for surface branch cells and interior branch cells of ammonia core Starburst PAMAM dendrimers.

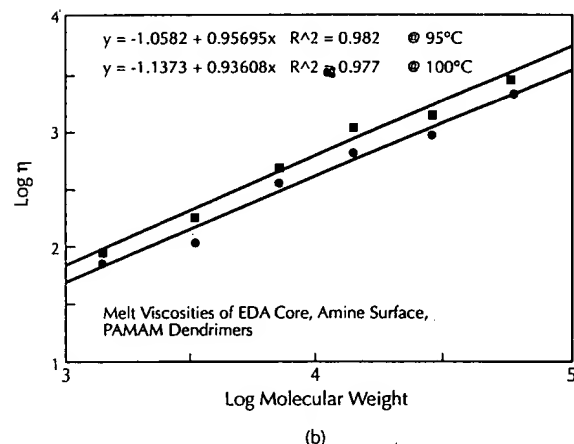
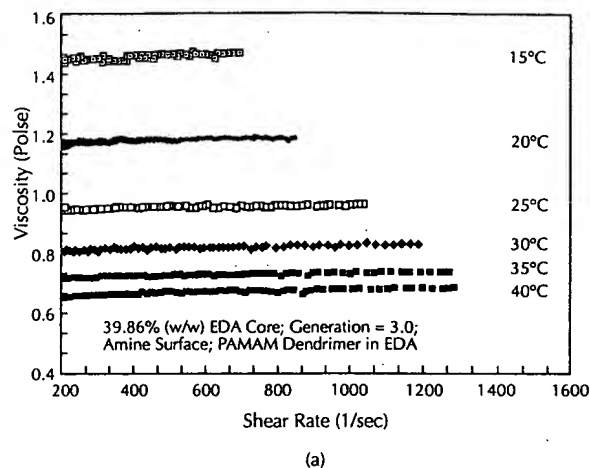


FIGURE 10. Rheological behavior of ethylene diamine core Starburst PAMAM dendrimers: (a) viscosity as a function of shear rate for a typical dendrimer and EDA solution; (b) viscosity as a function of molecular weight (i.e., generation) for neat dendrimer melts.

neighboring dendrimers (from the viscosity data), while retaining pronounced segmental mobility within the internal volume, possibly around the core and over the first two to three generations. The DSC results also suggest that at the fifth branch layer around the core (i.e., at generation 4), segmental motions responsible for the glass transition apparently reach their limiting values and cannot be extended any further. This limit is indicated by the sharp T_g increase from -11 °C for generation 0 to ~ 8 °C for generation 4 in Figure 11. In the case of higher generation dendrimers, T_g values are unaffected by further increases in molecular weight.

The molecular dimensions of PAMAM dendrimers have been examined by computer modeling and by size exclusion chromatography.^{4,5} In general, excellent agreement between calculated and experimental results was observed. These

GLASS TRANSITION TEMPERATURES OF PAMAM DENDRIMERS

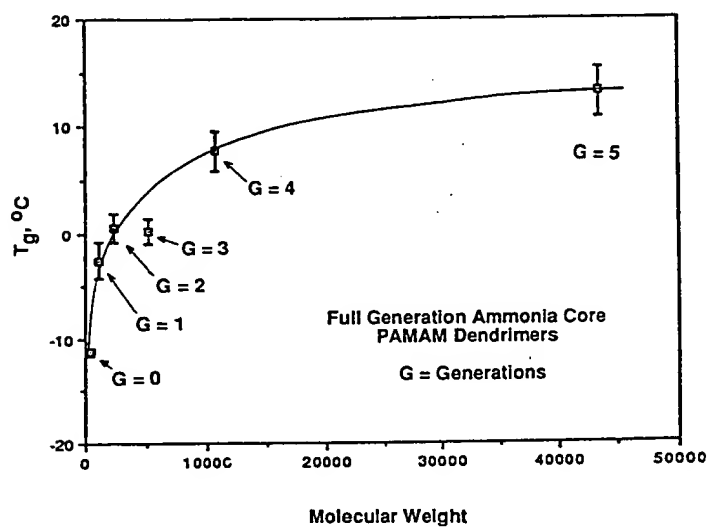


FIGURE 11. Glass transition temperature (T_g) as a function of molecular weight (i.e., generation) of full generation ammonia core Starburst PAMAM dendrimers. Note asymptotic leveling at generations 4 and 5.

ELECTROSPRAY MASS SPECTROSCOPY OF PAMAM DENDRIMERS

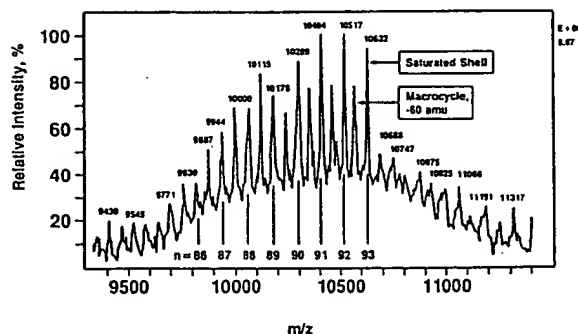
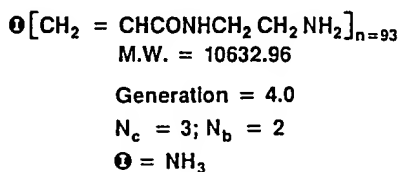
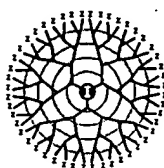


FIGURE 12. Typical electrospray mass spectrum of a generation 4 ammonia core Starburst PAMAM dendrimer. Note peaks corresponding to the missing arm and looped mutant structures.

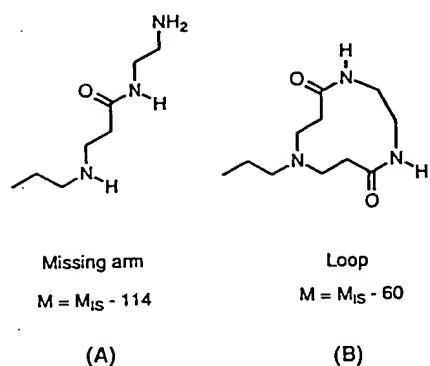


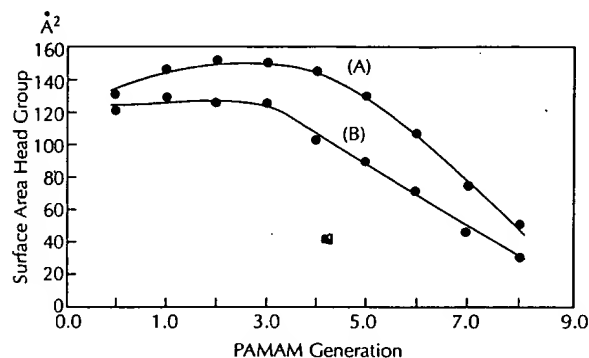
FIGURE 13. Structures of the missing arm and loop defects in the Starburst PAMAM dendrimers.

studies indicate diameters over a range of 1 to 10 nm from generation 0 to generation 8, respectively, with a linear enhancement of 0.7 and 1.2 nm per generation.^{4,5} At these nanoscopic dimensions, direct observation of single dendrimer molecules are possible with electron microscopy. These studies showed that dendrimers were observable as highly monodispersed spheroids.² For example, the sodium salt of generation 3.5 PAMAM dendrimer showed that almost 90% of all particles had diameters ranging within 10% of the average value determined by computer simulations. This feature seems to result directly from the control that a synthetic chemist has over critical molecular design parameters such as size, shape, surface chemistry, flexibility, and topology. The complexity of this dendritic architecture also reflects the extraordinary control provided by the excess monomer method. Analytical methods, such as ES-MS, allow the ideal construction to be examined in great detail.⁴⁵ For example, in generation 4 PAMAM (Figure 12) and in addition to the expected ideal structure ($M_{IS} = 10,632$), a series of the so-called missing arm (at $M = M_{IS} - \times 114$) and looped (at $M = M_{IS} - \times 60$) defects is also formed.^{46,47}

The missing arm defects (Figure 13A) correspond to products of incomplete alkylation, or retro-Michael reaction, leading to a mass defect of one or more units (i.e., $\times \cdot (-CH_2CH_2C(O)N(H)CH_2CH_2N)$ or $\times \cdot 114$ amu). However, loops (Figure 13B) result from intramolecular bridging of a neighboring carbomethoxy group by an amine-terminated functionality (i.e., $\times \cdot (NH_2CH_2CH_2NH_2)$ units or a mass defect of $\times \cdot 60$ amu).⁴⁵ Statistical treatments of these data show that despite these minor structural imperfections, the molecular weight distributions of the resulting dendrimers are narrow and are routinely observed to be as low as $\bar{M}_w/\bar{M}_n = 1.0003$ to 1.0005. Clearly, these results represent a significant step toward preparing perfectly isomolecular, high molecular weight polymers.

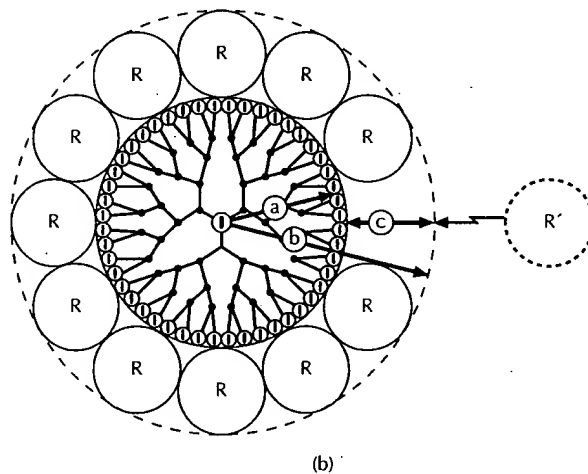
The dendrimer surface group reactivity changes little until the de Gennes dense-packed stage is approached. Within the PAMAM series, this stage occurs at about generation 7, above which the reactivity decreases significantly, indicating considerable constrictions in the surface area per terminal group as Figure 14 shows (compare also with Figure 4).⁵

Above generation 4, the surface area available per terminal group decreases dramatically. The surface area approaches the cross-sectional area of the amine-terminated



Curve (A): Assumes 95% of theoretical surface groups/generation
Curve (B): Assumes 100% of theoretical surface groups/generation

(a)



(b)

FIGURE 14. Sterically induced stoichiometry (SIS) in chemical reactions involving dendrimers as substrates: (a) plot of surface area per terminal group \bar{Z} as a function of generation for ammonia core Starburst PAMAM dendrimers, assuming 95% of the theoretical number of terminal groups are present. (b) schematic representation of steric hindrances to the incoming reactant (R') to a terminal group above the critical dendrimer generation for SIS, assuming 100% of terminal groups are present.

branch segment (i.e., $\cong 33\text{\AA}$) at generation 8, leading to increased steric hindrance to approaching reagents (Figure 14B). Sterically induced stoichiometry (SIS) results.⁴ At higher generations (i.e., greater than $G = 7$ in PAMAM series), the rate constants and conversions on these dendrimer surfaces decrease substantially, resulting in longer reaction times and larger populations of imperfect structures.

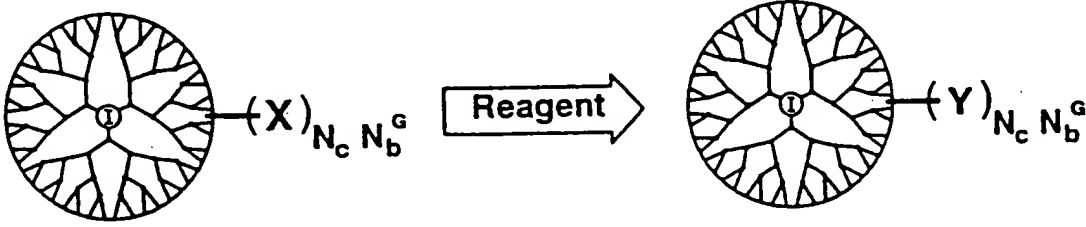
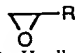
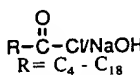
Dendrimer interiors and surfaces can be readily modified to possess chemically reactive or passive functional groups. Currently, over thirty different interiors have been synthesized in our laboratory and elsewhere. Dendrimer interiors may contain carbon, nitrogen, oxygen, silicon, phosphorous, metals, or virtually any element found in the periodic table. Over 100 dendrimer surface modifications have been reported to date. A few of the functional groups integrated into PAMAM dendrimer surfaces are illustrated in Table 2.

Generally, dendrimer surfaces can be modified to contain electrophilic or nucleophilic, hydrophobic or hydrophilic, and cationic or anionic moieties. Thus, dendrimer surface

modification allows virtually every known bonding mode to integrate onto the surface of these precisely controlled nanoscopic structures. As such, dendrimers possess highly reactive surfaces that may participate in either classical (sub-nanoscale chemistry) or novel nanoscopic conversions (Figure 15). In the latter, dendrimers have been validated as reactive nanoscopic building blocks suitable for constructing various megamolecular structures. These building blocks follow basic rules of chemical combination with nano-particles such as proteins, poly(nucleic acids), DNA, RNA, or other dendrimers to produce nanoscopic compounds, clusters, and assemblies.

Many of these new nanostructures exhibit commercial promise as gene transfection and drug delivery agents, immuno-diagnostic reagents, nano-catalysts, magnetic resonance imaging contrast agents, nano-reactors, and nano-calibrators.^{48,50-55} In conclusion, dendrimers should play a significant role in the systematic investigation of nanoscopic chemistry, architecture, and properties in biological and abiotic areas of interest.

TABLE 2. Dendrimer Surface Reactions with Various Electrophiles and Nucleophiles

					
	DENDRIMER TYPE	DENDRIMER SURFACE, (X)	GENERATIONS	REAGENT	DENDRIMER SURFACE, (Y)
ELECTROPHILIC REAGENTS					
1.	PAMAM	-NH ₂	0-10	CH ₂ =CHCO ₂ Me	-N-(CH ₂ CH ₂ CO ₂ Me) ₂
2.	PAMAM	-NH ₂	0-4	BrCH ₂ CO ₂ Me	-N-(CH ₂ CO ₂ Me) ₂
3.	PAMAM	-NH ₂	0-10	 (R=H, alkyl, aryl)	-N-(CH ₂ CHOHR) ₂
4.	PAMAM	-NH ₂	0-6	 R = C ₄ - C ₁₈	-NHCOR
5.	PAMAM	-NH ₂	0-4	Aryl-CH ₂ -Cl	-NH-CH ₂ -Aryl
NUCLEOPHILIC REAGENTS					
6.	PAMAM	-CO ₂ Me	0-10	H ₂ N(CH ₂) ₂ -NH ₂	-CONH(CH ₂) ₂ -NH ₂
7.	PAMAM	-CO ₂ Me	0-3	H ₂ N(CH ₂) ₆ -NH ₂	-CONH(CH ₂) ₆ -NH ₂
8.	PAMAM	-CO ₂ Me	0-3	N-(CH ₂ CH ₂ NH ₂) ₃	-CONH(CH ₂) ₂ -N[(CH ₂) ₂ -NH ₂] ₂
9.	PAMAM	-CO ₂ Me	0-9	H ₂ NCH ₂ CH ₂ OH	-CONHCH ₂ CH ₂ OH
10.	PAMAM	-CO ₂ Me	0-4	H ₂ N-(CH ₂) ₂ -NH(CH ₂) ₂ -OH	-CONH(CH ₂) ₂ -NH(CH ₂) ₂ -OH

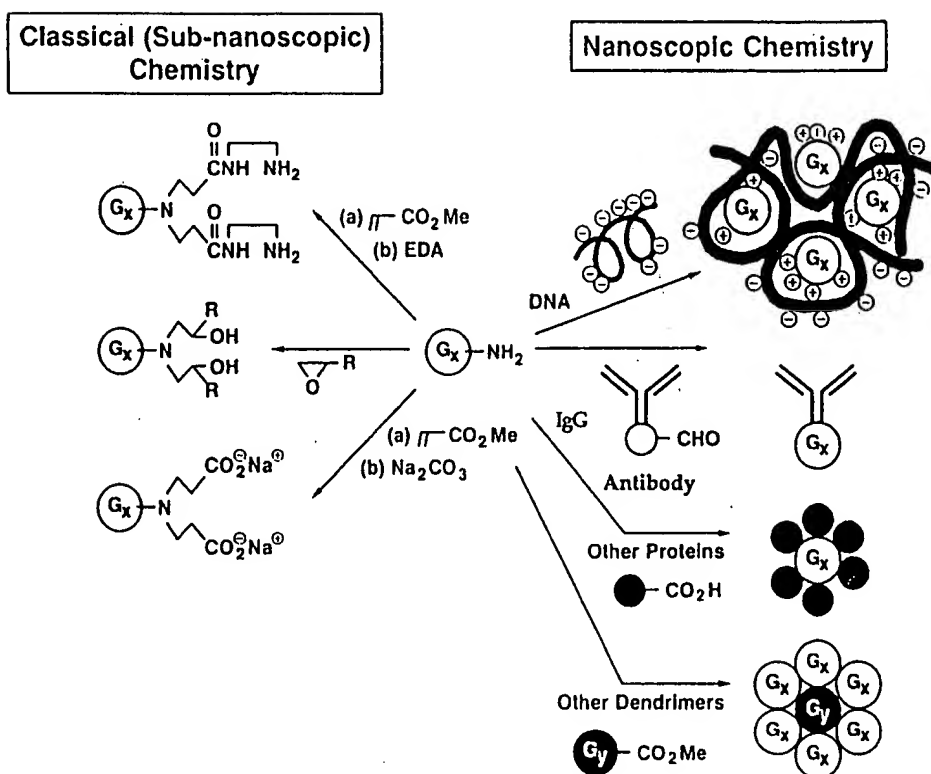


FIGURE 15. Sub-nanoscale and nanoscale chemistry on dendrimer surfaces, where $G_x = G_y$ = generations 1–7.

REFERENCES

- Tomalia, D. A.; Dewald, J. R.; Hall, M. J. et al. *Preprints 1st Society Polymer Science Japan International Polymer Conference* Kyoto, Japan, 1984; 65.
- Tomalia, D. A.; Baker, H.; Dewald, J. R. et al. *Polymer J. (Tokyo)* **1985**, *17*, 117.
- Tomalia, D. A.; Baker, H.; Dewald, J. R. et al. *Macromolecules*, **1986**, *19*, 2466.
- Tomalia, D. A.; Naylor, A. M.; Goddard, W. A., III *Angew. Chem. Int. Ed. Engl.* **1990**, *29*, 138.
- Tomalia, D. A.; Durst, H. D. *Topics in Current Chemistry* Vol. 165: *Supramolecular Chemistry I—Directed Synthesis and Molecular Recognition*; Weber, E., Ed.; Springer Verlag: Berlin, 1993; p 193–313.
- Fréchet, J. M. J.; Jiang, Y.; Hawker, C. J. et al. In *Proceedings of IUPAC International Symposium on Macromolecules* Seoul, Korea, 1989.
- Hawker, C. J.; Fréchet, J. M. J. *J. Am. Chem. Soc.* **1990**, *112*, 7638.
- Hawker, C. J.; Fréchet, J. M. J. *J. Chem. Soc., Chem. Commun.* **1990**, 1010.
- Hawker, C. J.; Fréchet, J. M. J. *Macromolecules* **1990**, *23*, 4726.
- Miller, T. M.; Neenan, T. X. *Chem. Mater.* **1990**, *2*, 346.
- Bochkarev, M. N. *Organomet. Chem. USSR* **1988**, *1*, 115.
- Kim, Y. H.; Webster, O. W. *Polym. Prepr. Am. Chem. Soc.* **1988**, *29*, 310.
- Kim, Y. H.; Webster, O. H. *J. Am. Chem. Soc.* **1990**, *112*, 4592.
- Hawker, C. J.; Lee, R.; Fréchet, J. M. J. *J. Am. Chem. Soc.* **1991**, *113*, 4583.
- Mathias, L. J.; Carothers, T. W. *Polym. Prepr. Am. Chem. Soc.* **1991**, *32*, 633.
- Mathias, L. J.; Carothers, T. W. *J. Am. Chem. Soc.* **1991**, *113*, 4043.
- Denkewalter, R. G.; Kole, J. F.; Lukasavage, W. J. U.S. Patent 4 410 688, 1983; *Chem. Abstr.* **11**, 103907.
- Hall, H.; Padias, A.; McConnell, R. et al. *J. Org. Chem.* **1987**, *52*, 5305.
- Newkome, G. R.; Yao, Z.-Q.; Baker, G. R. et al. *J. Org. Chem.* **1985**, *50*, 2003.
- Tomalia, D. A.; Dewald, J. R. U.S. Patent 4 507 466, 1985.
- Tomalia, D. A.; Dewald, J. R. U.S. Patent 4 558 120, 1985.
- Tomalia, D. A.; Dewald, J. R. U.S. Patent 4 568 737, 1986.
- Tomalia, D. A.; Dewald, J. R. U.S. Patent 4 587 329, 1986.
- Tomalia, D. A.; Dewald, J. R. U.S. Patent 4 631 337, 1986.
- Tomalia, D. A.; Dewald, J. R. U.S. Patent 4 694 064, 1987.
- Tomalia, D. A.; Dewald, J. R. U.S. Patent 4 713 975, 1987.
- Tomalia, D. A.; Dewald, J. R. U.S. Patent 4 737 550, 1988.
- Tomalia, D. A.; Dewald, J. R. U.S. Patent 4 871 779, 1989.
- Tomalia, D. A.; Dewald, J. R. U.S. Patent 4 857 599, 1989.
- Buhleier, F.; Wehner, W.; Vogtle, F. *Synthesis* **1978**, 155.
- Tomalia, D. A.; Baker, H.; Dewald, J. R. et al. *Macromolecules* **1986**, *19*, 2466.
- Tomalia, D. A.; Swanson, D. R.; Klimash, J. W. et al. *Polym. Prepr., Am. Chem. Soc. Div. Polym. Chem.* **1993**, *34*(1), 52.
- Swanson, D. R.; Savickas, P.; Kallos, G. et al. unpublished results.

34. Swanson, D. R.; Brothers, H. M., II unpublished results.
35. Dvornic, P. R.; Tomalia, D. A. *Chem. Br.* **1994**, *30*, 641.
36. de Gennes, P. G.; Hervet, H. J. *Phys. Lett. (Paris)* **1983**, *44*, 351.
37. Dvornic, P. R.; Tomalia, D. A. *Macromol. Chem., Macromol. Symp.* **1994**, *88*, 123.
38. Naylor, A. M.; Goddard, W. A., III; Kiefer, G. E. et al. *J. Am. Chem. Soc.* **1989**, *111*, 2339.
39. Meltzer, A. D.; Tirrell, D. A.; Jones, A. A. et al. *Macromolecules* **1992**, *25*, 4549.
40. Ottaviani, M. F.; Bossmann, S.; Turro, N. J. et al. *J. Am. Chem. Soc.* **1994**, *116*, 661.
41. Gopidas, K. R.; Leheny, A. R.; Caminati, G. et al. *J. Am. Chem. Soc.* **1991**, *113*, 7335.
42. Tomalia, D. A. *Proceedings of SFC 91, 4e Congres de la Societe Francaise de Chimie* Strasbourg, France, 1991; p 31.
43. Jansen, J. F. G. A.; de Brabander-van den Berg, E. M. M.; Meijer, E. W. *Science* **1994**, *266*, 1226.
44. Uppuluri, S.; Dvornic, P. R.; Tomalia, D. A. unpublished results.
45. Dvornic, P. R.; Tomalia, D. A. *Macromol. Chem., Macromol. Symp.* in press.
46. Tomalia, D. A.; Hedstrand, D. M. Presented at The Taniguchi Conference on Precision Polymer Synthesis Preprints; Kyoto, Japan, May, 1991.
47. Kallos, G. J.; Tomalia, D. A.; Hedstrand, D. M. et al. *Rap. Commun. Mass Spec.* **1991**, *5*, 383.
48. Haensler, J.; Szoka, F. C., Jr. *Bioconjugate Chem.* **1993**, *4*, 372.
49. Smith, P. B.; Martin, S. J.; Hall, M. J. et al. In *Applied Polymer Analysis and Characterization*; Mitchell, J., Jr., Ed.; Hanser: München/New York, 1987; p 357.
50. Singh, P.; Moll, F., III; Lin, S. H. et al. *Clin. Chem.* **1994**, *40*, 1845.
51. Knapen, J. W. J.; van der Made, A. W.; de Wilde, J. C. et al. *Nature* **1994**, *372*, 659.
52. Tomalia, D. A.; Dvornic, P. R. *Nature* **1994**, *372*, 617.
53. Wiener, E. C.; Brechbiel, M. W.; Brothers, H. et al. *Magnetic Resonance in Medicine* **1994**, *31*, 1.
54. Turro, N. J.; Barton, J. K.; Tomalia, D. A. *Acc. Chem. Res.* **1991**, *24*, 332.
55. Dandliker, P. J.; Diederich, F.; Gross, M. et al. *Angew. Chem. Int. Ed. Engl.* **1994**, *33*, 1739.

DENDRITIC POLYRADICALS

Suchada Rajca and Andrzej Rajca*

Department of Chemistry
University of Nebraska

Synthesis of highly branched, dendritic macromolecules underwent a rapid development in the 1980s.¹⁻³ Elegant methodologies that merge the repetitive reactions of polymer chemistry with stepwise execution of synthetic organic chemistry allow for synthesis of monodisperse macromol-

ecules with MW on the order of 10^4 in good yield, typically after only a few synthetic steps.¹ In the convergent syntheses,⁴⁻⁷ where rigorous purification can be carried out after each synthetic step, not only monodisperse but pure macromolecules are obtained. Furthermore, a high degree of branching in dendrimers shows promise for control of molecular shape.⁸⁻¹¹

Properly designed dendritic macromolecules may be viewed as finite fragments of Bethe lattice, which is one of the important models for phenomena related to condensed matter physics and materials science (Figure 1).¹² For example, functionalization with ferromagnetically coupled "unpaired" electrons would allow us to examine some fundamental questions concerning magnetic phenomena in nanometer-size magnetic particles.¹³⁻¹⁶ 1,3-Connected triarylmethyl-based polyradicals, which are derived from almost century-old Gomberg triphenylmethyl radical and homologous Schlenk hydrocarbon diradical,¹⁷⁻¹⁹ were selected as the building blocks. Our earlier studies established that an intramolecular ferromagnetic coupling was maintained in a series of polyradicals with up to 10 "unpaired" electrons (e.g., high-spin ground state with spin, $S = 5$ for a decaradical) and polyradicals could be handled in solution at low temperature and inert atmosphere.²⁰⁻²⁹

Here we summarize the synthesis leading to the dendritic polyradical with 31 triarylmethyl sites for "unpaired" electrons (Figures 1 and 2).¹⁵

PREPARATION

Synthesis of Polyethers

Preparation of 1,3-connected polyarylmethyl polyethers is based upon a convergent synthetic route, in which branched polymeric arms are built "inward" toward the central core.^{6,15,30} We employ three steps: (a) Br/Li exchange, (b) addition of aryllithium to carbonyl compound, and (c) conversion of the alcohol to the corresponding methyl ether. Sequential iterations of steps (a)–(c) yield dendritic polyethers (Figure 3).^{15,30}

The intermediates and products after steps (b) and (c) are isolated and purified; that is, the alternating polarity in the alcohol/ether/alcohol/ether/...sequence of isolated compounds greatly aids purification by chromatography. Further advantage in purification is gained from the convergent character of the synthesis, which implies that the molecular weight after step (b) is approximately doubled and the amount of the side products with molecular weights similar to the product is minimized. General procedure for each synthetic step is described below:

Step (a): Aryllithium is obtained by monolithiation of bromobenzene derivative in ether (distilled from sodium-benzophenone in a nitrogen atmosphere), at low tempera-

*Author to whom correspondence should be addressed.

POLYMERIC MATERIALS ENCYCLOPEDIA

Editor-in-Chief
JOSEPH C. SALAMONE
Professor Emeritus
University of Massachusetts, Lowell

VOLUME
3
—
D — E



CRC Press
Boca Raton New York London Tokyo

Acquiring Editor: *Joel Claypool*
Senior Project Editor: *Andrea Demby*
Editorial Assistant: *Maureen Aller*
Marketing Manager: *Greg Daurelle*
Marketing Manager Direct Reponse: *Arline Massey*
Cover Designer: *Denise Craig*
Interior Designer: *Jonathan Pennell*
Manufacturing Assistant: *Sheri Schwartz*
Compositor: *RTIS*

TP1110
P65
1996
vol. 3
COPY 2

Library of Congress Cataloging-in-Publication Data

Polymeric materials encyclopedia / editor-in-chief Joseph C. Salamone.

p. cm.

Includes bibliographical references and index.

ISBN 0-8493-2470-X

1. Plastics—Encyclopedia. 2. Polymers—Encyclopedia

I. Salamone, Joseph C., 1939—

TP1110.P65 1996

668.9'03—dc20

96-12181
CIP

This book contains information obtained from authentic and highly regarded sources. Reprinted material is quoted with permission, and sources are indicated. A wide variety of references are listed. Reasonable efforts have been made to publish reliable data and information, but the author and the publisher cannot assume responsibility for the validity of all materials or for the consequences of their use.

Neither this book nor any part may be reproduced or transmitted in any form or by any means, electronic or mechanical, including photocopying, microfilming, and recording, or by any information storage or retrieval system, without prior permission in writing from the publisher.

All rights reserved. Authorization to photocopy items for internal or personal use, or the personal or internal use of specific clients, may be granted by CRC Press, Inc., provided that \$.50 per page photocopied is paid directly to Copyright Clearance Center, 27 Congress Street, Salem, MA 01970 USA. The fee code for users of the Transactional Reporting Service is ISBN 0-8493-2470-X/96/\$0.00+.50. The fee is subject to change without notice. For organizations that have been granted a photocopy license by the CCC, a separate system of payment has been arranged.

The consent of CRC Press does not extend to copying for general distribution, for promotion, for creating new works, or for resale. Specific permission must be obtained in writing from CRC Press for such copying.

Direct all inquiries to CRC Press, Inc., 2000 Corporate Blvd., N.W., Boca Raton, Florida 33431.

Trademark Notice: Product or corporate names may be trademarks or registered trademarks, and are used only for identification and explanation, without intent to infringe.

© 1996 by CRC Press, Inc.

No claim to original U.S. Government works

International Standard Book Number 0-8493-2470-X

Library of Congress Card Number 96-12181

Printed in the United States of America 1 2 3 4 5 6 7 8 9 0

Printed on acid-free paper



In Vivo Delivery to Tumors of DNA Complexed with Linear Polyethylenimine

JEAN-LUC COLL,¹ PATRICE CHOLLET,¹ ELISABETH BRAMBILLA,¹ DOMINIQUE DESPLANQUES,¹
JEAN-PAUL BEHR,² and MARIE FAVROT¹

ABSTRACT

Synthetic gene delivery vectors have shown promise in several organs, including brain and lung. Tumor cell targeting, however, is still hindered by their low efficacy. A linear polyethylenimine (L-PEI, Exgen 500) was found to be effective *in vivo*. Our first attempts to use L-PEI for intratumoral gene delivery were not successful, presumably because of poor diffusion of the complexes within the tumor mass after injection with a syringe. Here we show that L-PEI-mediated transfection can be strongly enhanced when the complexes are delivered slowly into a solid tumor mass, using a micropump. Furthermore, L-PEI/DNA complexes actively transfect pseudocystic tumor cells when injected into the cyst cavity. In both cases L-PEI induced a significant and long-lasting (≥ 15 days) expression of the reporter gene. Finally, even though systemic delivery of L-PEI/DNA complexes leads to high levels of expression in the lung, this method is not adapted for transfection of subcutaneous tumors implanted in the thigh nor for transfection of lung metastases. Altogether, these results show that L-PEI has promising features for transfection of tumor cells, provided that the mode of delivery is adapted.

OVERVIEW SUMMARY

A cationic polymer, linear polyethylenimine (L-PEI), was used for transfection of tumor cells *in vivo*. We describe here a solid subcutaneous tumor mass that expresses the luciferase reporter gene at a significant level, ca. 10^6 RLU/mg protein/10 sec, for at least 15 days, provided the L-PEI/DNA complexes are injected intratumorally using a micropump. Similarly, L-PEI/DNA complexes can efficiently transfect pseudocystic tumors when they are injected in the cyst. Conversely, the same tumor cells implanted subcutaneously, as well as lung metastases, are not transfected when L-PEI/DNA complexes are injected intravenously. Thus, L-PEI is a suitable vector for intratumoral gene delivery, when its mode of delivery is adapted.

INTRODUCTION

GENE TRANSFER can be achieved by using viral or synthetic gene delivery systems. At present, retroviruses and adeno-

viruses are the preferred vectors for clinical protocols even though they present several drawbacks. They carry only a limited size of DNA and require the production of a special construct for each gene to be transfected; they are immunogenic and potentially hazardous for the patients and their environment. Synthetic delivery systems can in principle overcome these limitations, but their efficiency is still low.

Complexes consisting of negatively charged DNA associated with positively charged macromolecules mimic viruses in their ability to act as DNA carriers from the extracellular space to the cell nucleus. *In vitro*, their efficiency will depend on their ability to carry out multiple roles, including DNA compaction, protection, and transfer across physical barriers such as the plasma and nuclear membranes. Despite intensive efforts to understand how these molecules work *in vitro* (Balasubramaniam *et al.*, 1996; Labat-Moleur *et al.*, 1996; Koltover *et al.*, 1998; Pollard *et al.*, 1998) and *in vivo* (Zhu *et al.*, 1993; Egilmez *et al.*, 1996; Liu *et al.*, 1997; Templeton *et al.*, 1997; Goula *et al.*, 1998b; Li *et al.*, 1998), little is known about the performances of cationic molecules for the transfection of tumor cells *in vivo*. Promising results were initially described in melanoma (Nabel

¹Lung Cancer Research Group, Institut Albert Bonniot, Université Joseph Fourier, 38706 Grenoble, France.

²Laboratoire de Chimie Génétique, UMR 7514, Faculté de Pharmacie, Université Louis Pasteur, Strasbourg, France.

et al., 1993), following direct intratumoral injection of DNA-liposome complexes. More recent studies analyzed the outcome of using nonviral methods in brain tumors (Zhu *et al.*, 1996; Goldman *et al.*, 1997) or in subcutaneous tumor xenografts (Egilmez *et al.*, 1996). Nevertheless, despite intensive research efforts in this area, nonviral transfection of tumor cells *in vivo* was not really successful (Egilmez *et al.*, 1996; Coll *et al.*, 1998).

Several types of cancer lead to pseudocystic instead of solid tumors. The efficiency of gene transfer into these tumors has not been documented at all, presumably because of the lack of a relevant animal model. This type of tumor is frequently observed in glioma and ovary cancers, where a tumor wall will expand and form a liquid-filled cavity where the inner layer of tumor cells is directly in contact with the liquid. Pseudocystic tumors are theoretically well suited for gene therapy protocols, since the complexes can be injected directly into the cavity and will eventually line the cells.

Using another route, early studies described the interest in using nonviral vectors for intravenous DNA delivery (Stewart *et al.*, 1992; Zhu *et al.*, 1993). Later on, several groups presented additional data sustaining the general idea that cationic complexes injected intravenously will efficiently transfect the lungs and to a lesser extent the heart, spleen, and liver (Liu *et al.*, 1997; Goula *et al.*, 1998a). Angiogenic endothelial cells were also shown to pick up preferentially DOTAP-cholesterol complexes injected intravenously (Thurston *et al.*, 1998). Here, too, transfection of tumor cells by cationic complex-mediated intravenous gene delivery still remains a challenge.

In this work, we analyzed the potential of a synthetic polycation, polyethylenimine (PEI) (Boussif *et al.*, 1995), to achieve efficient *in vivo* gene transfer into tumor cells. To do so, we compared three routes of administration of the L-PEI/DNA complexes: intratumoral injections into solid tumors, intracystic injection into a model of cyst-forming tumors, and intravenous delivery to subcutaneous tumors and lung metastases.

MATERIALS AND METHODS

Cell lines and culture conditions

H322 (CRL5806; American Type Culture Collection [ATCC], Rockville, MD) and H358 (ATCC CRL5807), human non-small cell lung carcinoma (NSCLC) cell lines of bronchioalveolar origin (Clara cells), have been described previously (Coll *et al.*, 1998). H358NL is a subclone of H358 obtained in our laboratory. TS/Apc is a mouse mammary carcinoma cell line (Lollini *et al.*, 1995). Cells were cultured as adherent monolayers in RPMI 1640 medium (GIBCO, Gaithersburg, MD) containing 10% (v/v) heat-inactivated fetal calf serum (GIBCO) at 37°C under 5% CO₂ in a humidified atmosphere.

Plasmid constructs

Plamid pCMV-LacZ was purchased from Clontech (Palo Alto, CA). Plamid pCMV-Luc was constructed by subcloning the firefly luciferase cDNA from pGL3 (Promega, Madison, WI) in place of the Renilla luciferase fragment of pRL-CMV (Promega), using *NheI* and *XbaI* restriction enzymes (Promega).

These plasmids were extracted with Qiagen Endo-free-Mega-prep columns (Qiagen, Chatsworth, CA).

PEI/DNA complexes

Linear polymers of ethylenimine with a mean molecular mass of 22 kDa (Exgen 500; Euromedex, Souffleweyheim, France) was used as transfection reagent. Linear PEI (L-PEI)/DNA complexes with different ratios of L-PEI nitrogen to DNA phosphate (N/P ratio) were prepared in 5% (w/v) glucose (Goula *et al.*, 1998b).

β -Galactosidase and luciferase measurements

LacZ expression was evaluated by the *in situ* color reaction with the β -galactosidase (β -Gal) substrate 5-bromo-4-chloro-3-indolyl- β -D-galactopyranoside (X-Gal; GIBCO). Tissues were fixed with a solution of 4% paraformaldehyde in phosphate-buffered saline (PBS) for 4 hr at 4°C, rinsed twice in PBS, and then exposed to X-Gal (0.4 mg/ml) in PBS in the presence of 4 mM potassium ferricyanide, 4 mM ferrocyanide, 0.02% Nonidet P-40 (NP-40), and 2 mM MgCl₂ for 16 hr at 30°C.

The luciferase assay was performed using the luciferase assay system (Promega) as recommended. Briefly, tissues were extracted and macerated mechanically. They were then resuspended in 100 μ l of cell culture lysis reagent for each 20 mg of tissue. The cell debris were pelleted by a short centrifugation. Ten microliters of extract were then mixed with 100 μ l of luciferase assay substrate and the luciferase activity was measured in a photoluminometer (Promega) over 10 sec. The concentration of protein was measured using the DC-comp assay (Bio-Rad, Hercules, CA), and the luciferase activities were calculated as the number of reference light units per 10 sec per milligram (RLU/10 sec/mg) of protein. By using purified firefly luciferase under the same experimental conditions, we determined that 2 ng of this enzyme produced 10⁸ RLU/10 sec.

Animal administrations

Four-week-old female Swiss nude mice (IFFA-Credo, Marcy l'Etoile, France) were injected subcutaneously in the right thigh with 20 \times 10⁶ H322, H358, or H358NL cells. Two to 3 weeks later, the tumor sizes ranged between 4 and 5 mm in diameter. H358NL is a subclone of H358 obtained in our laboratory. This clone developed the ability to form pseudocystic tumors (thin layer of tumor cells forming a pocket filled with liquid [up to 5 ml]).

Artificial lung metastases were obtained by injecting 10⁵ TS/Apc cells in 100 μ l of PBS in the tail vein.

For intratumoral injections of naked DNA, 10 μ g of DNA was diluted into 100 μ l of 5% (w/v) glucose and injected with insulin syringes with 29-gauge, 0.5-inch needles (Becton Dickinson, Meylan, France) or with a micropump (KD Scientific; Biobloc, Illkirch, France) using the same syringes. In general, large (7-mm) tumors were used for intratumoral injections. When L-PEI/DNA complexes were used, 10 μ g of DNA diluted into 50 μ l of 5% glucose was mixed with an equal volume of glucose containing the desired concentration of L-PEI.

For systemic administrations, 50 μ g of DNA was complexed with various amounts of L-PEI in a final volume of 200 μ l of glucose (5%, w/v). Injections were performed in the tail vein.

At various times after intravenous injections, the mice were killed by cervical dislocation. Heart, lung, spleen, liver, blood, tumors, and kidneys were collected, washed with PBS, and used for X-Gal staining or luciferase activity measurements.

Statistical analysis

The Student *t* test was used for statistical analysis when two different groups of samples were compared. A *p* value of less than 0.05 was considered significant.

RESULTS

Injection into solid tumors

We first tested whether L-PEI had a beneficial effect on DNA delivery in H322 subcutaneous tumors. L-PEI/DNA complexes with N/P ratios of L-PEI nitrogen to DNA phosphate varying from 0 (i.e., naked DNA) to 20 (large excess of L-PEI) were prepared in 100 μ l of glucose (5%, w/v) and injected with a syringe directly into the tumors. The reporter gene used was one encoding the firefly luciferase, under control of a cytomegalovirus (CMV) promoter. Under these conditions, naked DNA gave a strong level of luciferase 24 hr after DNA injection [$1.2 \pm 0.3 \times 10^6$ RLU/mg protein/10 sec; *n* = 5), while L-PEI-formulated DNA was less efficient [$1.3 \pm 0.5 \times 10^5$ RLU/mg protein/10 sec for N/P ratio of 1; *n* = 3). We then injected 10 μ g of DNA formulated with biotinylated PEI (kind

gift of P. Erbacher, CNRS, Strasbourg, France), in order to follow the distribution of the complexes in tumors. Tumor sections were incubated with alkaline phosphatase-conjugated streptavidin and stained with naphthol red. Strong positive staining was observed at the periphery of the tumors in stromal cells only (mainly fibroblasts). This clearly suggested that most of the liquid injected rapidly with the syringe flowed out along the needle track and wrapped the tumor. To overcome this problem, we changed to a slow injection rate in order to augment the quantity of complexes trapped in the tumors. We thus repeated the experiment, using a micropump to inject the same amount of L-PEI/DNA complexes with N/P ratios varying from 0 to 20 at a rate of 20 μ l/min. Naked DNA (Fig. 1; N/P ratio of 0) led to low transfection levels (luciferase activities of 1.1×10^4 and 4×10^4 RLU/mg protein/10 sec when the tumors were extracted 24 or 72 hr after DNA injection, respectively). In the presence of L-PEI, luciferase expression increased up to 10^6 RLU/mg protein/10 sec with an N/P ratio of 10 and remained constant for at least 4 days. Increasing the N/P ratio resulted in a lower expression of the reporter gene. Further analysis were performed using the *lacZ* reporter gene (10 μ g; N/P ratio of 10) injected with the micropump. Five days later the tumors were removed, fixed, stained with X-Gal, and sectioned. Stained cells were found scattered in the tumor mass at a low frequency (estimated at 0.1%). Only tumor cells were labeled by this method (data not shown).

The same L-PEI-formulated DNA, injected with a micropump, was found to be more efficient than naked DNA in an-

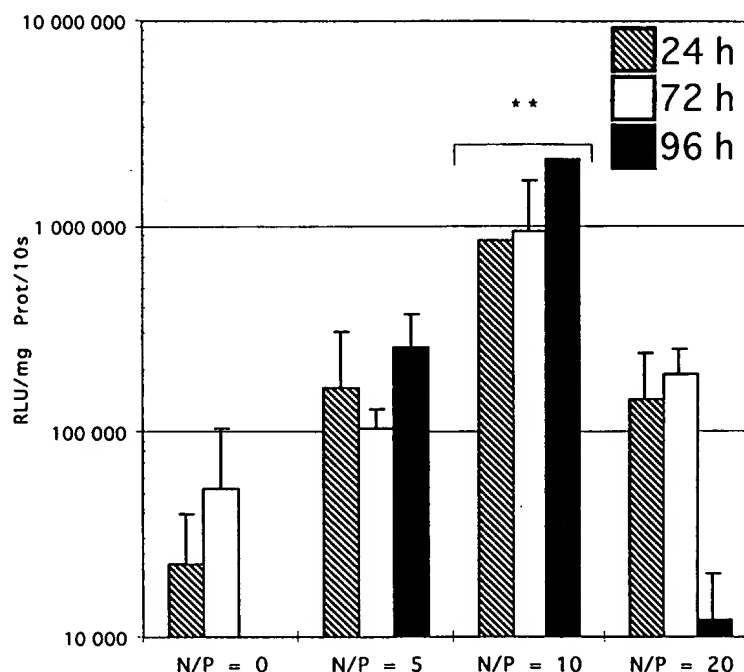


FIG. 1. Micropump injections of L-PEI/pCMV-*Luc* into subcutaneous H322 tumors. One hundred microliters of a 5% (w/v) glucose solution containing 10 μ g of DNA and increasing concentrations of L-PEI was injected intratumorally, using a micropump delivering 20 μ l/min. N/P, Ratio between the number of L-PEI nitrogen and DNA phosphate groups. Tumors were extracted 24, 72, or 96 hr after DNA injection, homogenized in lysis buffer, and centrifuged for 5 min at $8000 \times g$ and the supernatant was assayed for luciferase activity and protein concentration. The results are expressed as relative light units per 10 sec per milligram of protein (*n* = 3). ***p* < 0.01.

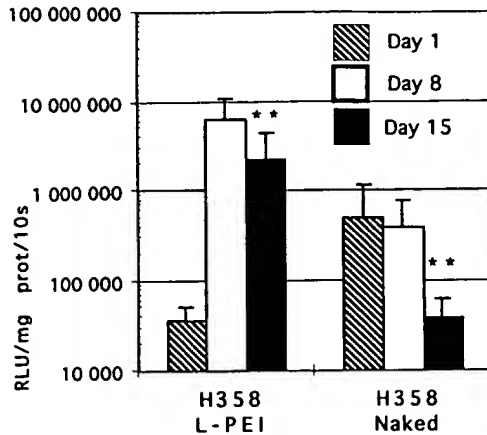


FIG. 2. Micropump injections of L-PEI/pCMV-Luc into subcutaneous H358 tumors. One hundred microliters of a 5% (w/v) glucose solution containing 10 μ g of DNA with L-PEI (N/P = 10) or without L-PEI (naked) was injected intratumorally, using a micropump delivering 20 μ l/min. Tumors were extracted 1, 8, or 15 days after DNA injection, and luciferase activity measured as described in Fig. 1 ($n = 3$). ** $p < 0.01$.

other NSCLC cell line (H358). L-PEI/DNA complexes yielded low levels of luciferase 1 day after injection (Fig. 2), but luciferase activity increased to more than 7×10^6 RLU/mg protein/10 sec on day 8. Interestingly, transgene expression remained elevated during the first 15 days. Conversely, syringe-injected naked DNA performed poorly and expression decreased rapidly with time.

Injections into pseudocystic tumors

We obtained a subclone of H358, named H358NL, which developed the ability to form pseudocystic tumors. The pseudocysts are made of a thin layer of tumor cells forming a pocket filled with several milliliters of liquid (up to 5 ml). This type of tumor is a good model for analyzing both the protective and transfection capacities of L-PEI. Naked DNA and L-PEI/DNA complexes were prepared in 150 μ l of glucose (5%, w/v). The liquid present in the cyst was aspirated with a syringe and replaced with the transfection solution. When compared with naked DNA (less than 5×10^4 RLU/mg protein/10 sec), the presence of excess L-PEI yielded strong (7.6×10^6 RLU/mg protein/10 sec on day 8) and long-lasting expression of the transgene (2.1×10^6 RLU/mg protein/10 sec on day 15) (Fig. 3).

Transfection of subcutaneous NSCLC tumors after intravenous injection of L-PEI-formulated DNA

An interesting therapy-oriented question was whether tumor cells could be transfected after remote intravenous administration of L-PEI/DNA complexes.

Animals carrying subcutaneous H322 tumors implanted in the right thigh were given one shot of 50 μ g of L-PEI-formulated DNA (N/P ratio of 10, in 200 μ l of glucose [5%, w/v]) in the tail vein. One day later, tumors were extracted and luciferase activities were measured. Results presented in Fig. 4

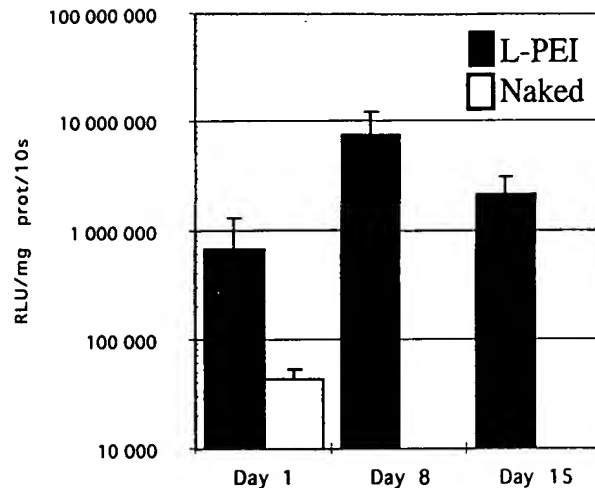


FIG. 3. Intracystic injections of L-PEI/pCMV-Luc into subcutaneous H358NL tumors. The liquid present in pseudocystic H358NL subcutaneous tumors was aspirated with a syringe and replaced by 150 μ l of L-PEI/DNA complexes (10 μ g of DNA and an N/P ratio of 10 for the L-PEI) or with 10 μ g of naked DNA. Tumors were extracted 1, 8, or 15 days after DNA injection, and luciferase activity was measured as described in Fig. 1 ($n = 3$).

show that tumor cells did not express the reporter gene 24 hr after DNA injection. The same results were obtained when the luciferase level was measured 5 or 8 days after L-PEI/DNA injection (data not shown). In contrast, the expected transfection of the lungs was observed, indicating that L-PEI/DNA complexes were efficient (Goula *et al.*, 1998a). Finally, the size of these highly vascularized subcutaneous tumors did not influence transfection efficiency since expression of the transgene was not observed in large (more than 1 cm of diameter) or small tumors (data not shown).

Transfection of lung metastases after intravenous injection of L-PEI-formulated DNA

We implanted artificial lung metastases by injecting 10^5 TS/Apc cells intravenously. In contrast to H322 and H358 cells, which invade the cervical lymph nodes, TS/Apc cells originating from a mouse mammary carcinoma form lung metastases in every injected animal. Tumor growth is rapid enough to kill the mice within the first 20 days after the injection of the cells. At death the mass of the lungs can be as much as 1 g, compared with a normal mass of 180 mg in Swiss nude mice.

In normal lungs, X-Gal staining of L-PEI/pCMV-LacZ-treated animals showed an intense staining of the alveoli (Fig. 5A). In invaded lungs, however, no X-Gal-positive cells were visible (Fig. 5B). This showed not only that tumor cells were difficult to transfect, but also that normal lung cells became resistant. We further analyzed this phenomenon by injecting luciferase reporter gene complexes into the tail veins of mice carrying increasing amounts of tumor cells in the lungs. Lung metastasis-carrying mice were given a single injection of 50 μ g of L-PEI-formulated DNA (N/P ratio of 10) 4, 11, or 18 days after implantation of the TS/Apc cells. Twenty-four hours af-

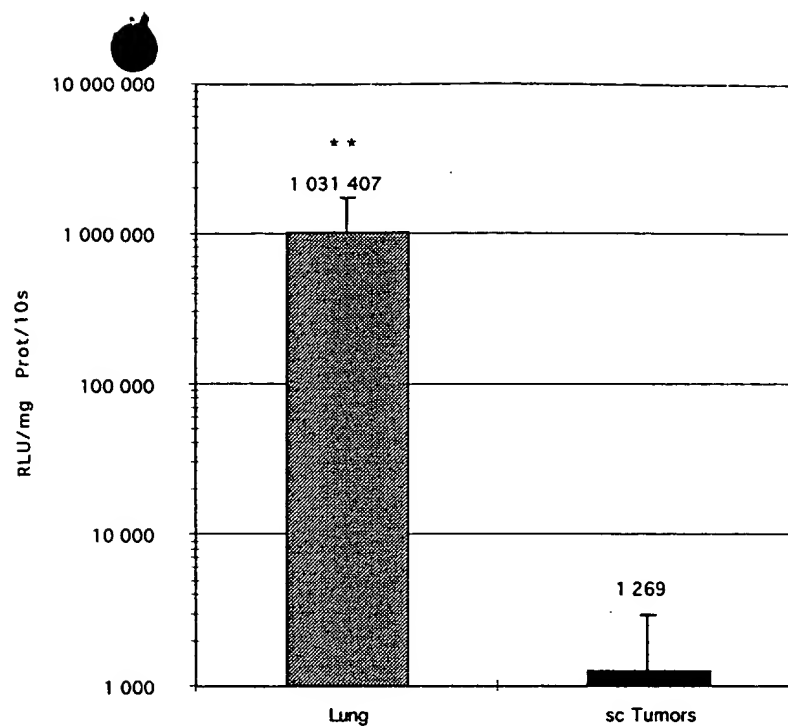


FIG. 4. Intravenous injections of L-PEI/pCMV-*Luc* and transfection of subcutaneous H322 tumors. PEI/pCMV-*Luc* complexes (N/P ratio of 10; 50 μ g of DNA in 200 μ l of glucose [5%, w/v]) were injected into the tail veins of mice carrying subcutaneous H322 tumors. The next day, the lungs and tumors were extracted and the luciferase activity measured. The results are expressed as relative light units per 10 sec per milligram of protein ($n = 5$). ** $p < 0.05$.

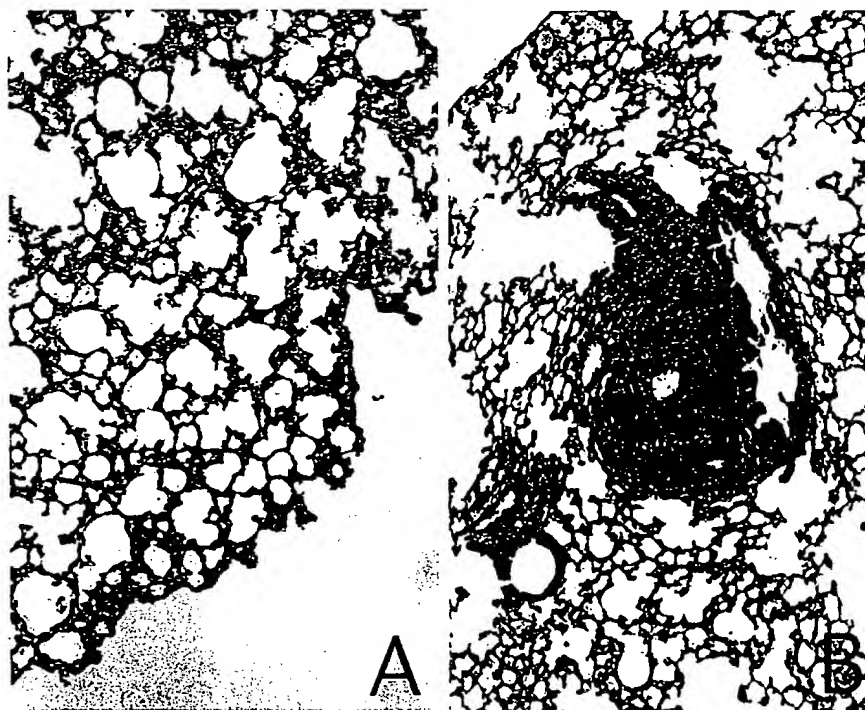


FIG. 5. After intravenous injection, transgene expression is found in normal lungs (A) but not in invaded lungs (B). Typical sections show LacZ-expressing cells [blue staining in (A)]. A pCMV-*LacZ* construct used at 50 μ g/200 μ l in 5% glucose was complexed with L-PEI (N/P ratio of 10) and injected into the tail vein of a normal mouse or of a mouse in which TS/Apc tumors cells had been injected intravenously 17 days earlier. Under these conditions, TS/Apc cells invade the lungs, forming large metastases [visible in (B)]. The animals were killed 24 hr after DNA injection. Dissected lungs were fixed and treated as whole mounts for X-Gal staining. Stained tissues were then dehydrated in ethanol, embedded in paraffin, and sectioned (3 μ m). The sections were then counterstained with hematoxylin and eosin. Original magnification: $\times 100$.

ter DNA injection, the animals were sacrificed and luciferase activity was measured in the lungs. Results presented in Fig. 6 show that the transfection efficiency decreased as the mass of the lungs (i.e., the tumor mass) increased.

DISCUSSION

The literature shows that cationic vectors can be used to transfer a gene into normal cells *in vivo*. This was observed after a direct injection into the brain (Abdallah *et al.*, 1996; Zhu *et al.*, 1996; Goldman *et al.*, 1997; Goula *et al.*, 1998b) but also after a systemic administration of the complexes, with a predominant transfection of the lungs (Zhu *et al.*, 1993; Liu *et al.*, 1997; Templeton *et al.*, 1997; Goula *et al.*, 1998a; Li *et al.*, 1998). Despite intensive efforts, cancer cells seem to be more difficult to transfect by nonviral methods. Indeed, only a few studies demonstrate that tumor cells can be good targets for cation-based gene delivery after a direct, intratumoral injection (Nabel *et al.*, 1993; Egilmez *et al.*, 1996; Zhu *et al.*, 1996; Goldman *et al.*, 1997). This suggested either that cationic complexes had lost their activity once injected into a tumor, or that the mode of delivery of the complexes was not adapted. We favored the second hypothesis since we observed that most of an injected solution did not diffuse properly into a tumor but had a strong tendency to spout out. We thus analyzed the influence of the mode of intratumoral delivery by comparing the transfection efficiencies obtained after a slow injection using a micropump versus a normal, rapid injection using a syringe.

Micropump-injected L-PEI complexes produced a high and

long-lasting expression of the transgene, whereas the same complexes were inefficient when injected with a syringe. When compared with naked DNA, the level of luciferase expressed in H358 tumors treated with L-PEI/DNA was still 500-fold higher 15 days after injection. Conversely, we observed that naked DNA was less efficient when injected with the micropump. A possible explanation for this phenomenon could be that the high hydrostatic pressure provided by a rapid injection with a syringe is necessary to ensure that the damage done to the plasma membranes of the cells allowing DNA entry is reversible. L-PEI-formulated DNA, on the other hand, would not need this pressure to enter the cells. A slow rate of injection would favor its diffusion and increase the concentration of DNA remaining in the tumor, while a rapid injection would result in a significant reflux of the complexes along the needle track, eventually leading to a loss of transfection agent. To be efficient, the complexes need to contain a small excess of L-PEI positive charges. Indeed, the best transfection is obtained with an N/P ratio of 10 and decreases when the N/P ratio reaches 20. In these experiments L-PEI/DNA complexes were made in glucose. It has been shown that in such a nonionic solution, the complexes are small (50 to 60 nm) and do not aggregate (Goula *et al.*, 1998b). Thus, use of glucose instead of saline augments the diffusion of these nanostructures and will certainly participate to the maintenance of their appropriate biophysical structure until they are in contact with the tumor cell surface.

Another advantage of using L-PEI is found in cystic tumors. Pseudocystic tumors are often observed in glioma and ovary tumors. In addition, the main tumor mass is frequently surgically removed before injection of the therapeutic gene, leaving a cav-

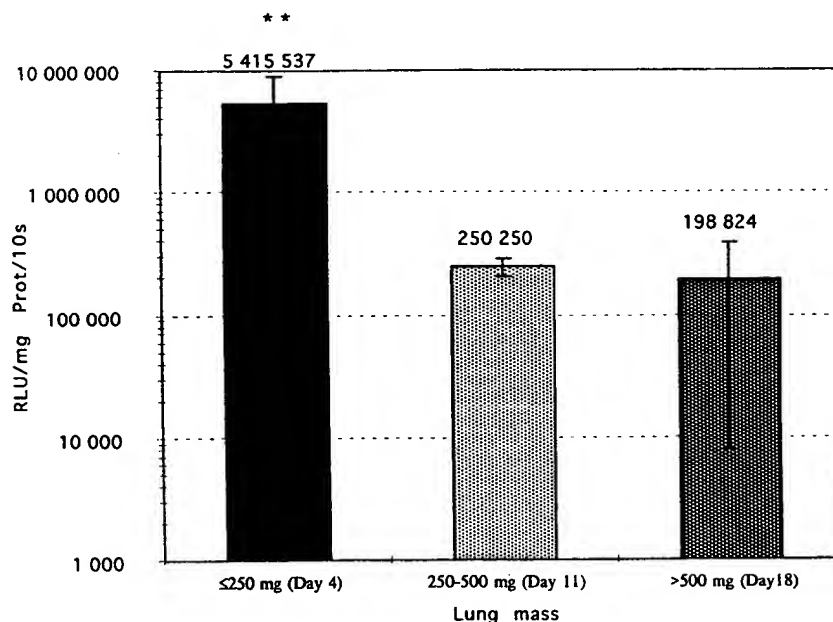


FIG. 6. Intravenous injections of L-PEI/pCMV-Luc and transfection of the colonized lungs. TS/Apc cancer cells were injected into the tail veins of mice. Four, 11, or 18 days later, L-PEI/pCMV-Luc complexes (N/P ratio of 10; 50 μ g of DNA in 200 μ l of glucose [5%, w/v]) were administered systemically. The next day, the lungs were extracted and weighed and the luciferase activity was measured as described in Fig. 1. The mean mass of normal lungs is about 180 mg. This mass increases after invasion of the lungs by tumor cells. The results are expressed as relative light units per 10 sec per milligram of protein ($n = 5$). ** $p < 0.05$.

ity surrounded by unresectable tumor cells. Such tumors are good candidates for gene delivery, since the DNA complexes can be injected into the cavity, where they will be in close contact with the neighboring tumor cells. Since these cavities can be rich in DNases, the cationic vector will have to protect the DNA efficiently. The high levels and long-lasting expression of the transgene in our model of pseudocystic tumors suggest that L-PEI is a good candidate for this purpose.

According to experimental *in vitro* data (Boussif *et al.*, 1996) and our *in vivo* experiments, we estimated that the luciferase activity (10^7 RLU/mg protein/10 sec) obtained by using L-PEI in H358 tumors is equivalent to 1% X-Gal-positive cells. In addition, the level of luciferase was constant for 15 days. Two hypotheses can be raised from these observations: (1) 1% of the cells are transfected and express the gene for 2 weeks or (2) L-PEI stabilizes the DNA complexes and forms a reservoir in the tumor that releases DNA and transfects fresh cells regularly. In this latter hypothesis, newly transfected cells would show up regularly while the expression of the transgene would vanish in formerly transfected cells. The true number of transfected cells would then be greater than 1%. It is important to demonstrate which hypothesis is valid in order to choose the most appropriate therapeutic gene. Indeed, by allowing the expression of a transgene in about 1% of the tumor cells for at least 15 days, L-PEI would be a suitable vector for the long-term production of diffusible therapeutic molecules such as cytokines. If the second hypothesis is true, L-PEI would also be appropriate for the delivery of suicide or corrective genes, for example, since the therapeutic genes would be expressed in a higher quantity of cells.

Our study shows that the mode of delivery influences the efficiency of intratumoral gene transfer. It is reasonable to assume that large tumors will behave differently than the 4- to 7-mm tumors used in our model. Thus it would be important to address this issue in larger animal models before injecting DNA complexes into large, solid human tumors.

Transfection of subcutaneous tumors implanted in the thigh after systemic injection of L-PEI/DNA complexes into the tail vein was not observed. This suggests that highly vascularized, rapidly growing tumors are not transfected any better than normal organs such as liver, heart, kidneys, spleen, dorsal skin, or quadriceps (data not shown), even though L-PEI is highly effective in transfecting lungs. One explanation for this phenomenon would be that the lung is the only organ in which the diameter of the capillaries and the blood flow rate are adapted to both the size and adhesion properties of the DNA complexes.

Accordingly, any change in one of these parameter in the lung would result in the loss of transfection efficiency. This could happen if the lungs were invaded by tumor cells. We noticed that as soon as tumor cells were microscopically detectable in the alveoli, L-PEI complexes administered systemically lost their normal ability to transfect normal pneumocytes (Goula *et al.*, 1998a) but did not gain the ability to transfect tumor cells. This resulted in the disappearance of X-Gal staining and in a dramatic diminution of luciferase activity in tumor-bearing lungs.

In conclusion, our study demonstrates that L-PEI-formulated DNA can efficiently and stably transfect tumor cells provided complexes are injected directly and slowly with a micropump into a tumor, or in a pseudocystic tumor.

ACKNOWLEDGMENTS

Many thanks to Dr. François Berger and Corine Tenaud for their help and encouragement. This study was funded in part by the Ligue Nationale pour la Recherche sur le Cancer, the ARC (Association pour la Recherche sur le Cancer), the Fondation pour la Recherche Médicale, the GEFLUC, and CNRS (Action Concertée).

REFERENCES

- ABDALLAH, B., HASSAN, A., BENOIST, C., GOULA, D., BEHR, J.P., and DEMENEIX, B.A. (1996). A powerful nonviral vector for *in vivo* gene transfer into the adult mammalian brain: Polyethylenimine. *Hum. Gene Ther.* 7, 1947-1954.
- BALASUBRAMANIAM, R.P., BENNETT, M.J., ABERLE, A.M., MALONE, J.G., NANTZ, M.H., and MALONE, R.W. (1996). Structural and functional analysis of cationic transfection lipids: The hydrophobic domain. *Gene Ther.* 3, 163-172.
- BOUSSIF, O., LEZOUALC'H, F., ZANTA, M.A., MERGNY, M.D., SCHERMAN, D., DEMENEIX, B., and BEHR, J.P. (1995). A versatile vector for gene and oligonucleotide transfer into cells in culture and *in vivo*: Polyethylenimine. *Proc. Natl. Acad. Sci. U.S.A.* 92, 7297-7301.
- BOUSSIF, O., ZANTA, M.A., and BEHR, J.P. (1996). Optimized galenics improve *in vitro* gene transfer with cationic molecules up to 1000-fold. *Gene Ther.* 3, 1074-1080.
- COLL, J.L., NEGOCESCU, A., LOUIS, N., SACHS, L., TENAUD, C., GIRARDOT, V., DEMEINEX, B., BRAMBILLA, E., BRAMBILLA, C., and FAVROT, M. (1998). Antitumor activity of *bax* and *p53* naked gene transfer in lung cancer: *In vitro* and *in vivo* analysis. *Hum. Gene Ther.* 9, 2063-2074.
- EGILMEZ, N.K., YOSHIMI, I., and BANKERT, R.B. (1996). Evaluation and optimization of different cationic liposome formulations for *in vivo* gene transfer. *Biochem. Biophys. Res. Commun.* 221, 169-173.
- GOLDMAN, C.K., SOROCANU, L., SMITH, N., GILLESPIE, Y.C., SHAW, W., BURGESS, S., BILBAO, G., and CURIEL, D.T. (1997). *In vitro* and *in vivo* gene delivery mediated by a synthetic polycationic amino polymer. *Nature Biotechnol.* 15, 462-466.
- GOULA, D., BENOIST, C., MANTERO, S., MERLO, G., LEVI, G., and DEMENEIX, B.A. (1998a). Polyethylenimine-based intravenous delivery of transgenes to mouse lung. *Gene Ther.* 5, 1291-1295.
- GOULA, D., REMY, J.S., ERBACHER, P., WASOWICZ, M., LEVI, G., ABDALLAH, B., and DEMENEIX, B.A. (1998b). Size, diffusibility and transfection performance of linear PEI/DNA complexes in the mouse central nervous system. *Gene Ther.* 5, 712-717.
- KOLTOVER, I., SALDITT, T., RÄDLER, J.O., and SAFINYA, C.R. (1998). An inverted hexagonal phase of cationic liposome-DNA complexes related to DNA release and delivery. *Nature (London)* 391, 78-81.
- LABAT-MOLEUR, F., STEFFAN, A.M., BRISSON, C., PERRON, H., FEUGEAS, O., FURSTENBERGER, P., OBERLING, F., BRAMBILLA, E., and BEHR, J.P. (1996). An electron microscopy study into the mechanism of gene transfer with lipopolyamines. *Gene Ther.* 3, 1010-1017.
- LI, S., RIZZO, M.A., BATTACHARYA, S., and HUANG, L. (1998). Characterization of cationic lipid-protamine-DNA (LPD complexes) for intravenous gene delivery. *Gene Ther.* 5, 930-937.
- LIU, Y., MOUNKES, L.C., LIGGITT, H.D., BROWN, C.S., SOLODIN, I., HEATH, T.D., and DEBS, R.J. (1997). Factors influencing the efficiency of cationic liposome-mediated intravenous gene delivery. *Nature Biotechnol.* 15, 167-173.

- LOLLINI, P.L., DE GIOVANNI, C., LANDUZZI, L., NICOLETTI, G., FRABETTI, F., CAVALLO, F., GIOVARELLI, M., FORNI, G., MODICA, A., MODESTI, A., MUSLANI, P., and NANNI, P. (1995). Transduction of genes coding for a histocompatibility (MHC) antigen and for its physiological inducer interferon- γ in the same cell: Efficient MHC expression and inhibition of tumor and metastasis growth. *Hum. Gene Ther.* 6, 743-752.
- NABEL, G.J., NABEL, E.G., YANG, Z.Y., FOX, B.A., PLAUTZ, G., GAO, X., HUANG, L., SHU, S., GORDON, D., and CHANG, A.E. (1993). Direct gene transfer with DNA-liposome complexes in melanoma: Expression, biologic activity, and lack of toxicity in humans. *Proc. Natl. Acad. Sci. U.S.A.* 90, 11307-11311.
- POLLARD, H., REMY, J.S., LOUSSOUARN, G., DEMOLOMBE, S., BEHR, J.P., and ESCANDE, D. (1998). Polyethylenimine but not cationic lipids promotes transgene delivery to the nucleus in mammalian cells. *J. Biol. Chem.* 273, 7507-7511.
- STEWART, M.J., PLAUTZ, G., DEL BUONO, L., YANG, Z.Y., XU, L., GAO, X., HUANG, L., NABEL, E.G., and NABEL, G.J. (1992). Gene transfer in vivo with DNA-liposome complexes: Safety and acute toxicity in mice. *Hum. Gene Ther.* 3, 267-275.
- TEMPLETON, N.S., LASIC, D.P., FREDERIK, P.M., STREY, H.H., ROBERTS, D.D., and PAVLAKIS, G.N. (1997). Improved DNA: liposome complexes for increased systemic delivery and gene expression. *Nature Biotechnol.* 15, 647-652.
- THURSTON, C., McLEAN, J.W., RIZEN, M., BALUK, P., HASKELL, A., MURPHY, T.J., HANAHAN, D., and McDONALD, D.M. (1998). Cationic liposomes target angiogenic endothelial cells in tumors and chronic inflammation in mice. *J. Clin. Invest.* 101, 1401-1413.
- ZHU, J., HANISH, U.K., FELGNER, P.L., and RESZKA, R. (1996). A continuous intracerebral gene delivery system for in vivo liposome-mediated gene therapy. *Gene Ther.* 3, 472-476.
- ZHU, N., LIGGITT, D., LIU, Y., and DEBS, R. (1993). Systemic gene expression after intravenous DNA delivery into adult mice. *Science* 261, 209-211.

Address reprint requests to:

Dr. Jean-Luc Coll
GRCPVA, Institut Albert Bonniot
Université Joseph Fourier
Domaine de la Merci
38706 Grenoble, France

Received for publication December 11, 1998; accepted after revision April 16, 1999.

Human Gene Therapy

Editor-in-Chief:

W. French Anderson

Associate Editors:

Malcolm K. Brenner

James M. Wilson

European Editors:

Claudio Bordignon

Jean Michel Heard

Asian Pacific Associate Editor:

Shuichi Kaneko

Full Text Online: www.liebertonline.com

Mary Ann Liebert, Inc. publishers



Review

Poly(ethylenimine) and its role in gene delivery

W.T. Godbey^a, Kenneth K. Wu^b, Antonios G. Mikos^{c,*}

^aDepartment of Biochemistry and Cell Biology, Rice University, P.O. Box 1892, MS 140, Houston, TX 77251-1892, USA

^bDivision of Hematology and Vascular Biology Research Center, The University of Texas Health Science Center at Houston, 6431 Fannin Street, Houston, TX 77030, USA

^cDepartment of Bioengineering, Rice University, P.O. Box 1892, MS 142, Houston, TX 77251-1892, USA

Received 8 February 1999; accepted 25 March 1999

Abstract

Since the first published examination of poly(ethylenimine) (PEI) as a gene delivery vehicle, there has been a flurry of research aimed at this polycation and its role in gene therapy. Here we will briefly review PEI chemistry and the characterization of PEI/DNA complexes used for gene delivery. Additionally, we will note various PEI transfection considerations and examine findings involving other polycationic gene delivery vehicles used with cellular targeting ligands. The current state of our knowledge regarding the mechanism of PEI/DNA transfection will also be discussed. Finally, we will survey toxicity issues related to PEI transfection. © 1999 Elsevier Science B.V. All rights reserved.

Keywords: Poly(ethylenimine); PEI; Polycation; Nonviral gene delivery; Transfection; Cell trafficking

1. Introduction

The popular press has taken numerous opportunities to herald the promise of gene therapy as a potential cure for several genetic diseases. Although this news might seem fresh and innovative, the transfer of genetic material into living cells has been around for decades. Even in 1966, transfection techniques for mammalian cells were already touted as part of the future of medicine [1]. However, after

over 30 years of research, the field of gene therapy has yet to provide an acceptable treatment as a cure for a human disease.

This is not to say that gene therapy has made no progress in the last three decades. Both viral and nonviral gene delivery systems have been used in clinical trials to treat maladies such as cystic fibrosis [2–7] and several forms of cancer [8–11]. With each successive trial the prospect of successful gene therapy treatment for human disease has become more feasible. However, the majority of gene delivery methods have involved primarily adenoviral or liposomal vectors. There exist numerous other possible vectors that are currently under intense scientific investigation. One such vector, poly(ethylenimine) (PEI), has recently appeared as a possible alternative to viral and liposomal routes of gene delivery.

*Corresponding author. Tel.: +1-713-285-5355; fax: +1-713-285-5353.

E-mail address: mikos@rice.edu (A.G. Mikos)

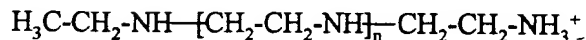
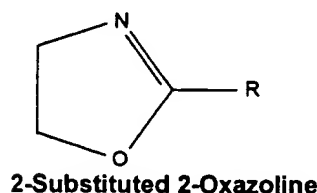
¹Invited Award Contribution of 1998 Young Investigator Award Recipient.

2. PEI chemistry

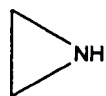
PEI is a polymer that has been used for years in common processes such as paper production, shampoo manufacturing, and water purification. The polymer comes in two forms: linear and branched. The branched form is produced by cationic polymerization from aziridine monomers (Fig. 1) via a chain-growth mechanism, with branch sites arising from specific interactions between two growing polymer molecules. Polymer growth is terminated by "back biting," or intramolecular macrocyclic ring formation. The linear form of PEI also arises from cationic polymerization, but from a 2-substituted 2-oxazoline monomer (Fig. 1) instead. The product (for example linear poly(N-formalethylenimine)) is then hydrolyzed to yield linear PEI. The linear form of PEI is also attainable from the same process as that used to attain branched PEI, but the reaction

must take place at relatively low temperature. This method will produce linear PEI molecules with higher molecular weights (up to 25 000 Da), with the linear PEI separating from the branched PEI molecules via precipitation. (These methods are described and reviewed in Ref. [12].) The branched form of PEI has yielded significantly greater success in terms of cell transfection, and is therefore the standard form of PEI that is used for gene delivery. Unless otherwise noted, all references to PEI ascribe to the branched form of the molecule.

The basic unit of PEI has a backbone of two carbons followed by one nitrogen atom; as already mentioned, the complete polymer can be linear or branched (Fig. 1). The branched form of PEI contains 1°, 2°, and 3° amines, each with the potential to be protonated. This gives PEI the attribute of serving as an effective buffer through a wide pH range. With nitrogens appearing as one out of every three atoms



Linear PEI*



Aziridine

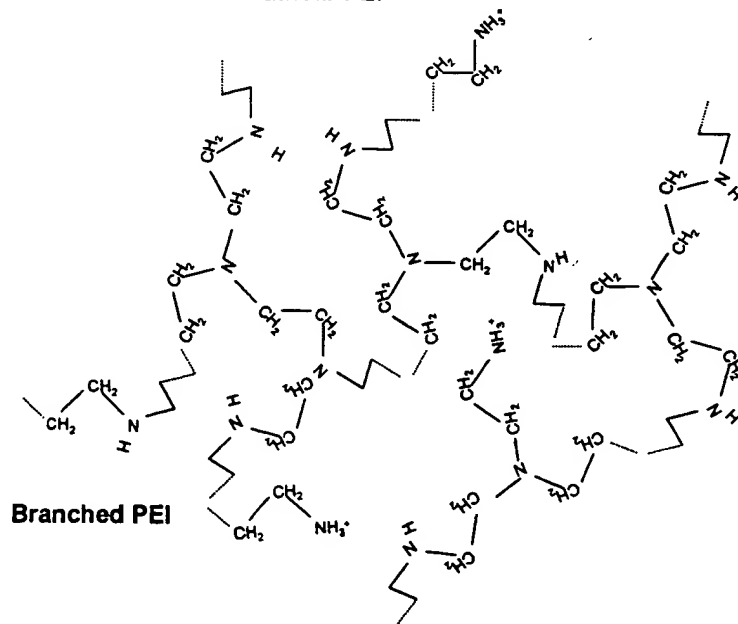


Fig. 1. Structures of PEI precursors and end products. *Aziridine can also yield linear PEI under certain conditions.

in the PEI backbone, any benefits of branching and protonability quickly accumulate in relation to the overall polymer size.

Several suppliers offer PEI in a variety of reported molecular weights. However, the actual molecular weight of a given PEI product appears to be reported differently depending upon the particular company supplying the chemical. There are three PEI products that predominate in the transfection literature — one available from Fluka (Milwaukee, WI, USA; Cat. No. 03880) with a reported molecular weight of 600 000–1 000 000, one from Polysciences (Warrington, PA, USA; Cat. No. 00618) with a reported molecular weight of 70 000, and one from Sigma (St. Louis, MO, USA; Cat. No. 40 872-7) with a reported weight average molecular weight of 25 000. Fig. 2 shows the results of gel fractionation chroma-

tography performed on the three products (against seven polyethylene glycol (PEG) standards in 0.5 M NaCl, using a Hydropore 87-S03-C5 size exclusion column (Varian, Walnut Creek, CA, USA)). The molecular weights reported in the figure vary from those reported by suppliers because of differences in the analytical methods and/or standards used.

The protonability of PEI has already been mentioned as important to PEI's success as a gene delivery vehicle. A useful descriptor of PEI's protonability is its pK_a , which has remained elusive because rigorous analysis of experimental data to obtain PEI's pK_a would require one to include an ionization constant for every amine group [13]. The number of amine groups can easily exceed 1000, depending on the molecular weight of the PEI being analyzed. Suh et al. reported on the percentage of

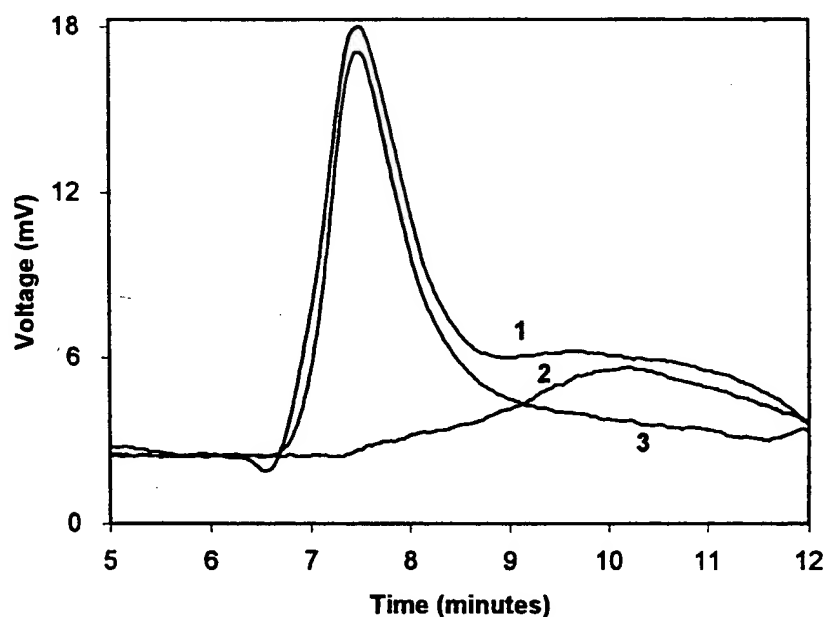


Fig. 2. Gel fractionation chromatographs of three PEI products used for gene delivery, measured against PEG standards. (NMW=nominal molecular weight.) (1) Polysciences NMW 70 000; (2) Sigma NMW 25 000; (3) Fluka NMW 600 000–1 000 000. The number average molecular weights, \bar{M}_n , weight average molecular weights, \bar{M}_w , and polydispersity indexes, P.I., for the three PEIs as determined by gel fractionation chromatography [25] are as follows:

	Polysciences	Sigma	Fluka
\bar{M}_n	$8\,400 \pm 2\,800$	700 ± 200	$75\,800 \pm 12\,700$
\bar{M}_w	$133\,800 \pm 10\,800$	8000 ± 2800	$155\,500 \pm 4\,500$
P.I.	16.99 ± 5.20	11.66 ± 4.82	2.08 ± 0.31

unprotonated nitrogens at various pHs for two concentrations of one molecular weight of PEI [13]. The data reported imply that the amount of PEI protonation depends, in part, on its concentration. However, the concentrations of PEI that are used for transfection were not examined in the paper, so the protonation values reported do not accurately reflect what occurs in transfecting PEI, and they should not be used for such a purpose. With each PEI nitrogen having its own local environment influencing its protonability, perhaps what is more important than obtaining a particular PEI molecule's pK_a is its overall buffering capacity over a range of pHs.

3. Characterization of PEI/DNA complexes

In the presence of sufficient PEI, DNA will condense [14]. The extent of condensation depends on the polymer:DNA ratio [15]. PEIs with branched structure condense to a greater extent than do linear PEIs [14]. The induction of DNA condensation, in addition to providing compact colloids for endocytosis, might also afford some protection to the carried DNA from nuclease digestion as has been shown for PEG–poly(L-lysine)/DNA complexes [16].

The shape of polycation-condensed DNA has been examined in great detail, with condensate shapes taking on a variety of forms. A given plasmid/polycation combination can condense into more than one configuration, as shown with T7 DNA condensing into both toroids and tubular micelles (rods) in the presence of polylysine [17]. However, differences in specimen preparations can alter the morphology of condensed complexes [18], and it has been suggested that rod conformations are actually artifacts induced by sample preparations [19]. Many laboratories have examined the effects of different polycationic condensing agents on DNA conformation, and toroidal condensates have predominated [19–23]. This suggests that the ultimate shape of polycation/DNA complexes might not depend on the specific polycation used, but might be due to a more general factor such as the kinetics behind polycation-induced DNA condensation. Kinetics have been pointed out by Dunlap et al. as a possible explanation for the rounded, globular forms taken on by

DNA in the presence of linear or branched PEI [14]. This group also noted that in the presence of either form of PEI, plasmid DNA condensed into bundled, folded loops as opposed to winding.

The sizes of PEI/DNA complexes have been found to be within the range 20–40 nm using atomic force microscopy [14]. The sizes were fairly consistent between complexes made with linear or branched PEI, although the branched PEI also yielded a small amount of much larger condensates (over 240 nm in one case). Using electron microscopy, Tang and Szoka found toroidal PEI/DNA structures of 55 ± 12 nm [23]. The group also examined complexes in solution using dynamic light scattering and found apparent diameters ranging from 90 to 130 nm. The number of plasmids within a PEI/DNA complex remains unknown as of yet, but lipopolyamine/DNA complexes have been noted as containing approximately 100 plasmids [24].

The surface charge of PEI and PEI/DNA complexes has been examined in terms of ζ potential [25]. It was found that while a certain sample of branched PEI had a ζ potential of 37 mV in solution, this value was lowered significantly to 31.5 mV when the PEI was allowed to complex with DNA (at a 7.5:1 PEI nitrogen to DNA phosphate ratio). Centrifugation of PEI/DNA complexes was seen to lower the ζ potential further, this time to 29.2 mV. The surface charge of the transfecting colloids is thought to be an important factor in the complexes' association with plasma membranes.

4. Transfection considerations

DNA transfection using polycations such as PEI, as with adenoviral transfection, is transient because of the lack of integration into the host genome, as well as a lack of (episomal) replication [26]. However, unlike adenoviral transfection methods, PEI-mediated gene delivery has the potential to transfect cells with larger pieces of genetic material. (Reviewed by Abdallah et al. [27].) Upper limits to the size of virally-delivered plasmids are naturally set by the size of the particular viral head used: an adenovirus holds up to 7.5 kilobases (kb) [28], while an adeno-associated virus can carry between 2.5 kb [29] and 4.5 kb [30] of genetic material. Although

retroviral transfection does offer permanent expression of the delivered gene, retroviral transfection requires actively dividing cells [30,31].

The ability of PEI to transfect a wide variety of cells is well established. Boussif et al. have documented PEI-mediated transfection in 25 different cell types, including 18 human cell lines as well as pig and rat primary cells [32]. Gene delivery experiments have been performed in vivo using newborn [33] and adult [34] mice as well as on Sprague-Dawley rats [35]. Abdallah et al. reported no morbidity in the mice used over their 3 month experimental course [34].

The ratio of PEI nitrogens to DNA phosphates is important in terms of transfection efficiency and cell toxicity. Polymer/DNA complexes with an overall positive charge can activate complement, and reducing the $+/-$ charge ratio of the complexes reduces complement activation as well as the amount of cell death associated with transfection [36]. Ferrari et al. hypothesized that circulating proteins can bind to and inactivate cationic polymer/DNA complexes [37], and Boussif et al. have found that transfection efficiency is increased when serum is present by using a more-concentrated PEI/DNA solution for transfection, lending support to the hypothesis of circulating proteins binding to polycation/DNA complexes [32]. The binding of circulating proteins could also induce recognition by cells of the reticuloendothelial system, which would halt the transfection process in vivo.

One way to minimize the effects of protein binding to PEI/DNA is through manipulation of the PEI amine to DNA phosphate ratio. Ratios ranging from 5:1 to 13.5:1 have all been used successfully in the literature, with each proportion having its own merits. Boussif et al. tested branched-PEI transfection with charge ratios ranging from 4.5:1 to 135:1 and reported maximal transfection efficiency in vitro within the 9–13.5 PEI nitrogens per DNA phosphate range [33], while Ferrari et al. used linear PEI at a 5:1 ratio in an attempt to transfect cells with neutrally charged complexes [37].

Another way to minimize the binding of circulating proteins to polycationic transfection complexes is through surface modification. Several types of nanoparticles have undergone such alterations in the past in an attempt to circumvent uptake by

phagocytic cells. Examples of modified nanoparticles include polystyrene, poly(methyl methacrylate), poly(β -hydroxybutyrate), and poly(lactic acid), with surface modifiers including various polaxamers, ethoxylated glycerols, and PEG [38]. It has also been shown that PEG-epoxide will readily interact with PEI, and that polystyrene surfaces, after preadsorption of PEI and subsequent coupling with PEG, will act to exclude proteins such as fibrinogen from binding to the surface [39]. The idea that PEG can prevent protein binding has been carried to PEI/DNA complexes, with PEG and PEI being used together to form block copolymers. The PEI in these copolymers is still able to interact with DNA, and the resulting complexes have been described in some detail by Vinogradov et al. [40]. This type of complex modification shows promise for the in vivo use of PEI for gene delivery.

When forming transfection complexes by the addition of PEI to a DNA solution, it is unlikely that the PEI will form a continuous shell around the resulting complexes. These colloids will have areas where smaller molecules will be able to fit. It has been shown that a subsequent addition of smaller PEI molecules to formed PEI/DNA complexes will result in complexes with increased packing of amines about the DNA [25]. The larger number of PEI amines per PEI/DNA complex yielded complexes with higher buffering capacities, which presumably enabled more efficient endolysosomal escape. This, in turn, allowed a greater number of plasmids to reach the nucleus for transcription, as evidenced by increased transfection efficiency.

The pH and molecular weight of PEI used for transfection have also been examined. Although differing pHs of PEI solutions do not make any significant difference in transfection efficiency [33,41], the molecular weight of the PEI used for transfection does. Abdallah et al. examined the transfection efficiencies of three molecular weights of PEI in vivo and found that PEI with a reported molecular weight of 25 kD yields higher transfection efficiency than PEIs of higher reported molecular weights [34]. Godbey et al. also examined the effect of PEI molecular weight on transfection efficiency using PEIs with lower molecular weights in vitro. They determined that as molecular weight was increased, so was transfection efficiency (Fig. 3)

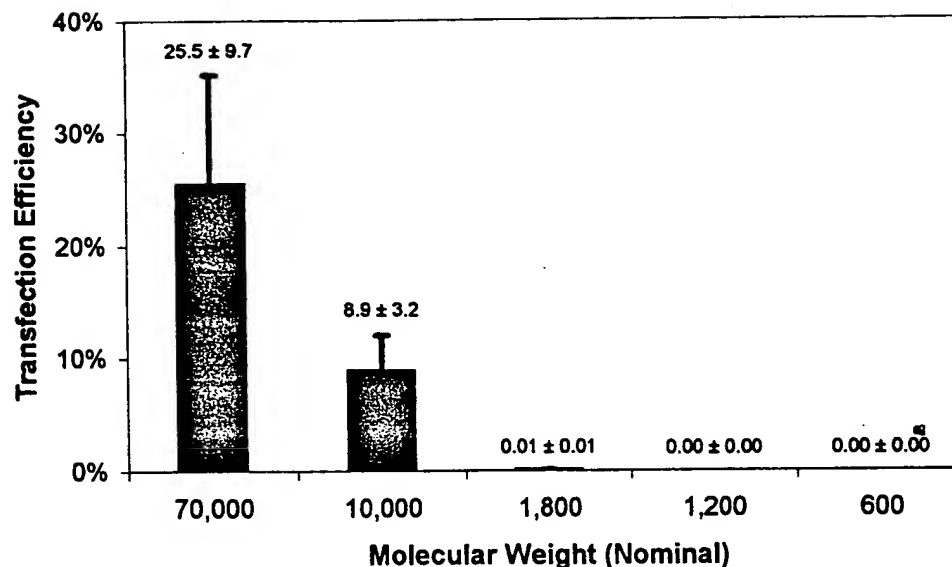


Fig. 3. Transfection efficiencies of five molecular weights of PEI, pH 7.0, 3 days posttransfection [41]. The cell line EA.hy926 was transfected with PEI supplied by Polysciences (Warrington, PA, USA) to produce these results. Error bars represent plus one standard deviation ($n \geq 4$).

[41]. This result for low molecular weight PEIs is consistent with the finding that interpolymer systems with relatively few salt bonds will dissociate during dilution [42], which implies that PEI/DNA complexes made with smaller PEI molecules will dissociate more easily and provide lower transfection yields.

However, the largest (and highest-transfecting) molecular weight of PEI tested by Godbey et al. had a similar weight average molecular weight to that of the largest (and lowest-transfecting) PEI examined by Abdallah et al. described above. To resolve the apparent conflict, the two PEI samples (from Polysciences and Fluka) have since been tested directly, with the Polysciences product yielding a significantly higher transfection efficiency [25]. This difference is most likely due to the differences in polydispersity between the two products. (Gel fractionation chromatography and polydispersity analyses of the two products are given in Fig. 2.)

Another consideration implied by the molecular weight verses transfection efficiency data is that it is the size of the resulting complexes that affects transfection efficiency. Ogris et. al. have found that smaller (40 nm) transferrin-PEI/DNA complexes, made at low salt concentrations, have lower transfection

efficiencies than larger (>1000 nm) complexes made from the same components at physiological salt levels [43]. Perhaps the smaller complexes have decreased cellular uptake or increased degradability levels. These are possibilities that are currently under investigation.

5. Targeting

PEI has been coupled with different ligands for the purpose of cell targeting. Examples of ligands used include RGD peptide sequences [44], antiCD3 [45], and galactose for hepatocyte targeting [46]. Additionally, because poly(L-lysine) (PLL) and PEI are both polycationic polyamines, any successful targeting methods that have been used for PLL/DNA complexes ought to apply to PEI/DNA complexes as well. One example of a targeting ligand that has been used with both polymers is transferrin, which has been attached to both PLL/DNA and PEI/DNA complexes for the purpose of targeting transfection to specific cell types [20,43,45,47]. Other ligands attached to PLL include antiCD4 [48], recombinant gp120 (the envelope protein of HIV) [48], folate

[49], and synthetic peptides (attached with an integrin binding segment) [50]. Even low density lipoprotein has been used as a ligand for cell targeting through attachment to stearyl (hydrophobized) PLL molecules [51]. This form of cell targeting is often responsible for improved uptake of transfecting complexes into cells, and will result in higher transfection efficiencies (provided the cell recognizes the targeting ligand used) [45].

While the attachment of ligands to transfecting complexes to achieve targeted endocytosis is one form of cell targeting, another method entails the use of cell-specific promoters to achieve targeted expression of delivered DNA. Using this sort of promoter targeting, many different cell types will endocytose the transfecting complexes but only those cells that recognize the delivered plasmids' promoter will transcribe and express the delivered gene. Cowan et al. used this method to target vascular endothelia by using the promoter for the intercellular adhesion molecule 2 gene [52]. Several different cell-specific promoters have been identified thus far, and each serves as a potential genetic marker for targeted gene delivery.

6. Mechanism

The mechanism by which PEI transfects cells begins with entry of PEI/DNA via endocytosis (Fig. 4A,B). In experiments involving fluorescently labeled PEI/DNA complexes, it has been shown that the complexes initially form aggregates on plasma membrane surfaces [53]. Experiments that used lipopolyamine/DNA particles for transfection revealed that such complexes bound to membrane components involved in Ca^{2+} -mediated cell anchoring to the extracellular matrix. Only adherent cells were involved with uptake of the complexes [24]. In examining CaPO_4 -mediated transfection, Coonrod et al. used vinblastulin to depolymerize microtubules and thus indicate entry of complexes into cells via endocytosis [54]. The same group also used cytochalasin B to interrupt microfilament formation and keep transfection complexes in the outer peripheries of cells after endocytosis, thus blocking DNA transport at endosome/lysosome fusion [54].

Following endocytosis, normal cellular trafficking

usually has endocytosed particles being directed to lysosomes for degradation. Improved transfection efficiency by the use of chloroquine, which represses lysosomal degradation, would imply endocytosed transfection complexes do eventually meet up with lysosomes for destruction. This has been shown to be the case with both PLL [49] and PEI [43]. Using a different approach, Chiu et al. demonstrated lysosomal degradability of PLL (as well as other α -amino acids) through detection of lower molecular weight fragments in cytoplasm after a time [55]. These results do not inherently translate to other gene delivery vehicles though, because the group did not see any degradation of poly(D-lysine) in the same experiments. It is generally assumed, however, that PEI/DNA complexes are trafficked to lysosomes for degradation after endocytosis.

Lysosomal membranes contain V-ATPases, which pump H^+ at the expense of ATP [56]. A charge gradient would theoretically build because of protons being pumped into the lysosomes, but there is also an influx of Cl^- which relieves this gradient [56]. It has been hypothesized that the increased Cl^- concentration, in turn, increases lysosomal osmolarity, with water rushing in to relieve the gradient resulting in lysosomal swelling and bursting [33,57]. Even though lysosomes eventually burst, they are still quite successful at degrading endocytosed particles beforehand. Transgene delivery is often interrupted within endolysosomes because of nucleases that reside within lysosomes. PEI is thought to be a good gene delivery vehicle because of its ability to accept the protons pumped into endolysosomes. By accepting protons, PEI could raise endolysosomal pH, which would alter protein folding within the endolysosome and perhaps inactivate degradative enzymes. The enzymes might be inactivated long enough for endolysosomal bursting to occur before plasmid digestion has taken place. As discussed earlier, modified PEI/DNA particles with increased buffering capacities have been shown to increase transfection efficiency, which lends support to the above hypothesis.

After endolysosomal disruption, the delivered plasmids eventually reach the nucleus for transcription. PEI/DNA complexes that were microinjected into cell cytoplasm were translocated into the nuclei of these cells, without dependence on membrane

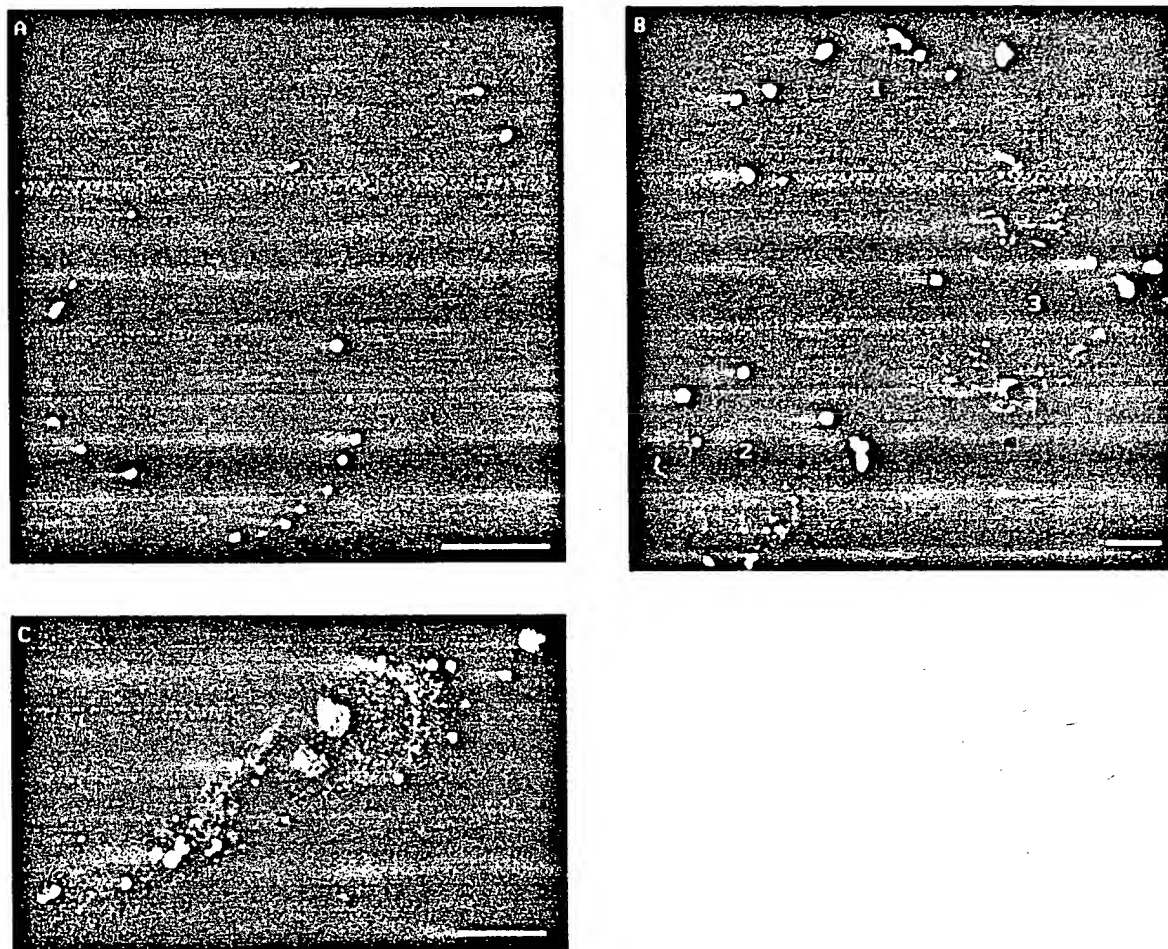


Fig. 4. Confocal images of cells transfected with labeled complexes [53]. Each bar represents 10 μm . (A) Initially, complexes aggregate in discrete patches on cell exteriors. (B) Aggregates of fluorescence are endocytosed. This frame pictures three cells in different stages of transfection. (B-1) Complexes initially form aggregates on plasma membranes. (B-2) Aggregates in the process of endocytosis. (B-3) Later in the process there are more endosomes and fewer cell surface aggregates. (Numbers were placed to correspond with cell nuclei.) (C.) After endocytosis but before gene expression, PEI/DNA complexes enter nuclei in the form of ordered structures.

rupture or cell mitosis [58]. The same result was also seen in experiments using exogenously-administered PEI/DNA particles that went through normal endocytotic trafficking, with complexes entering nuclei in the form of large, discrete structures (Fig. 4C) [53]. The fact that complexes made it into cell nuclei intact shows that it is not necessary for PEI and DNA to separate prior to nuclear entry of the delivered plasmids. The path of PEI/DNA complexes from endolysosome disruption to nuclear entry has not yet been fully explained, but it is doubtful that it

occurs by mere diffusion. Cytoplasmic diffusion has been projected as slow because of the cytoplasm's relatively-high viscosity [59]. Vesicle transport may depend on the cytoskeleton [60–63], and with endocytosed PEI/DNA complexes entering nuclei in what appear to be vesicles it might follow that the complexes also travel along cytoskeletal tracks.

The mechanism by which PEI/DNA complexes cross the nuclear membrane can only be speculated on at this time, but it may involve the coating of complexes with a lipophilic layer. Whether this

coating comes from anionic phospholipids adhering to the cationic exterior of the complexes, or the coating is actually made from fragments of the membrane of burst endolysosomes, it is possible that PEI/DNA complexes enter cell nuclei as the result of the coating's fusion with the nuclear membrane. Cationic liposomes have been shown to interact with anionic lipids [64], and to fuse with endosomal membranes to thereby release their carried DNA [65]. Phospholipid-coated PEI/DNA complexes might be released into cell nuclei in the same way.

7. Toxicity

Free PEI will harm cells, but when bound to DNA the detrimental effects are greatly lessened. A possible reason for toxic effects of PEI on cells is that PEI will permeabilize membranes. Permeabilizing effects of PEI on Gram negative bacterial outer membranes have been well-documented [66,67]. At concentrations of 0.001 M_{Amine} (molarity of PEI amines) and above, PEI has also been implicated in causing lysosomal disruption in rat hepatocytes [68]. Oku et al. have reported fusogenic effects of both branched and linear PEI on liposomes, with branched PEI disrupting liposomal membranes made from phosphatidyl serine [69].

When considering the above studies pointing out membrane disruption by PEI, it is not unreasonable to be concerned about the possibility that PEI/DNA complexes might permeabilize the plasma membranes of transfected cells. However, each of the above papers has a counterargument to this concern. The works by Helander et al. were performed on bacterial, not mammalian, cells [66,67]. Although Klemm et al. noted lysosomal disruption at PEI concentrations above 0.001 M_{Amine}, their data do not show any effects on lysosomal stability when the concentration of PEI is at or below 0.0002 M_{Amine} [68], which is more representative of the concentrations used to transfect cells. To further complicate matters, while Oku et al. demonstrated disruption of phosphatidyl serine liposomes by branched PEI, this effect was not seen to any great degree when the liposomes were constructed from phosphatidyl choline/phosphatidyl serine [69]. Further supporting the lack of plasma membrane disruption by PEI

during transfection is work performed by Lambert et al. regarding neuronal cell transfection, which demonstrated no excitation of neuronal cells caused by the transfection process (although PEI concentrations above 150 μ M were toxic to neuronal cells) [70]. These data collectively suggest that low concentrations of PEI will not harm plasma membranes. However, endosomal concentrations of PEI might be elevated to a point where permeabilizing effects might occur, although this has yet to be proven.

8. Conclusions

Although it has been used in a variety of chemical processes for many years, PEI has recently been used successfully for transfection both in vitro and in vivo. As a polycation, PEI will spontaneously adhere to and condense DNA to form toroidal complexes that are readily endocytosed by cells. The presence of multiple unprotonated amines in the complexes is thought to buffer endolysosomal pH, thus allowing cytoplasmic release of the PEI/DNA before lysosomal degradation can occur. The PEI/DNA complexes are eventually translocated into cell nuclei, but it remains to be seen what effects this has on host cell transcription.

Numerous physical characterizations have been performed on PEI/DNA complexes, including size, shape, surface charge concentration, and buffering capacity analyses. These characterizations describe properties that are important to the success of PEI transfection, and may be useful for other nonviral transfection methods as well (just as poly(L-lysine) targeting research has been applied to PEI-mediated gene delivery). Future nonviral vectors could also be designed based on data obtained for PEI mediated transfection. Increasing transfection efficiency while reducing toxicity must be accomplished before PEI can ultimately be used for efficacious gene therapies, although progress toward this end continues to be rapid.

Acknowledgements

This material is based upon work supported under a National Science Foundation Graduate Fellowship

(WTG) and the National Institutes of Health (R29-AR42639) (AGM), (PSO-NS-23327) (KKW), and (R01-HL-50675) (KKW).

References

- [1] E.L. Tatum, Molecular biology, nucleic acids and the future of medicine, *Perspect. Biol. Med.* 10 (1966) 19–32.
- [2] J. Zabner, L.A. Couture, R.J. Gregory, S.M. Graham, A.E. Smith, M.J. Welsh, Adenovirus-mediated gene transfer transiently corrects the chloride transport defect in nasal epithelia of patients with CF, *Cell* 75 (1993) 207–216.
- [3] R.G. Crystal, N.G. McElvaney, M.A. Rosenfeld, C.-S. Chu, A. Mastrangeli, J.G. Hay, S.L. Broday, H.A. Jaffe, N.T. Elissa, C. Danel, Administration of an adenovirus containing the human CFTR cDNA to the respiratory tract of individuals with cystic fibrosis, *Nat. Gen.* 8 (1994) 42–51.
- [4] M.R. Knowles, K.W. Hohnaker, Z. Zhou, J.C. Olsen, T.L. Noah, P. Hu, M.W. Leigh, J.R. Engelhardt, L.J. Edwards et al., A controlled study of adenoviral-vector-mediated gene transfer in the nasal epithelium of patients with cystic fibrosis, *New Engl. J. Med.* 333 (1995) 823–831.
- [5] N.J. Caplan, E. Alton, P.G. Middleton, J.R. Dorin, B.J. Stevenson, X. Gao, S.R. Durham, P.K. Jeffery, M.E. Hodson et al., Liposome-mediated CFTR gene transfer to the nasal epithelium of patients with cystic fibrosis, *Nat. Med.* 1 (1995) 39–46.
- [6] D.S. Porteous, J.R. Dorin, G. McLachlan, H. Davidson-Smith, H. Davidson, B.J. Stevenson, A.D. Carothers, A.J. Wallace, S. Moralle et al., Evidence for safety and efficacy of DOTAP cationic liposome mediated CFTR gene transfer to the nasal epithelium of patients with cystic fibrosis, *Gene Ther.* 4 (1997) 210–218.
- [7] D.R. Gill, K.W. Southern, K.A. Mofford, T. Seddon, L. Huang, F. Sorgi, A. Thompson, L.J. MacVinish, R. Ratcliff et al., A placebo controlled study of liposome mediated gene transfer to the nasal epithelium of patients with cystic fibrosis, *Gene Ther.* 4 (1997) 199–209.
- [8] G.J. Nabel, E.G. Nabel, Z.Y. Yang, B.A. Fox, G.E. Plautz, X. Gao, L. Huang, S. Sh, D. Gordon, A.E. Chang, Direct gene transfer with DNA–liposome complexes in melanoma: expression, biological activity and lack of toxicity in humans, *Proc. Natl. Acad. Sci. USA* 90 (1993) 11307–11311.
- [9] J. Rubin, E. Galanis, H.C. Pitot, R.L. Richardson, P.A. Burch, J.W. Charboneau, C.C. Reading, B.D. Lewis, S. Stahl et al., Phase I study of immunotherapy of hepatic metastases of colorectal carcinoma by direct gene transfer of an allogeneic histocompatibility antigen, HLA-B7, *Gene Ther.* 4 (1997) 419–425.
- [10] N.J. Vogelzang, T.M. Lestingi, G. Sudakoff, S.A. Kradjian, Phase I study of immunotherapy of metastatic renal cell carcinoma by direct gene transfer into metastatic lesions, *Hum. Gene Ther.* 5 (1994) 1357–1370.
- [11] N.J. Vogelzang, G. Sudakoff, E.M. Hersh, Clinical experience in Phase I and Phase II testing of direct intratumoral administration with allovectin-7: a gene-based immunotherapeutic agent, *Proc. Am. Soc. Clin. Oncol.* 15 (1996) 235.
- [12] D.A. Tomalia, G.R. Killat, in: J.I. Kroschwitz (Ed.), second ed., *Encyclopedia of Polymer Science and Engineering*, Vol. 1, Wiley, New York, 1985, pp. 680–739.
- [13] J. Suh, H.J. Paik, B.K. Hwang, Ionization of poly(ethylenimine) and poly(allylamine) at various pH's, *Bioorg. Chem.* 22 (1994) 318–327.
- [14] D.D. Dunlap, A. Maggi, M.R. Soria, L. Monaco, Nanoscopic structure of DNA condensed for gene delivery, *Nucleic Acids Res.* 25 (1997) 3095–3101.
- [15] K. Minagawa, Y. Matsuzawa, K. Yoshikawa, M. Matsumoto, M. Doi, Direct observation of the biphasic conformational change of DNA induced by cationic polymers, *FEBS Lett.* 295 (1991) 67–69.
- [16] P.R. Dash, V. Toncheva, E. Schacht, L.W. Seymour, Synthetic polymers for vectoral delivery of DNA: characterization of polymer–DNA complexes by photon correlation spectroscopy and stability to nuclease degradation and disruption by polyanions in vitro, *J. Control. Release* 48 (1997) 269–276.
- [17] U.K. Laemmli, Characterization of DNA condensates induced by poly(ethylene oxide) and polylysine, *Proc. Natl. Acad. Sci. USA* 72 (1975) 4288–4292.
- [18] D.K. Chatteraj, L.C. Gosule, J.A. Schellman, DNA condensation with polyamines. II. Electron microscopic studies, *J. Mol. Biol.* 121 (1979) 327–337.
- [19] K. Marx, G. Ruben, A study of Phi X-174 DNA torus and lambda DNA torus tertiary structure and the implications for DNA self-assembly, *J. Biomol. Struct. Dyn.* 4 (1986) 23–39.
- [20] E. Wagner, M. Cotten, R. Foisner, M.L. Birnstiel, Transferrin–polycation–DNA complexes: the effect of polycations on the structure of the complex and DNA delivery to cells, *Proc. Natl. Acad. Sci. USA* 88 (1991) 4255–4259.
- [21] M.A. Wolfert, L.W. Seymour, Atomic force microscopic analysis of the influence of the molecular weight of poly(L)lysine on the size of polyelectrolyte complexes formed with DNA, *Gene Ther.* 3 (1996) 269–273.
- [22] M.A. Wolfert, E.H. Schaht, V. Toncheva, K. Ulbrich, O. Nazarova, L.W. Seymore, Characterization of vectors for gene therapy formed by self-assembly of DNA with synthetic block co-polymers, *Hum. Gene Ther.* 7 (1996) 2123–2133.
- [23] M. Tang, F.C. Szoka Jr., The influence of polymer structure on the interactions of cationic polymers with DNA and morphology of the resulting complexes, *Gene Ther.* 4 (1997) 823–832.
- [24] F. Labat-Moleur, A.-M. Steffan, C. Brisson, H. Perron, O. Feugeas, P. Furstenberger, F. Oberling, An electron microscopy study into the mechanism of gene transfer with lipopolyamines, *Gene Ther.* 3 (1996) 1010–1017.
- [25] W.T. Godbey, K.K. Wu, A.G. Mikos, Improved packing of poly(ethylenimine)/DNA complexes increases transfection efficiency, *Gene Ther.* in press.
- [26] R.J. Cristiano, L.C. Smith, M.A. Kay, B.R. Brinkley, S.L.C. Woo, Hepatic gene therapy: efficient gene delivery and expression in primary hepatocytes utilizing a conjugated

- adenovirus–DNA complex, *Proc. Natl. Acad. Sci. USA* 90 (1993) 11548–11552.
- [27] B. Abdallah, L. Sachs, B.A. Demeneix, Non-viral gene transfer: applications in developmental biology and gene therapy, *Biol. Cell* 85 (1995) 1–7.
- [28] P. Lemarchand, H.A. Jaffe, C. Danel, M.C. Cid, H.K. Kleinman, L.D. Stratford-Perricaudet, M. Perricaudet, A. Pavirani et al., Adenovirus-mediated transfer of a recombinant human α_1 antitrypsin cDNA to human endothelial cells, *Proc. Natl. Acad. Sci. USA* 89 (1992) 6482–6486.
- [29] J.D. Harris, N.R. Lemoine, Strategies for targeted gene therapy, *Trends Genet.* 12 (1996) 400–405.
- [30] N. Miller, R. Vile, Targeted vectors for gene therapy, *FASEB J.* 9 (1995) 190–199.
- [31] T. Roe, T.C. Reynolds, G. Yu, P.O. Brown, Integration of murine leukemia virus DNA depends on mitosis, *EMBO* 12 (1993) 2099–2108.
- [32] O. Boussif, M.A. Zanta, J.P. Behr, Optimized galenics improve in vitro gene transfer with cationic molecules up to 1000-fold, *Gene Ther.* 3 (1996) 1074–1080.
- [33] O. Boussif, F. Lezoualc'h, M.A. Zanta, M.D. Mergny, D. Scherman, B. Demeneix, J.P. Behr, A versatile vector for gene and oligonucleotide transfer into cells in culture and in vivo: polyethylenimine, *Proc. Natl. Acad. Sci. USA* 92 (1995) 7297–7301.
- [34] B. Abdallah, A. Hassan, C. Benoist, D. Goula, J.P. Behr, B.A. Demeneix, A powerful non-viral vector for in vivo gene transfer into the adult mammalian brain: polyethylenimine, *Hum. Gene Ther.* 7 (1996) 1947–1954.
- [35] A. Boletta, A. Benigni, J. Lutz, G. Remuzzi, M. Soria, L. Monaco, Non-viral gene delivery to the rat kidney with polyethylenimine, *Hum. Gene Ther.* 8 (1997) 1243–1251.
- [36] C. Plank, K. Mechtler, F.C. Szoka Jr., E. Wagner, Activation of the complement system by synthetic DNA complexes: a potential barrier for intravenous gene delivery, *Hum. Gene Ther.* 7 (1996) 1437–1446.
- [37] S. Ferrari, E. Moro, A. Pettenazzo, J.P. Behr, F. Zaccello, M. Scarpa, ExGen 500 is an efficient vector for gene delivery to lung epithelial cells in vitro and in vivo, *Gene Ther.* 4 (1997) 1100–1106.
- [38] G. Storm, S.O. Belliot, T. Daemen, D.D. Lasic, Surface modification of nanoparticles to oppose uptake by the mononuclear phagocyte system, *Adv. Drug Deliv. Rev.* 17 (1995) 31–48.
- [39] K. Bergstrom, K. Holmberg, A. Safran, A.S. Hoffman, M.J. Edgell, A. Kozlowski, B.A. Hovanes, J.M. Harris, Reduction of fibrinogen adsorption on PEG-coated polystyrene surfaces, *J. Biomed. Mater. Res.* 26 (1992) 779–790.
- [40] S.V. Vinogradov, T.K. Bronich, A.V. Kabanov, Self-assembly of polyamine–poly(ethylene glycol) copolymers with phosphorothioate oligonucleotides, *Bioconjug. Chem.* 9 (1998) 805–812.
- [41] W.T. Godbey, K.K. Wu, A.G. Mikos, Size matters: molecular weight affects the efficiency of poly(ethyleneimine) as a gene delivery vehicle, *J. Biomed. Mater. Res.* 45 (1999) 268–275.
- [42] I.M. Papisov, A.A. Litmanovich, Molecular “recognition” in interpolymer interactions and matrix polymerization, *Adv. Polym. Sci.* 90 (1988) 139–179.
- [43] M. Ogris, P. Steinlein, M. Kurs, K. Mechtler, R. Kircheis, E. Wagner, The size of DNA/transferrin–PEI complexes is an important factor for gene expression in cultured cells, *Gene Ther.* 5 (1998) 1425–1433.
- [44] P. Erbacher, J.-S. Remy, J.-P. Behr, Gene transfer with synthetic virus-like particles via the integrin-mediated endocytosis pathway, *Gene Ther.* 6 (1999) 138–145.
- [45] R. Kircheis, A. Kichler, G. Wallner, M. Kurs, M. Ogris, T. Felzmann, M. Buchberger, E. Wagner, Coupling of cell binding ligands to polyethylenimine for targeted gene delivery, *Gene Ther.* 4 (1997) 409–418.
- [46] M.A. Zanta, O. Boussif, A. Adib, J.P. Behr, In vitro gene delivery to hepatocytes with galactosylated polyethylenimine, *Bioconjug. Chem.* 8 (1997) 839–844.
- [47] S.I. Michael, D.T. Curiel, Strategies to achieve targeted gene delivery via the receptor-mediated endocytosis pathway, *Gene Ther.* 1 (1994) 223–232.
- [48] M. Cotten, E. Wagner, M.L. Birnstiel, Receptor-mediated transport of DNA into eukaryotic cells, *Methods Enzymol.* 217 (1993) 618–644.
- [49] K.A. Mislick, J.D. Baldeschwieler, J.F. Kayyem, T.J. Meade, Transfection of folate–polylysine DNA complexes: evidence for lysosomal delivery, *Bioconjug. Chem.* 6 (5) (1995) 512–515.
- [50] L. Shewring, L. Collins, S.L. Lightman, S. Hart, K. Gustafsson, J.W. Fabre, A non-viral vector system for efficient gene transfer to corneal endothelial cells via membrane integrins, *Transplantation* 64 (1997) 763–769.
- [51] J.S. Kim, A. Maruyama, T. Akaike, S.W. Kim, In vitro gene expression on smooth muscle cells using a Terplex delivery system, *J. Control. Release* 47 (1997) 51–59.
- [52] P.J. Cowan, T.A. Shinkel, H.B. Witort, M.J. Pearse, J.F. d'Apice, Targeting gene expression to endothelial cells in transgenic mice using the human intercellular adhesion molecule 2 promoter, *Transplantation* 62 (1996) 155–160.
- [53] W.T. Godbey, K.K. Wu, A.G. Mikos, Tracking the intracellular path of poly(ethyleneimine) DNA complexes for gene delivery, *Proc. Natl. Acad. Sci. USA* 96 (1999) 5177–5181.
- [54] A. Coonrod, F.-Q. Li, M. Horwitz, On the mechanism of gene transfection: efficient gene transfer without viruses, *Gene Ther.* 4 (1997) 1313–1321.
- [55] H.C. Chiu, P. Kopeckova, S.S. Deshmene, J. Kopecek, Lysosomal degradability of poly(α -amino acids), *J. Biomed. Mater. Res.* 34 (1997) 381–392.
- [56] N. Nelson, Structure and pharmacology of the proton-AT-Pases, *Trends Pharmacol. Sci.* 12 (1991) 71–75.
- [57] J.P. Behr, Transfert de gènes par l'intermédiaire de lipides et de polymères aminés, *CR Soc. Biol.* 190 (1996) 33–38.
- [58] H. Pollard, J.S. Remy, G. Loussouarn, S. Demolombe, J.P. Behr, D. Escande, Polyethylenimine but not cationic lipids promotes transgene delivery to the nucleus in mammalian cells, *J. Biol. Chem.* 273 (1998) 7507–7511.
- [59] K. Luby-Phelps, P.E. Castle, D.L. Taylor, F. Lanni, Hindered diffusion of inert tracer particles in the cytoplasm of mouse 3T3 cells, *Proc. Natl. Acad. Sci. USA* 84 (1987) 4910–4913.
- [60] N.B. Cole, J. Lippincott-Schwartz, Organization of organelles and membrane traffic by microtubules, *Curr. Opin. Cell Biol.* 7 (1995) 55–64.

- [61] R.A. Walker, M.P. Sheetz, Cytoplasmic microtubule-associated motors, *Annu. Rev. Biochem.* 62 (1993) 429–451.
- [62] F. Feiguin, A. Ferreira, K.S. Kosik, A. Caceres, Kinesin-mediated organelle translocation revealed by specific cellular manipulations, *J. Cell Biol.* 127 (1994) 1021–1039.
- [63] P.J. Hollenbeck, J.A. Swanson, Radial extension of macrophage tubular lysosomes supported by kinesin, *Nature* 346 (1990) 864–866.
- [64] Y. Xu, F.C. Szoka Jr., Mechanism of DNA release from cationic liposome/DNA complexes used in cell transfection, *Biochemistry* 35 (1996) 5616–5623.
- [65] A. Noguchi, T. Furuno, C. Kawaura, M. Nakanishi, Membrane fusion plays an important role in gene transfection mediated by cationic liposomes, *FEBS Lett.* 433 (1998) 169–173.
- [66] I.M. Helander, H.L. Alakomi, K. Latva-Kala, P. Koski, Polyethyleneimine is an effective permeabilizer of Gram-negative bacteria, *Microbiology* 143 (1997) 3193–3199.
- [67] I.M. Helander, K. Latva-Kala, K. Lounatmaa, Permeabilizing action of polyethylenimine on *Salmonella typhimurium* involves disruption of the outer membrane with lipopolysaccharide, *Microbiology* 144 (1998) 385–390.
- [68] A.R. Klemm, D. Young, J.B. Lloyd, Effects of polyethylenimine on endocytosis and lysosome stability, *Biochem. Pharmacol.* 56 (1998) 41–46.
- [69] N. Oku, N. Yamaguchi, N. Yamaguchi, S. Shibamoto, F. Ito, M. Nango, The fusogenic effect of synthetic polycations on negatively charged lipid bilayers, *J. Biochem.* 100 (1986) 935–944.
- [70] R.C. Lambert, Y. Maulet, J.-L. Dupont, S. Mykita, P. Craig, S. Volsen, A. Feltz, Polyethylenimine-mediated DNA transfection of peripheral and central neurons in primary culture: probing Ca^{2+} channel structure and function with antisense oligonucleotides, *Mol. Cell. Neurosci.* 7 (1996) 239–246.

VOLUME 60 NOS. 2-3 5 AUGUST 1999
Completing vol. 60

JCREC 60(2-3) 149-428

ISSN: 0168-3659

Journal of controlled release: official
(IM)
v. 60, no. 2-3 (Aug 5 1999)
General Collection
W1 J0596C
Received: 08-30-1999

Journal of controlled release

OFFICIAL JOURNAL OF THE CONTROLLED RELEASE SOCIETY
AND THE JAPANESE SOCIETY OF DRUG DELIVERY SYSTEM



PROPERTY OF THE
NATIONAL
LIBRARY OF
MEDICINE

24
H

000006
JOURNAL OF CONTROLLED RELEASE
1999 VOLUME 60 ISSUES 2 AND 3
SISAC
0168-3659(1999)60:2/3;1-5
W1 J0596C
S203591/01
37662767

Elsevier

- Guidotti, G., and Craig, L. C. (1963), *Proc. Natl. Acad. Sci. U. S.* 50, 54.
- Guidotti, G., Konigsberg, W., and Craig, L. C. (1963), *Proc. Natl. Acad. Sci. U. S.* 50, 774.
- Hexner, P. E., Radford, L. E., and Beams, J. W. (1961), *Proc. Natl. Acad. Sci. U. S.* 47, 1848.
- Jeffrey, P. D., and Coates, J. H. (1966), *Biochemistry* 5, 489.
- Keresztes-Nagy, S., and Klotz, I. M. (1965), *Biochemistry* 4, 919.
- Keresztes-Nagy, S., Lazer, L., Klapper, M. H., and Klotz, I. M. (1965), *Science* 150, 357.
- Klapper, M. H., Barlow, G. H., and Klotz, I. M. (1966), *Biochem. Biophys. Res. Commun.* 25, 116.
- Klotz, I. M. (1966), *Arch. Biochem. Biophys.* 116, 92.
- Klotz, I. M. (1967), *Science* 155, 697.
- Klotz, I. M., and Keresztes-Nagy, S. (1963), *Biochemistry* 2, 455.
- Klotz, I. M., Klotz, T. A., and Fiess, H. A. (1957), *Arch. Biochem. Biophys.* 68, 284.
- LeBar, F. E., and Baldwin, R. L. (1962), *J. Phys. Chem.* 66, 1952.
- Millar, D. B., Frattali, V., and Willick, G. E. (1969), *Biochemistry* 8, 2416.
- Neer, E. J., Konigsberg, W., and Guidotti, G. (1968), *J. Biol. Chem.* 243, 1971.
- Perutz, M. F., and Lehmann, H. (1968), *Nature* 219, 902.
- Perutz, M. F., Muirhead, H., Cox, J. M., and Goaman, L. C. G. (1968), *Nature* 219, 131.
- Richards, E. G., Teller, D. C., and Schachman, H. K. (1968), *Biochemistry* 7, 1054.
- Rosemeyer, M. A., and Huehns, E. R. (1967), *J. Mol. Biol.* 25, 253.
- Schachman, H. K., and Edelstein, S. (1966), *Biochemistry* 5, 2681.
- Schellman, J. (1958), *Compt. Rend. Trav. Lab. Carlsberg* 30, 363.
- Steiner, R. F. (1952), *Arch. Biochem. Biophys.* 39, 333.
- Vinograd, S., and Hutchinson, W. O. (1960), *Nature* 187, 216.
- Yphantis, D. A. (1964), *Biochemistry* 3, 297.

Macromolecule-Small Molecule Interactions.

Strong Binding and Cooperativity in a Model Synthetic Polymer*

Irving M. Klotz, Garfield P. Royer,† and A. R. Sloniewsky

ABSTRACT: Exceptionally strong binding of organic anions is exhibited by polyethylenimine derivatives with apolar side chains. Conformationally compact, water-soluble polymers have been prepared with pendant butyryl, hexanoyl, or lauroyl aliphatic groups, or with carbobenzoxytyrosine or carbobenzoxytryptophan aromatic residues. All of these complex much more extensively with methyl orange than do proteins

such as serum albumin or β -lactoglobulin.

The dependence of binding on concentration of small anion as well as the spectra of the complexes show that strong cooperative interactions appear with increased uptake of small molecule. These polymers offer attractive macromolecules for insertion of catalytic sites in addition to binding sites.

The binding of small molecules and ions by serum albumin has been of interest for many years (Klotz *et al.*, 1946; Klotz, 1949) because these complexes provide an insight into general biomacromolecular interactions with substrates and modifiers. Stoichiometric and energetic quantities characteristic of these interactions were obtained readily, particularly by equilibrium-dialysis techniques. However, an understanding of the detailed molecular nature of binding has been more elusive, although it has been clear that a

combination of apolar and ionic interactions contribute to the strength of the complexes (Klotz, 1946).

If one truly understands a biochemical interaction it should be possible to reproduce it *de novo* with materials of non-biological origin. Thus one might expect water-soluble synthetic polymers containing suitable apolar and ionic side chains to exhibit strong affinities for small molecules. Many such polymers have been examined (for references see Klotz and Sloniewsky, 1968). In our previous experience, however, no linear-chain type of water-soluble polymer was found to bind small molecules with an avidity comparable to that of serum albumin.

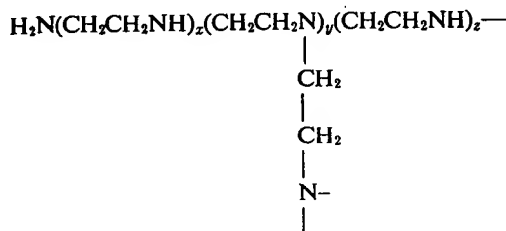
Such polymers, however, have highly swollen, extended conformations in aqueous solution, as is evident from their high intrinsic viscosities. In contrast serum albumin with an intrinsic viscosity near 4 ml/g must be relatively compact. It seemed possible, therefore, that if one could create a polymer with a high *local* concentration of apolar and ionic

* From the Biochemistry Division, Department of Chemistry, Northwestern University, Evanston, Illinois 60201. Received July 25, 1969. This investigation was supported in part by a grant from the National Science Foundation. It was also assisted by support made available by a U. S. Public Health Service training grant (5T1-GM-626) from the National Institute of General Medical Sciences.

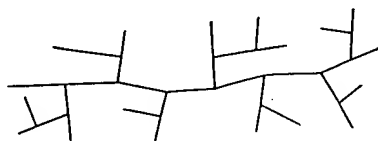
† Postdoctoral Fellow, National Institute of General Medical Sciences, 1968-1970.

groups but still water soluble, one might produce a macromolecule with strong binding properties. A class of such polymers has been produced in derivatives of polyethylenimine.

Polyethylenimine is a highly branched water-soluble polymer (Davis, 1968), a segment of which may be described as



Approximately 25% of the nitrogens are primary amines, 50% secondary, and 25% tertiary (Davis, 1968). The branching of the polymer may be represented schematically as



The primary amine groups form a very suitable locus for the attachment of apolar groups to the polymer. We have prepared, therefore, a number of derivatives with different side chains attached to a portion of the primary amine groups. These modified polymers show remarkable binding properties.

Experimental Section

Experiments described in this paper were all carried out with derivatives of PEI-600, a commercially available (Dow Chemical Co.) polyethylenimine with a molecular weight near 50,000.

Two types of acyl derivatives were prepared, one containing long-chain hydrocarbon groups and the other containing aromatic amino acid substituents.

The long-chain aliphatic acyl derivatives were prepared in the following manner. Water from the 33% aqueous solution of PEI-600 was removed in a rotary evaporator, the residue dissolved in dry ethanol, and the solvent again removed. The polymer was then dissolved in absolute ethanol to give a 35% solution. A measured quantity of the methyl ester of the appropriate acid (lauric, hexanoic, butanoic, or isobutyric) was then added to the solution of polymer. This mixture was refluxed, with stirring, for 48–72 hr. At the conclusion of the reaction, the mixture was diluted with ethanol to two to three times its original volume. Gaseous HCl was bubbled in to precipitate the polymer as its hydrochloride salt, which was washed with large quantities of ethanol containing dissolved HCl. The product was then dried for several days under vacuum at 45°. Drying was continued until the product showed no significant amount of ethanol as judged from its nuclear magnetic resonance spectrum. Nuclear magnetic resonance was also used to determine the extent of acylation

of the polymer. For this purpose 15% solutions of the hydrochloride salt of the polymer were dissolved in D₂O.

The amino acid derivatives were made with the appropriate nitrophenyl ester reagent. Measured quantities of a dry alcoholic solution of the nitrophenyl ester of either carbobenzoxytryptophan or carbobenzoxytyrosine were added dropwise with stirring to a dry alcoholic solution of PEI-600. The progress of the reaction could be followed by the appearance of the yellow color of the released nitrophenolate ion. The modified polymer was purified by gel filtration on Sephadex LH-20 with ethanol as solvent. The polymer appeared in the void volume of the eluent whereas nitrophenol and any unreacted ester emerged much later. Ethanol in the polymer fraction was removed by evaporation and an aqueous solution of the polymer was lyophilized to dryness. The content of carbobenzoxytryptophan or of carbobenzoxytyrosine was determined from the absorbance of the polymer derivative at about 280 nm. The extinction coefficients employed were those determined for carbobenzoxytyrosine propylamide and carbobenzoxytryptophan propylamide, 1600 and 5700, respectively. These reference amides were prepared from the appropriate nitrophenyl ester and propylamine.

The extent of binding of methyl orange was measured by equilibrium dialysis following procedures previously described (Klotz *et al.*, 1946; Hughes and Klotz, 1956; Rosenberg and Klotz, 1960). In this procedure, a pair of test tubes are filled with a measured quantity (10 ml) of buffer solution containing methyl orange at a known concentration. A dialysis bag containing (10 ml) polymer at a known concentration in buffer solution is immersed in one tube; a bag containing (10 ml) buffer only is immersed in the other. The tubes are shaken in a mechanical device overnight. The solutions external to the bag are then analyzed for equilibrium concentrations of methyl orange. From these measurements, the moles of bound small molecule/10⁵ g of polymer can be readily computed, after corrections have been made for binding of the dye by the cellulose bag. All experiments were carried out in a 0.1 M Tris-cacodylate buffer at pH 7 and at 25°. Since binding by the polymers, especially the lauroyl derivative, was so exceptionally high, polymer concentrations within the dialysis bag were reduced from the 0.2% commonly used with serum albumin to as low as 0.001%. Most of the measurements with the lauroyl derivative were made at polymer concentrations of 0.005–0.1%, with the hexanoyl derivative at approximately 0.025%, and with the butyryl derivatives at 0.04%. At the very lowest concentrations used, near 0.001%, binding measurements gave lower results which we attribute to significant depletion of the polymer from the extremely dilute solutions by absorption on the cellophane membrane. With lauroylpolyethylenimine, when the moles of bound methyl orange/10⁵ g of polymer exceeded approximately 470, an insoluble complex of macromolecule and small molecule was detected within the dialysis bag. Pronounced precipitation was observed as the extent of binding increased further.

Absorption spectra of the bound methyl orange were obtained by recording the difference spectrum between the inside of a dialysis bag and the external solution containing free methyl orange in equilibrium with the bound dye (Klotz and Shikama, 1968). When necessary, cells of very small light path were used and the values of absorbances were then normalized to a 1.0-cm path length.

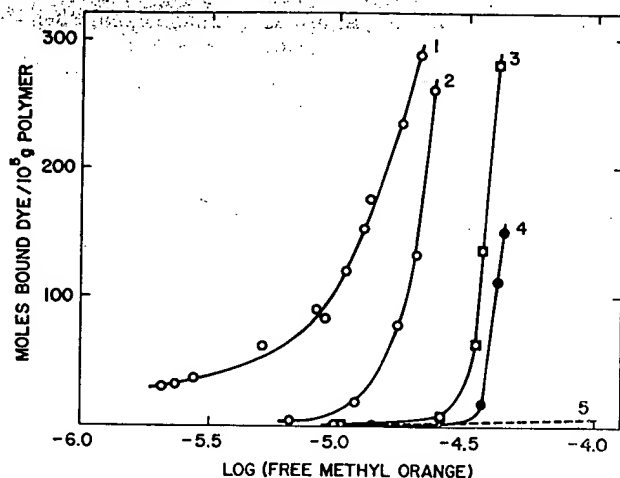


FIGURE 1: Extent of binding of methyl orange at pH 7.0 and 25° as a function of free (nonbound) dye concentration. (1) Polyethylenimine with 8.4% of residues acylated by lauroyl groups. (2) Polyethylenimine with 11.5% of residues acylated by hexanoyl groups. (3) Polyethylenimine with 10% of residues acylated by butyryl (○) or isobutyryl (□) groups. (4) Polyethylenimine, PEI-600. (5) Bovine serum albumin.

Results

To facilitate comparison of different macromolecules the extent of binding has been expressed in terms of a common unit of weight of 10^5 g of polymer or protein. Figure 1 illustrates the tremendously greater extent of binding by the acylpolyethylenimines as compared with serum albumin. At a free methyl orange concentration of 10^{-5} M, the lauroyl derivative binds over 100 moles of small dye molecule, the hexanoyl about 10, and the butyryl about 1, whereas earlier studies with bovine albumin (Klotz *et al.*, 1946) lead to values just below 1. Admittedly, lauroylpolyethylenimine has a very long apolar side chain. On the other hand, less than 10% of its residues are acylated, whereas serum albumin contains nearly 40% nonpolar amino acid residues. Furthermore, the hexanoyl and butyryl derivatives of polyethylenimine, in which side-chain lengths are comparable to those in proteins, show substantially greater binding of organic anions than does albumin.

Also remarkable in comparison with albumin is the very steep rise in binding with increasing concentration of methyl orange. In Figure 1 this is most strikingly apparent in the smaller chain derivatives of the polymer (curves 4, 3, and 2, compared with 5) but, as more sophisticated graphical analyses (Klotz, 1953), based on various linear transformations of the fundamental binding equations, indicate, it is equally true of the lauroyl derivative.

Figure 2 illustrates the extent of binding of methyl orange by polyethylenimine derivatives with aromatic amino acid acylating groups. Again it is immediately evident that these synthetic polymers exhibit much greater avidity for organic anions than does serum albumin. Particularly striking, perhaps, is the substantial increase in binding upon introduction of carbobenzoxytryptophan groups on only 2% of the ethylenimine residues.

In connection with widespread interest in the effect of urea on proteins and their interactions it seemed relevant to

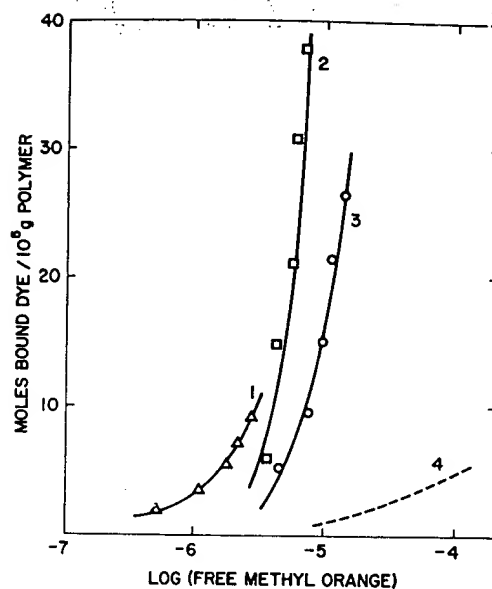


FIGURE 2: Extent of binding of methyl orange at pH 7.0 and 25° as a function of free (nonbound) dye concentration. (1) Polyethylenimine with 10% of residues acylated by carbobenzoxytyrosine. (2) Polyethylenimine with 8% of residues acylated by carbobenzoxytryptophan. (3) Polyethylenimine with 2% of residues acylated by carbobenzoxytryptophan. (4) Bovine serum albumin.

examine binding by substituted polyethylenimines in the presence of this denaturant. These results, together with an extension of the concentration range for binding in the absence of urea, are shown in Figure 3. Obviously the presence of urea markedly reduces the binding affinity of lauroylpolyethylenimine.

The spectra of bound methyl orange are shown in Figure 4. Free, nonbound methyl orange has an absorption maximum at 464 nm. When the moles of bound methyl orange/ 10^5 g of polymer is near 100 or below, the spectrum of the bound dye shows a peak near 420 nm. At higher ratios of bound anion, particularly above 150 moles/ 10^5 g, a new sharp peak appears near 375 nm.

Discussion

It is obvious from the results shown in Figures 1 and 2 that acylated derivatives of polyethylenimine, in which the acyl group is apolar, possess very strong affinities for organic anions. The extent of binding exceeds substantially that observed with serum albumin, which is the best of the proteins in general binding ability (Klotz and Urquhart, 1949b). At the lowest experimental level this is strikingly shown by the fact that a 0.001% concentration of lauroylpolyethylenimine (8.4%) is as effective as a 0.2% concentration of bovine albumin in depleting a solution of free methyl orange anions.

In principle it is possible to evaluate the first binding constant, k_1 , for anion-macromolecule complexes by suitable extrapolation of binding data to infinitely dilute small molecule concentration (Klotz and Urquhart, 1949a), even when there are strong interactions between successively bound small molecules. For methyl orange-serum albumin complexes, k_1 is of the order of 5×10^4 (Klotz *et al.*, 1946). For the corre-

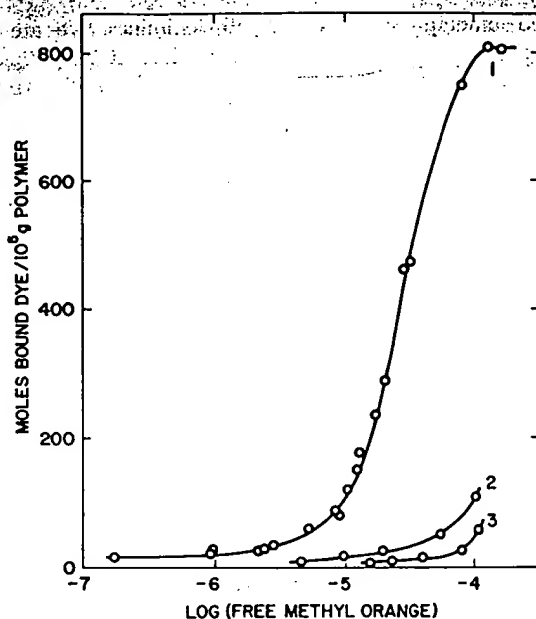


FIGURE 3: Effect of urea on extent of binding of methyl orange, at pH 7 and 25°, by polyethylenimine with 8.4% of residues acylated by lauroyl groups. (1) Tris-cacodylate buffer, 0.1 M. (2) Buffer and 6.0 M urea. (3) Buffer and 9.0 M urea.

sponding complex with lauroylpolyethylenimine, $k_1 \gg 10^6$. In fact the stability constant for the polymer-dye complex is so great that it has not been possible to evaluate it. As Figure 1 shows, even at free methyl orange concentrations of $\sim 10^{-6}$ M, the moles of bound dye are $\sim 10/10^5$ g of polymer. In practice to evaluate k_1 one must find the range of free methyl orange concentration at which the moles of bound dye are $\leq 1/10^5$ g of polymer. The results in Figure 1 suggest that this concentration of free methyl orange will lie well below 10^{-7} M, a range too low for customary procedures using equilibrium dialysis.

The marked increment in binding produced by the tryptophan derivatives (Figure 2) is of interest in connection with the possible involvement of this aromatic residue in binding by proteins. X-Ray diffraction has established the presence of tryptophan in the cleft in which substrate is held in lysozyme (Blake *et al.*, 1967; Phillips, 1967). There is also optical evidence that tryptophan residues are at the binding site of avidin (Green, 1963), antibody γ -globulins (Little and Eisen, 1967), and serum albumin (Reynolds *et al.*, 1967; Herskovits and Sorensen, 1968).

Also of relevance to the molecular basis of protein behavior are the observations (Figure 3) that urea strongly suppresses the binding ability of lauroylpolyethylenimine, just as it does that of serum albumin (Klotz *et al.*, 1948). Classically the effects of urea on proteins have been attributed to the disruption of peptide hydrogen bonds by this solute. In view of the present results with polyethylenimines, however, it seems unlikely that the mechanism of urea action in proteins involves disruption of $N-H \cdots O=C$ bonds. Similar conclusions have been reached previously from studies of the effect of urea on binding of anions by polyvinylpyrrolidone (Klotz and Shikama, 1968) and on the acid-base behavior of organic molecules attached to proteins and polymers (Klotz and

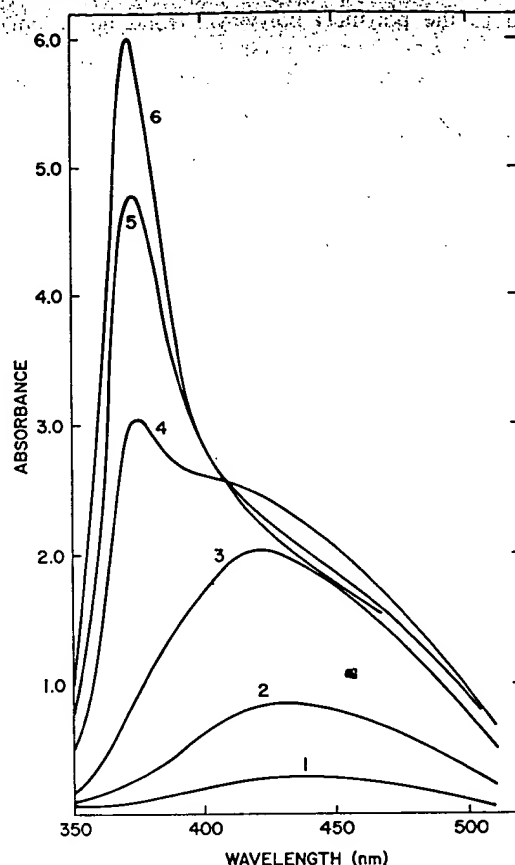


FIGURE 4: Absorption spectra of bound methyl orange on lauroylpolyethylenimine (8.4%) in Tris-cacodylate buffer (pH 7.0) and at 25°. Polymer concentration 0.0100%. Moles bound of methyl orange/ 10^5 g of polymer varied as follows: curve 1, 9.1; curve 2, 28.3; curve 3, 82.4; curve 4, 174; curve 5, 233; curve 6, 287.

Stryker, 1960). Also it has been shown (Hammes and Schimmel, 1967) that urea perturbs the ultrasonic attenuation in aqueous solutions of polyethylene glycol, and that it decreases the solubilization affinity of (nonionized) polymethacrylic acid for hydrocarbons (Barone *et al.*, 1967). Since urea has similar effects on aqueous solutions of synthetic and biopolymers of such very different molecular structure and conformation, it seems unlikely that it exerts its perturbing effects by direct combination with these different macromolecules. The very fact that large concentrations of urea are necessary for all of these effects indicates that its action is due to a change in the character of the solvent environment of the macromolecule, *i.e.*, *alloplastic* factors (Klotz, 1966) are involved.

The spectra of bound methyl orange on polyethylenimines (Figure 4) are distinctly different from those previously seen with this colored probe (Klotz, 1946; Klotz *et al.*, 1952; Klotz and Shikama, 1968). The free dye in bulk aqueous solution has a peak near 464 nm, in various organic solvents (ranging from benzene to ethanol to substituted acetamides) near 420–430 nm. Methyl orange bound to bovine albumin or to β -lactoglobulin shows an absorption maximum in the range 420 to 435 nm, presumably a reflection of the apolar character of the binding region. On the other hand, the dye

bound to the polymers polyvinylpyrrolidone or polylysine has a peak near 470 nm; evidently the open swollen conformation of these macromolecules exposes the bound dye to a largely aqueous milieu.

Bound to lauroylpolyethylenimine, methyl orange has a spectrum which depends on the number of anions attached to the polymer (Figure 4). When the moles of bound dye/ 10^5 g of polymer is less than 100, the spectrum has a peak near 420 nm, a position in consonance with the apolar environment of pendant lauroyl groups. When the moles bound/ 10^5 g reaches about 150, the 420-nm absorption maximum begins to be replaced by an entirely new and unique peak near 375 nm, which becomes more intense and sharper as the moles of bound dye increases even further.

The fact that the blue shift in the spectrum of bound dye occurs near 150 moles of bound dye/ 10^5 g of polymer is noteworthy, for 150 is also (approximately) the number of lauroyl groups attached to (10^5 g of) the polyethylenimine. It seems, therefore, that up to this point, each methyl orange anion is exposed largely to a lauroyl environment. Above 150, however, bound dye anions go to sites that already have one (or more) bound methyl orange molecules. A new type of interaction thus arises between the aromatic rings of neighboring azobenzene molecules, similar to interactions which lead to stacking in other systems, and this is reflected in the appearance of a peak at 375 nm, not previously encountered.

It is, furthermore, noteworthy that the transition concentration for the spectroscopic blue shift is also that at which cooperativity in binding manifests itself. With lauroylpolyethylenimine, appropriate graphical analysis using linear transformations of the fundamental binding equations (Klotz, 1953) shows that cooperative binding of methyl orange sets in at a free concentration (see Figure 1) near 10^{-5} M, that is when the moles of bound dye/ 10^5 g of polymer approaches 150. Cooperativity is more evident the smaller the aliphatic acyl side chain of the polymer (Figure 1). In fact the rise in binding is sharpest with unmodified polyethylenimine (curve 4 of Figure 1). In this case each methyl orange anion as it is bound simultaneously creates a new stronger apolar site for further binding of additional anions, as their concentration is increased. This interpretation is also supported by the spectra of this series of complexes. When about 2 moles of dye is bound per 10^5 g of unmodified polyethylenimine, the absorption maximum is at 470 nm; in the neighborhood of 15 moles (and perhaps even lower) a sharp peak at 380 nm is observed.

Thus cooperativity may reflect not only "conformational adaptability" (Karush, 1950) of a macromolecule but also modifications in local environment which are a consequence of the mere presence of bound small molecule.

Summarizing, we see that a compact, branched water-soluble polymer with apolar pendant groups shows very strong binding affinity for small molecules. Having intro-

duced binding sites into polyethylenimines, we are now inserting potential catalytic groups also. It may then be possible to achieve rate enhancements by such synthetic polymer catalysts which may approach those observed with enzymes.

References

- Barone, G., Crescenzi, V., Liquori, A. M., and Quadrifoglio, F. (1967), *J. Phys. Chem.* 71, 2341.
- Blake, C. C. F., Johnson, L. N., Mair, A. G., North, A. T. C., Phillips, D. C., and Sarma, V. R. (1967), *Proc. Roy. Soc. (London)* B167, 378.
- Davis, L. E. (1968), in *Water-Soluble Resins*, Davidson, R. L., and Sittig, M., Ed., New York, N. Y., Reinhold, p 216.
- Green, N. M. (1963), *Biochem. J.* 89, 599.
- Hammes, G. G., and Schimmel, P. R. (1967), *J. Am. Chem. Soc.* 89, 442.
- Herskovits, T. T., and Sorensen, M., Sr. (1968), *Biochemistry*, 7, 2533.
- Hughes, T. R., and Klotz, I. M. (1956), *Methods Biochem. Anal.* 3, 265.
- Karush, F. (1950), *J. Am. Chem. Soc.* 72, 2705.
- Klotz, I. M. (1946), *J. Am. Chem. Soc.* 68, 2299.
- Klotz, I. M. (1949), *Cold Spring Harbor Symp. Quant. Biol.* 14, 97.
- Klotz, I. M. (1953), in *The Proteins*, Neurath, H., and Bailey, K., Ed., New York, N. Y., Academic, Chapter 8.
- Klotz, I. M. (1966), *Arch. Biochem. Biophys.* 116, 92.
- Klotz, I. M., Burkhard, R. K., and Urquhart, J. M. (1952), *J. Am. Chem. Soc.* 56, 77.
- Klotz, I. M., and Shikama, K. (1968), *Arch. Biochem. Biophys.* 123, 551.
- Klotz, I. M., and Sloniewsky, A. R. (1968), *Biochem. Biophys. Res. Commun.* 31, 421.
- Klotz, I. M., and Stryker, V. H. (1960), *J. Am. Chem. Soc.* 82, 5169.
- Klotz, I. M., Triwush, H., and Walker, F. M. (1948), *J. Am. Chem. Soc.* 70, 2935.
- Klotz, I. M., and Urquhart, J. M. (1949a), *J. Phys. Colloid Chem.* 53, 100.
- Klotz, I. M., and Urquhart, J. M. (1949b), *J. Am. Chem. Soc.* 71, 1597.
- Klotz, I. M., Walker, F. M., and Pivan, R. B. (1946), *J. Am. Chem. Soc.* 68, 1486.
- Little, J. R., and Eisen, H. N. (1967), *Biochemistry* 6, 3119.
- Phillips, D. C. (1967), *Proc. Natl. Acad. Sci. U. S. A.* 57, 484.
- Reynolds, J. A., Herbert, S., Polet, H., and Steinhardt, J. (1967), *Biochemistry* 6, 937.
- Rosenberg, R. M., and Klotz, I. M. (1960), in *Analytical Methods of Protein Chemistry*, Alexander, P., and Block, R. J., Ed., Oxford, Pergamon, Vol. 2, pp 133-168.

LIBRARY
DEC 31 1969

Biochemistry



Officially published by the American Chemical Society

Editor: H. G. Othman